



Universidade do Minho

Instituto de Investigação em Biomateriais,
Biodegradáveis e Biomiméticos

Ana Sofia Martins Olival

Erythrocyte-derived liposomes for the treatment of inflammatory diseases

Dissertação de Mestrado

Mestrado Integrado em Engenharia Biomédica

Ramo de Biomateriais, Reabilitação e Biomecânica

Trabalho realizado sob a orientação de

Professor Nuno João Meleiro Alves das Neves

Doutora Helena Susana Costa Machado Ferreira

Setembro de 2020

Declaração

Nome: Ana Sofia Martins Olival

Endereço electrónico: a75473@alunos.uminho.pt

Telefone: 939473137

Número do Bilhete de Identidade: 15141881

Título da dissertação: Erythrocyte-derived liposomes for the treatment of inflammatory diseases

Orientador(es): Professor Nuno João Meleiro Alves das Neves

Doutora Helena Susana Costa Machado Ferreira

Ano de conclusão: 2020

Designação do Mestrado: Mestrado Integrado em Engenharia Biomédica

Área de Especialização: Biomateriais, Reabilitação e Biomecânica

Unidade de Investigação 3B's - Biomateriais, Biodegradáveis e Biomiméticos da Universidade do Minho

É AUTORIZADA A REPRODUÇÃO INTEGRAL DESTA TESE/TRABALHO APENAS PARA EFEITOS DE INVESTIGAÇÃO, MEDIANTE DECLARAÇÃO ESCRITA DO INTERESSADO, QUE A TAL SE COMPROMETE;

Universidade do Minho, ____/____/____

Assinatura: _____

Agradecimentos

Em primeiro lugar, gostaria de agradecer ao Professor Rui Reis pela oportunidade de desenvolver a minha dissertação de mestrado num centro de excelência, Instituto de Investigação em Biomateriais, Biodegradáveis e Biomiméticos (I3Bs), na Universidade do Minho.

Ao meu orientador, Professor Nuno Neves, agradeço pela oportunidade de desenvolver este projeto sob a sua orientação, pelo conhecimento transmitido, pelo espírito crítico, e, especialmente, pela força e confiança depositadas neste projeto.

À minha co-orientadora, Helena Ferreira, por toda a ajuda, disponibilidade e conhecimento que tornaram este projeto possível de realizar. Obrigada por me aconselhar sempre da melhor forma e por toda a paciência para me ajudar enfrentar os desafios que surgiram.

Um especial agradecimento aos projetos FROnTHERA - RL3 e Cells4_IDs que providenciaram financiamento necessário para a elaboração do trabalho experimental desta tese.

Um particular agradecimento à Aline Barros e à professora Madalena Vieira, do departamento de Engenharia Biológica da Universidade do Minho, pela ajuda incansável na utilização do GC e pelo conhecimento que partilharam comigo.

Agradeço também à CEF Taipas Saúde, pela disponibilidade de fazer as colheitas de sangue, essenciais para este projeto, e a todas as pessoas que doaram sangue para que esta tese fosse possível.

À Sara Vieira, pela constante compreensão e paciência para me ensinar e ajudar no trabalho laboratorial. Obrigada.

Ao João, pela infinita paciência para me ouvir todos os dias, pela compreensão, pelo carinho imensurável e por me fazeres rir, mesmo quando era um desafio. Obrigada.

Agradeço à minha família, à minha mãe, ao meu pai e ao meu irmão, por sempre me apoiarem no meu percurso académico e por me incentivarem a querer ser sempre melhor. Ao Gonçalinho, por ser a melhor prenda de Natal e por tornar mágica esta etapa da minha vida e à minha avó por me animar sempre que foi preciso.

À Leonor, à Patrícia, à Patrícia e à Virgínia, pela companhia, disponibilidade, paciência para me ouvirem falar infinitamente sobre esta tese e por terem sempre os melhores conselhos para me dar. Obrigada pelos risos e por estarem lá para mim em todos os momentos (e pela terapia). Principalmente tu, Leonor.

Aos meus amigos que conheci em Leuven, no início desta experiência, que me acompanharam mesmo aqui e me ajudaram a sobreviver à quarentena. Obrigada pelas Sextas-feiras e pelos jogos de mafia.

Aos meus amigos de casa, que mesmo em locais diferentes sempre me incentivaram e divertiram. Obrigada.

Agradeço também a todas as pessoas que passaram na biblioteca desde que eu cheguei. Trabalhar horas sem fim num laboratório é um bocadinho difícil, mas vocês tornaram-no mais fácil. Só tenho boas memórias (hilariantes, mas boas). Obrigada.

Finalmente, é com grande orgulho e satisfação que termino esta tese. Foi uma oportunidade de aprendizagem pessoal e académica melhor do que eu poderia ter imaginado.

Obrigada Ana, conseguimos.

STATEMENT OF INTEGRITY

I hereby declare having conducted this academic work with integrity. I confirm that I have not used plagiarism or any form of undue use of information or falsification of results along the process leading to its elaboration.

I further declare that I have fully acknowledged the Code of Ethical Conduct of the University of Minho.

Lipossomas derivados de membranas de eritrócitos para o tratamento de doenças inflamatórias

Resumo

As doenças inflamatórias crônicas são das principais causas de morbidade e mortalidade mundialmente. Desta forma, existe uma necessidade urgente de desenvolver novas alternativas terapêuticas que sejam eficazes na redução da inflamação crônica. Neste trabalho, lipossomas preparados a partir de eritrócitos foram desenvolvidos para combater a inflamação. Os eritrócitos são os componentes sanguíneos mais abundantes e as suas membranas contêm os principais ácidos gordos, incluindo os ácidos gordos ômega-3. Estes ácidos gordos têm demonstrado possuir vários benefícios para a saúde, incluindo a redução do risco de paragem cardíaca, morte cardíaca súbita e doença cardíaca isquêmica fatal. Para além disso, os ácidos gordos ômega 3 também estão envolvidos na resolução da inflamação, tendo atividade anti-inflamatória. Consequentemente, as membranas dos eritrócitos foram utilizadas como fonte lipídica para a preparação de lipossomas para combater a inflamação. O diclofenac, um fármaco anti-inflamatório não esteroide amplamente utilizado no tratamento de doenças inflamatórias como osteoartrite e artrite reumatoide, foi incorporado nos lipossomas para demonstrar o potencial dos lipossomas como veículos para entrega de fármacos no tratamento de doenças inflamatórias. Os lipossomas à base de eritrócitos foram preparados pelo método de hidratação do filme lipídico, seguido de extrusão. Posteriormente, os lipossomas foram funcionalizados com ácido fólico para que a sua ação fosse mais seletiva nos macrófagos ativos durante a resposta inflamatória. O tamanho dos lipossomas resultantes foi de aproximadamente 222 e 297 μm para lipossomas vazios e incorporando diclofenac, respectivamente. A concentração de diclofenac encapsulado determinada por HPLC foi aproximadamente 193 μM . Ensaio *in vitro* demonstraram que os lipossomas desenvolvidos não alteram a atividade metabólica e a proliferação de macrófagos diferenciados a partir de monócitos (células THP-1 diferenciadas por PMA). A atividade anti-inflamatória de ambas as formulações estudadas foi avaliada após estimulação dos macrófagos com lipopolissacarídeo. Os lipossomas vazios ou incorporando diclofenac apresentaram capacidade de reduzir aproximadamente a concentração de IL-6 em 88% e 76%, e de reduzir a concentração de TNF- α em 65% e 77%, respetivamente. Isto demonstra o potencial dos lipossomas desenvolvidos para serem usados como veículos de fármacos no tratamento de doenças inflamatórias.

Palavras-chave: Doenças inflamatórias, entrega de fármacos, eritrócitos, lipossomas.

Erythrocyte-derived liposomes for the treatment of inflammatory diseases

Abstract

Chronic inflammation-related diseases are the main cause of morbidity and mortality worldwide. Consequently, there is an urgent demand for the development of new and effective approaches to counteract the persistent inflammation. Here, a novel anti-inflammatory erythrocyte-based liposome was developed. Erythrocytes represent the most abundant blood component and their membranes present the major classes of fatty acids, including omega-3 fatty acids that have several health benefits throughout human life, including the reduction of risk of cardiac arrest, sudden cardiac death and fatal ischemic heart disease. Omega-3 fatty acids also play an important role in the resolution phase of inflammation, having anti-inflammatory activity. Consequently, erythrocytes membranes were used as a lipidic source for the preparation of liposomes with anti-inflammatory activity. Diclofenac, a widely used nonsteroidal anti-inflammatory drug (NSAID), was incorporated into the liposomes to demonstrate their potential as drug delivery devices for inflammatory diseases treatment. Erythrocyte-based liposomes were prepared by the thin film hydration method, followed by extrusion. Subsequently, the liposomes were functionalized with folic acid to target active macrophages during an inflammatory scenario. The size of the resulting vesicles was approximately 222 and 297 μm for empty liposomes and incorporating diclofenac, respectively. The concentration of diclofenac encapsulated determined by HPLC was around 193 μM . *In vitro* assays demonstrated that the developed liposomes do not alter the metabolic activity and proliferation of monocyte-differentiated macrophages (PMA-differentiated THP-1 cells). The anti-inflammatory activity of both formulations was evaluated after macrophages stimulation with lipopolysaccharide. Liposomes incorporating or not diclofenac presented ability to reduce approximately the IL-6 concentration in a percentage of 88% and 76%, and to reduce the concentration of TNF- α in a percentage of 65% and 77%, respectively. This demonstrates the potential of the developed liposomes to be used as drug carriers for the treatment of inflammatory diseases.

Keywords: Active targeting, drug delivery, erythrocytes, inflammatory diseases, liposomes

TABLE OF CONTENTS

Agradecimentos.....	iv
Lipossomas derivados de membranas de eritrócitos para o tratamento de doenças inflamatórias	vii
Erythrocyte-derived liposomes for the treatment of inflammatory diseases.....	viii
List of Abbreviations	xii
List of Figures.....	xv
List of Tables	xvii
CHAPTER I. General Introduction	3
1.1 Chronic inflammatory Diseases	3
1.1.1 Immune response: inflammation	3
1.1.2 Current therapeutic solutions.....	12
1.2 Drug delivery systems for inflammatory diseases	16
1.2.1 Liposomes	17
1.2.2. Cell-based approaches.....	21
1.2.2.4. Stem Cells.....	28
1.3 Erythrocytes as a lipidic source for drug delivery.....	29
1.3.1 Membrane structure, composition and function	29
1.4 Purpose of this work	31
1.5 References	32
CHAPTER II. Materials and Methods.....	50
2.1. Materials	50
2.1.1. Phosphatidylcholine from egg yolk.....	50
2.1.2. Erythrocytes.....	51
2.1.3. Diclofenac	53
2.1.4. Folic acid.....	54
2.2. Methods	55
2.2.1. Extraction of lipids from erythrocytes	55

2.2.2. Fatty acids profile	56
2.2.3. Preparation of erythrocyte-based LUVs incorporating or not diclofenac.....	57
2.2.4. Preparation of phosphatidylcholine liposomes.....	58
2.2.5. Characterization of LUVs	58
2.3. References	69
CHAPTER III. Erythrocyte-derived liposomes for the treatment of inflammatory diseases.....	76
Abstract.....	76
3.1. Introduction	77
3.2. Materials and Methods.....	79
3.2.1. Materials	79
3.2.2. Extraction of lipids from erythrocytes membranes and evaluation of their profile	79
3.2.3. Preparation erythrocyte-based LUVs incorporating or not diclofenac	80
3.2.4. Preparation of PC liposomes	81
3.2.5. Diclofenac concentration into liposomes.....	81
3.2.6. Size distribution and zeta potential measurements	81
3.2.7. LUVs morphology.....	81
3.2.8. Differential scanning calorimetry	82
3.2.9. THP-1 cell culture	82
3.2.10. Cell metabolic activity and proliferation assessment.....	82
3.2.11. Cell morphology analysis	83
3.2.12. Evaluation of anti-inflammatory activity	83
3.3. Statistical analysis.....	84
3.4. Results	84
3.4.1. Fatty acids profile evaluation	84
3.4.2. PC liposomes characterization	85
3.4.3. Erythrocyte-derived liposomes characterization	85

3.4.4. Thermal stability of erythrocyte-based liposomes	86
3.4.5. Biological assays.....	87
3.4.6. Anti-inflammatory activity of the LUVs.....	90
3.5. Discussion	92
3.6. Conclusions	96
3.7. References	97
CHAPTER IV. General Conclusions and Future Work.....	104
4.1. General Conclusions	104
4.2. Future Work.....	105

List of Abbreviations

µg	Microgram
µm	Micrometer
nm	Nanometer
mL	Milliliter
µM	Micromolar
mV	Milivolt
°C	Degree Celsius

B

BSE	Backscattered electrons
-----	-------------------------

C

Ca ²⁺	Calcium ions
CAMs	Cell adhesion molecules
COX	Cyclooxygenase

D

DHA	Docosaeicosanoic acid
DLS	Dynamic light scattering
DMARDs	Disease-modifying antirheumatic drugs
DSC	Differential scanning calorimetry

E

ED	Erythrocyte-derived
ELISA	Enzyme-linked immunosorbent assay
EPA	Eicosapentaenoic acid

F

FA	Folic acid
FDA	Food and drug administration
FEG	Field emission gun

G

GC-MS	Gas chromatography coupled to mass spectrometry
-------	---

GM-CSF	Granulocyte-macrophage colony-stimulating factor
--------	---

GUVs	Giant Unilamellar vesicles
------	----------------------------

H

HPLC	High performance liquid chromatography
------	---

I

IC ₅₀	Half-maximal inhibitory concentration
------------------	--

IFN γ	Interferon gama
--------------	-----------------

IKK	I κ B kinase
-----	---------------------

IL	Interleukin
----	-------------

J

JAK	Janus kinase
-----	--------------

K

KCl	Potassium chloride
-----	--------------------

L

LOX	Lipoxygenase
-----	--------------

LPS	Lipopolysaccharide
-----	---------------------------

LUVs	Large Unilamellar vesicles
------	----------------------------

M

MAPK	mitogen-activated protein kinase
------	-------------------------------------

MCP-1	Monocyte chemoattractant protein-1
-------	---------------------------------------

MgSO ₄	Magnesium Sulphate
-------------------	--------------------

MSCs	Mesenchymal stem cells
N	
NaCl	Sodium chloride
NF- κ B	nuclear factor kappa-light-chain-enhancer of activated B cells
NSAIDs	nonsteroidal anti-inflammatory drugs
NSC	Neural stem cells
P	
PAMPs	pathogen-associated molecular patterns
PC	Phosphatidylcholine
PDI	Polydispersity index
PE	Phosphatidylethanolamine
PEG	Polyethylene glycol
PER	Packed erythrocytes
PGs	Prostaglandins
PMA	phorbol 12-myristate-13-acetate
PPP	Platelet poor plasma
PRP	Platelet rich plasma
PRRs	Pattern-recognition receptors
PUFAs	Polyunsaturated fatty acids
R	
RES	Reticuloendothelial system
RPMI	Roswell Park Memorial Institute
S	
SE	Secondary electrons
SEM	Scanning electron microscopy

STAT	signal transducer and activator of transcription
STEM	Scanning transmission electron microscopy
SUVs	Small Unilamellar vesicles
T	
TEM	Transmission electron microscopy
TGF	Transforming growth factor
TLRs	Toll-like receptors
TNF- α	Tumor necrosis factor α

List of Figures

CHAPTER I. General Introduction

Figure 1.1. The main components and kinetics of the response of the innate and adaptive immune system.....	4
Figure 1.2. Exogenous and endogenous inducers of inflammation.....	5
Figure 1.3. The NF- κ B pathway is triggered by TLRs and inflammatory cytokines, such as TNF α and IL-1.	6
Figure 1.4. Arachidonic acid cascade..	8
Figure 1.5. Leukocytes (represented by neutrophils in the image) migration through blood vessels.	11
Figure 1.6. Differences between the active sites of COX-1 and COX-2.....	14
Figure 1.7. Relative COX-1/COX-2 selectivity of NSAIDs at their IC ₅₀ (half-maximal inhibitory concentration).....	15
Figure 1.8. Schematic representation of the different types of liposomes functionalization..	19

CHAPTER II. Materials and Methods

Figure 2.1. Chemical structure of phosphatidylcholine (16:0/18:1) from egg..	50
Figure 2.2. Scanning electron micrograph of erythrocytes (colored, $\times 2500$).	51
Figure 2.3. Model of the erythrocyte membrane (a) composed of phospholipids, cholesterol, proteins, and carbohydrates.	52
Figure 2.4. Chemical structure of diclofenac enclosed on COX-2 receptor	54
Figure 2.6. Schematics of a GC system.	57
Figure 2.7. General schematics of a HPLC system.....	60
Figure 2.8. Schematics of charge distribution around a nanoparticle in solution.	62
Figure 2.9. Schematics of a STEM system.	63
Figure 2.10. Characteristic thermodynamic parameters of a DSC curve.	64
Figure 2.11. Types of signals resulting from the interaction between the electron beam and the specimen.	66

CHAPTER III. Erythrocyte-derived liposomes for inflammatory diseases treatment

Figure 3.1. STEM images of erythrocyte-derived LUVs (A) and erythrocyte-derived LUVs incorporating diclofenac (B).....	86
--	----

Figure 3.2. DSC Thermograms of the erythrocyte-derived (ED) liposomes encapsulating or not diclofenac (DF).....	86
Figure 3.3. Metabolic activity (A) and cell proliferation (B) of non-stimulated macrophages in the presence of either LUVs prepared with erythrocytes membranes lipids or PC (phospholipid concentration of ~124 μ M) incorporating or not diclofenac (DF)) and of the free drug (55 μ M, concentration similar to the one incorporated in the PC and erythrocyte-derived (ED) LUVs).	87
Figure 3.5. Cell proliferation of LPS-stimulated macrophages..	89
Figure 3.6. SEM micrographs of non-stimulated macrophages and LPS stimulated macrophages in the presence of cell medium (control), empty erythrocyte-derived liposomes (ED LUVs) or incorporating diclofenac (ED LUVs with DF).	90
Figure 3.7. Concentration of IL-6 produced by LPS-stimulated macrophages..	91
Figure 3.8. Concentration of TNF- α produced by LPS-stimulated macrophages.	92

List of Tables

CHAPTER I. General Introduction

Table 1.1. Main mediators of inflammation..	7
Table 1.2. Cytokines and their role in inflammation.	9
Table 1.3. Clinically approved liposome-based formulations.....	18
Table 1.4. Classification of liposomes according to their lamellarity and size, and respective characteristics..	20
Table 1.5. Comparative analysis of different cell-based strategies.	22

CHAPTER II. Materials and Methods

Table 2.1. Fatty acids occurrence (%) in the erythrocyte membrane lipids.	53
---	----

CHAPTER III. Erythrocyte-derived liposomes for inflammatory diseases treatment

Table 3.1. Concentration of stearic acid (18:0), EPA (20:5 ω 3) and DHA (22:6 ω 3) in the lipidic extracts and LUVs.....	85
Table 3.2. Size, PDI and zeta potential of PC liposomes with and without diclofenac (DF).....	85
Table 3.3. Size, PDI and zeta potential of erythrocyte-derived (ED) liposomes with and without diclofenac (DF).....	85
Table 3.4. Concentration of phosphorus, cholesterol and diclofenac in erythrocyte-derived (ED) liposomes.	85

CHAPTER I

General Introduction

CHAPTER I. General Introduction

1.1 Chronic inflammatory Diseases

According to World Health Organization, chronic inflammatory-mediated disorders, such as autoimmune diseases (e.g. type 1 diabetes), atherosclerosis, cancer, chronic obstructive pulmonary disease, asthma and inflammatory bowel disease, are among the main causes of death worldwide [1]. These diseases are life-long debilitating illnesses, decreasing tremendously the quality of life of the affected patients and are associated with social and economic high costs [2]. Therefore, effective strategies to control chronic inflammation are crucial.

1.1.1 Immune response: inflammation

Inflammation is a biological and vital response of the immune system against harmful factors, such as pathogens, damaged cells and toxins [3]. The immune system can provide two types of response: innate immunity and adaptive immunity (Figure 1.1.). The innate immune system provides the first line of defense against infectious pathogens and includes physical barriers (e.g. skin), different immune cells (e.g. macrophages and neutrophils) and soluble factors (e.g. cytokines and chemokines) [4]. Posteriorly, the adaptive immune system is activated to destroy the foreign organisms/substances. The adaptive immune system consists of lymphocytes and their products, such as antibodies [3–4]. The responses of the adaptive immunity can be divided in two types: humoral immunity, mediated by antibodies produced by B lymphocytes, and cell-mediated immunity, mediated by T lymphocytes. Antibodies provide protection against extracellular pathogens in the blood, mucosal surfaces, and tissues and T lymphocytes are important in the defense against intracellular microbes [4]. They kill the infected cells directly or activate phagocytes to kill ingested microbes, via the production of soluble protein mediators called cytokines [4].

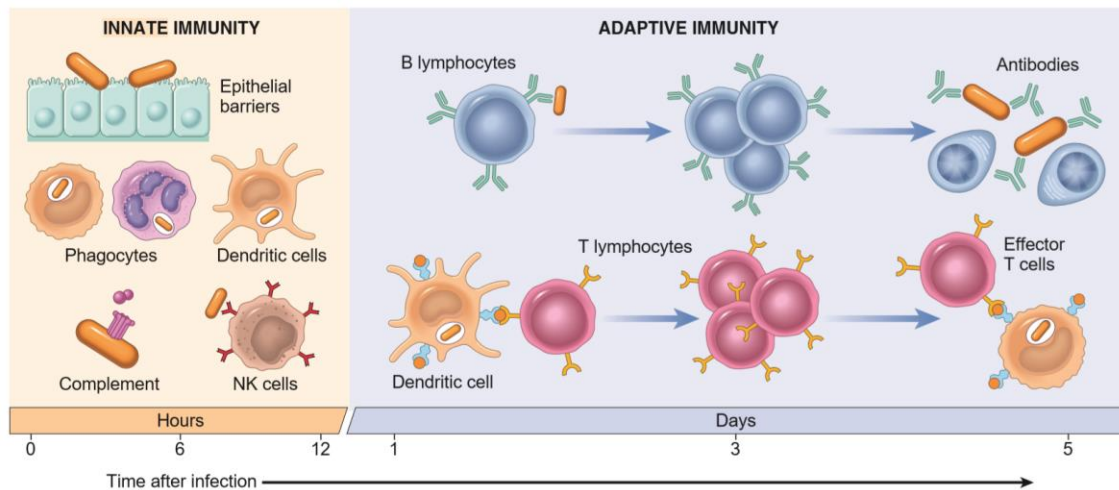


Figure 1.1. The main components and kinetics of the response of the innate and adaptive immune system. NK cells, Natural killer cells. Adapted from [4].

Inflammation was primarily described in the first century AD, by Celsus, as the tissue response to injury. This response is characterized by four signs: *(i) rubor* or redness (caused by the increased blood flow), *(ii) edema* or swelling (increased permeability of the microvasculature and leakage of proteins into the interstitial space), *(iii) calor* or heat (associated with the increase of blood flow and metabolic activity of the cellular mediators of inflammation), and *(iv) dolor* or pain (due to alterations in the perivasculature and associated nerve terminations) [5–6]. These four signals are appropriated for a successful immune response, by the activation of a series of organized and coordinated pathways against noxious compounds, pathogens or tissue injury that restores the body homeostasis [6]. Unfortunately, the immune response can become uncontrolled leading to tissue damage. In the 1850s, Rudolf Virchow described the fifth signal of inflammation, *functio laesa* or loss of function of the organs involved. Although the four cardinal signs of Celsus are only related to acute inflammation, *functio laesa* is involved in chronic inflammation. Indeed, the natural biological response of the immune system can be classified as acute or chronic and local or systemic [3]. Despite the complex nature of inflammation, there are four components that are common to any inflammatory response: the inflammatory stimuli; the sensing receptors, which recognize the stimuli; the inflammatory mediators, induced by the sensing receptors; and the target tissues that are affected by the inflammatory mediators [6–8].

The inflammatory stimuli can have an exogenous or endogenous origin (Figure 1.2.) [8–9]. Exogenous signals can be classified into two groups: microbial and non-microbial. Microbial stimuli can be further divided in two classes: pathogen-associated molecular patterns (PAMPs) and virulence factors. PAMPs are a limited and defined set of conserved molecular patterns present in

all microorganisms of a given class, and are recognized by the host germline-encoded pattern-recognition receptors (PRRs) [10]. Classes of PRR families include the Toll-like receptors (TLRs), C-type lectin receptors, retinoic acid-inducible gene receptors, and NOD-like receptors [11]. TLRs are a family of highly conserved mammalian PRRs that participate in the activation of the inflammatory response [12]. One important exogenous trigger of these PRRs is the bacterial endotoxin, also known as lipopolysaccharide (LPS), a component of the cell wall of Gram-negative bacteria. LPS can directly activate monocytes and macrophages and, consequently, different cytokines production, such as tumor necrosis factor- α (TNF- α); interleukin-1 (IL-1) and IL-6 [13]. Exogenous inducers of inflammation that are of non-microbial origin include allergens, irritants, foreign bodies and toxic compounds. Finally, endogenous inducers of inflammation include signals produced by stressed, damaged or malfunctioning tissues.

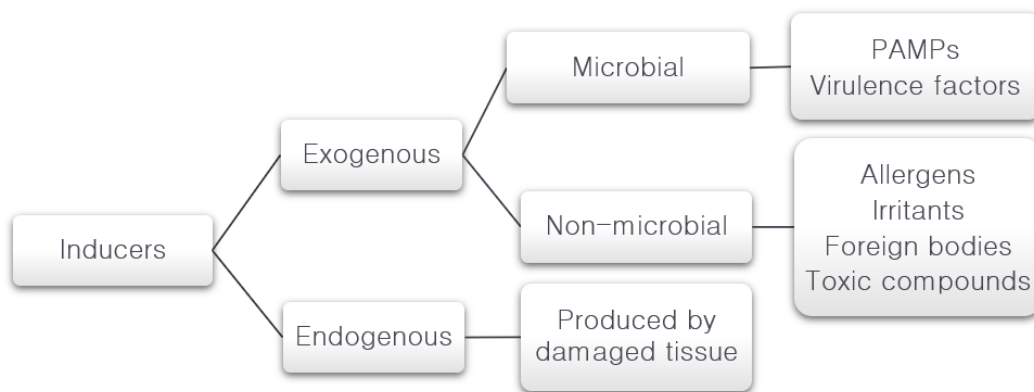


Figure 1.2. Exogenous and endogenous inducers of inflammation. ECM, extracellular matrix; PAMP, pathogen-associated molecular pattern. Adapted from [9]

The resident cells, such as macrophages, dendritic cells and mast cells, detect the harmful stimuli and trigger important intracellular signaling pathways, including the mitogen-activated protein kinase (MAPK), nuclear factor kappa-light-chain-enhancer of activated B cells (NF- κ B), and Janus kinase (JAK) and signal transducer and activator of transcription (STAT) pathways [7, 14].

MAPKs are a family of serine/threonine protein kinases that direct cellular responses, namely cell proliferation, differentiation, survival and apoptosis, to several stimuli, including osmotic stress, mitogens, heat shock, and inflammatory cytokines (such as IL-1, TNF- α , and IL-6) [15–16]. Activation of the MAPKs results, therefore, in the phosphorylation and activation of p38 transcription factors present in the cytoplasm or nucleus, initiating the inflammatory response [16–17].

The NF- κ B is not a single nuclear factor, as the name suggests, but a family of inducible transcription factors. This family is composed of five structurally related members, including p50, p52, relA, rel B and cRel [15]. Under unstimulated conditions, NF- κ B is in the cytoplasm in its inactive form, sequestered by a family of inhibitor proteins, known as I κ B proteins (Figure 1.3.) [7]. However, in the presence of inflammatory mediators, such as TNF- α and IL-1, the I κ B kinase (IKK) phosphorylates the I κ B protein leading to their degradation [7]. Once free, the NF- κ B complex can enter into the nucleus, initiating gene transcription [18]. This pathway regulates the production of pro-inflammatory cytokines and the recruitment of inflammatory cells.

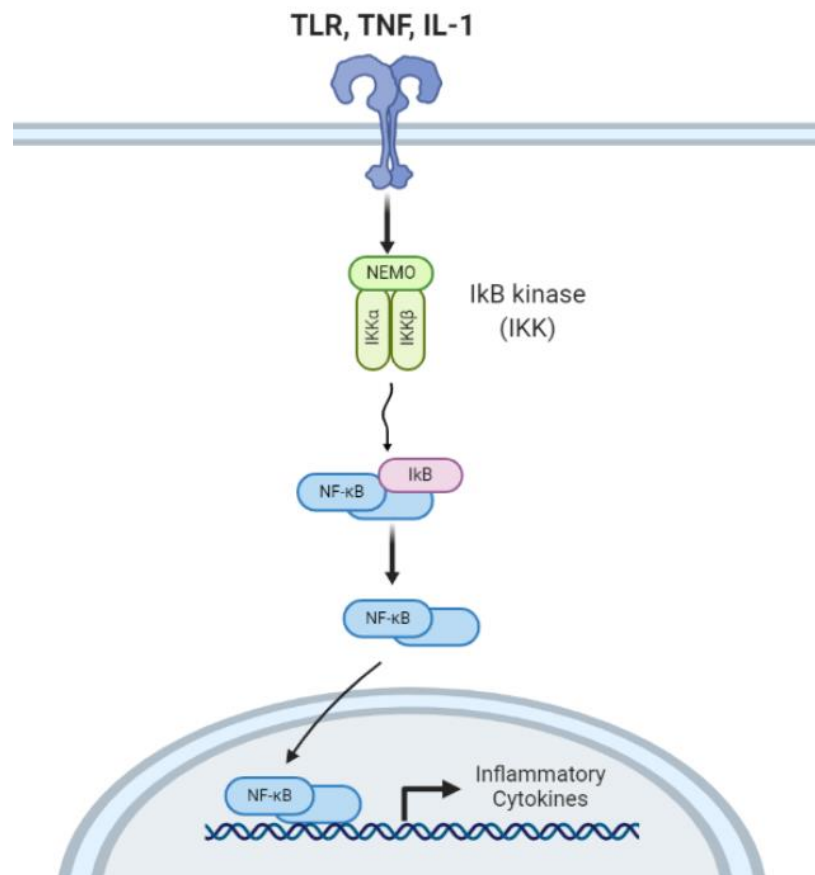


Figure 1.3. The NF- κ B pathway is triggered by TLRs and inflammatory cytokines, such as TNF α and IL-1. This leads to the activation of I κ B kinase (IKK), which then phosphorylates the I κ B proteins leading to their degradation. The NF- κ B complex, once free, can translocate to the nucleus and initiate gene transcription to produce inflammatory cytokines. Adapted from [7].

Inflammatory signals from the activated NF- κ B and MAPK pathways result in the production of various effector molecules, including cytokines that activate the JAK-STAT pathway [19]. The interaction between cytokines and their receptors causes the phosphorylation of JAKs, which phosphorylate STATs [20]. Then, STATs form a dimer, and these dimers translocate into the nucleus to modulate the expression of specific cytokine-responsive genes [20].

The activation of the NF- κ B, MAPK and JAK-STAT inflammatory pathways results in the secretion of inflammatory mediators, which can be classified into seven groups according to their biochemical properties: vasoactive amines, vasoactive peptides, fragments of complement components, lipid mediators, cytokines, chemokines and cell adhesion molecules (CAMs) (Table 1.1.) [9, 21].

Table 1.1. Main mediators of inflammation. Adapted from [9, 21–22].

Mediator	Examples	Source	Action
Vasoactive amines	Histamine	Mast cells, basophils, platelets	Vasodilation, increased vascular permeability, endothelial activation
Vasoactive peptides	Thrombin, bradykinin, plasmin	Plasma	Increased vascular permeability, smooth muscle contraction, vasodilation, pain
Complement components	Complement proteins (C3, C5)	Plasma	Leukocyte activation and chemotaxis, vasodilation (through mast cell stimulation)
Lipid mediators	Prostaglandins	Mast cells, leukocytes	Vasodilation, pain, fever
	Leukotrienes	Mast cells, leukocytes	Increased vascular permeability, chemotaxis, leukocyte adhesion and activation
Cytokines	TNF- α , IL-1 and IL-6	Macrophages, endothelial cells, mast cells	Local: endothelial activation Systemic: fever, metabolic abnormalities, hypotension (shock)
Chemokines	IL-18, MCP-1	Leukocytes, activated macrophages	Chemotaxis, leukocyte activation
CAMs	Selectins, integrins	Endothelial cells, leukocytes	Rolling, adhesion and transmigration of leukocytes

Abbreviations: IL – interleukin; TNF- α – tumor necrosis factor- α ; MCP-1 – Monocyte Chemoattractant Protein-1; CAMs – cell adhesion molecules

Vasoactive amines, such as histamine, produced when mast cells and platelets degranulate, act on the vasculature, causing increased vascular permeability and vasodilation [9, 21]. Vasoactive peptides (e.g. thrombin or plasmin) cause vasodilation and increase vascular permeability [9, 21]. Specifically, the vasoactive peptide bradykinin contributes to vasodilation and

has a potent pain-stimulating effect. The complement fragments (e.g. C3 or C5) are produced by several pathways after complement activation and promote granulocyte and monocyte recruitment as well as histamine release from mast cells, thus increasing vascular permeability and vasodilation. [9, 21]. Lipid mediators (e.g. prostaglandins and leukotrienes) are derived from phospholipids, that are present in the inner leaflet of the cellular membranes [9, 21]. After activation by intracellular calcium ions (Ca^{2+}), the cytosolic phospholipase A_2 hydrolyses arachidonic acid, releasing it from the cellular phospholipids [9, 21]. Arachidonic acid can be then metabolized to form eicosanoids either by the epoxygenase, cyclooxygenase (COX) or lipoxygenase (LOX) pathways (Figure 1.4.) [21, 23]. The epoxygenase pathway is responsible for the formation of epoxyeicosatetraonic acid, which is reported to have a regulatory role in inflammation [23]. The COX pathway leads to the generation of prostaglandins (PGs), prostacyclin and thromboxane, while the LOX pathway originates leukotrienes and lipoxins [23]. Of these lipid mediators, PGs, prostacyclin, thromboxane and leukotrienes have pro-inflammatory effects, such as causing vasodilation, being hyperalgesic and inducing fever, while lipoxins have major anti-inflammatory effects such as suppressing neutrophils chemotaxis, fibrosis and pain [9, 21].

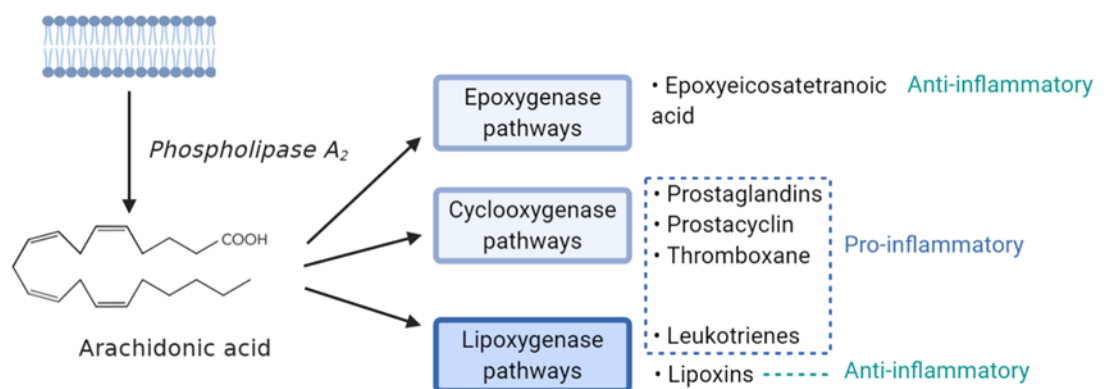


Figure 1.4. Arachidonic acid cascade. Phospholipase A_2 acts on the membrane phospholipids to release arachidonic acid, which, in turn, is the substrate for the COX, LOX and epoxygenase pathways. The epoxygenase pathway produces epoxyeicosatetraonic acid, COX pathways produce prostaglandins, prostacyclin, and thromboxane, and the LOX pathways produce leukotrienes and lipoxins.

Inflammatory cytokines (e.g. $\text{TNF-}\alpha$, IL-1, and IL-6) are released from different immune cells, including monocytes, macrophages and lymphocytes and have several roles in the inflammatory response (Table 1.2) [9, 21].

Table 1.2. Cytokines and their role in inflammation. Adapted from [7, 21].

Cytokine	Family	Main cell sources	Function
IL-1 β	IL-1	Macrophages, monocytes	Stimulates the expression of endothelial adhesion molecules, leukocyte recruitment and secretion of other cytokines; systemic acute-phase response (specially fever)
IL-6	IL-6	Macrophages, T-cells, adipocyte	Systemic effects (acute phase response)
IL-8	CXC	Macrophages, epithelial cells, endothelial cells	Pro-inflammatory, chemotaxis, angiogenesis
TNF- α	TNF	Macrophages, NK cells, CD4+ lymphocytes, adipocyte	Stimulates the expression of endothelial adhesion molecules, leukocyte recruitment and secretion of other cytokines; systemic acute-phase response
IFN- γ	IFN	T-cells, NK cells, NKT cells	Pro-inflammatory, innate and adaptive immunity
GM-CSF	IL-4	T-cells, macrophages, fibroblasts	Pro-inflammation, macrophage activation, increase of neutrophil and monocyte function
IL-4	IL-4	Th-cells	Anti-inflammation, T-cell and B-cell proliferation, B-cell differentiation
IL-10	IL-10	Monocytes, T-cells, B-cells	Anti-inflammation, inhibition of the pro-inflammatory cytokines production
IL-11	IL-6	Fibroblasts, neurons, epithelial cells	Anti-inflammation, differentiation, induces acute phase protein
TGF- β	TGF	Macrophages, T-cells	Anti-inflammation, inhibition of pro-inflammatory cytokines production

Abbreviations: IL – interleukin; TNF– tumor necrosis factor; IFN – Interferon; GM-CSF – Granulocyte-macrophage colony-stimulating factor; TGF– transforming growth factor.

Chemokines (e.g. IL-18, MCP-1) are produced by leukocytes and activated macrophages after inflammatory response initiation and they control leukocyte extravasation and chemotaxis towards the affected tissues [9, 21].

Selectins and integrins, receptors expressed on leukocytes and endothelial cells, respectively, are the two major families of molecules involved in leukocyte adhesion and migration through blood vessels. In the absence of an inflammatory scenario, endothelial selectins are expressed at low levels and integrins present on leukocytes' membranes are in a low affinity conformation (Figure 1.5). Thus, leukocytes flow in the blood stream without binding to the endothelial surfaces [3, 8]. However, during an inflammatory response, leukocytes and endothelial cells become active. Selectins upregulated in the endothelial cells, will first interact weakly with leukocyte integrins. These initial interactions are easily disrupted by the flowing blood and, consequently, leukocytes will roll along the endothelial surface. However, the activation of integrins by chemokines will lead to their conformational change, acquiring high affinity to endothelial selectins. This results in a strong integrin-mediated binding of the leukocytes to the endothelium at the site of inflammation. Afterwards, the leukocytes will extravasate squeezing between cells at intercellular junctions, by a phenomenon called transmigration, and continue to move along the chemical gradient (chemokines) to the inflammation site by a process called chemotaxis. Additionally, during the inflammatory process, a reversible opening of endothelial cells tight junctions will occur. This will allow for protein and fluids to leak from the vascular to the extravascular compartment, leading to edema.

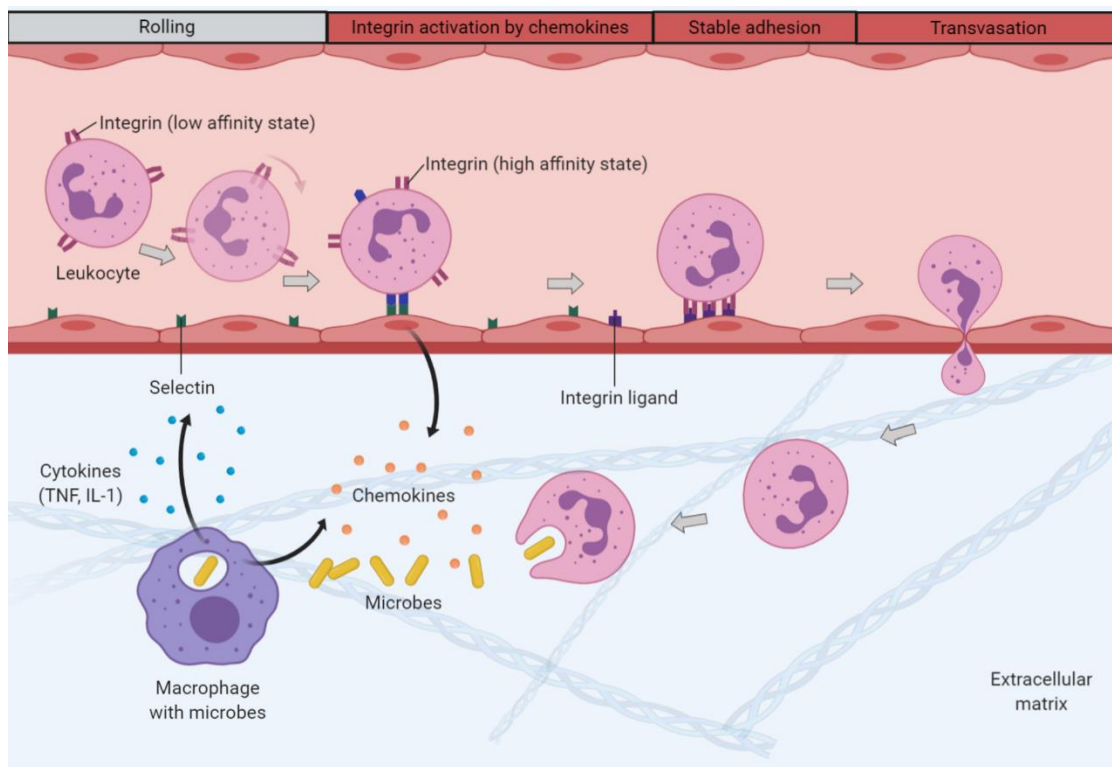


Figure 1.5. Leukocytes (represented by neutrophils in the image) migration through blood vessels. The leukocytes first roll due to weak interactions with selectins, and later bind to the endothelium due to integrin-mediated interactions. Subsequently, leukocytes migrate across the endothelium, pierce the basement membrane, and move toward chemokines released at the inflammation site. TNF, tumor necrosis factor; IL-1, interleukin-1. Adapted from [21].

Another event of the inflammatory response is the platelet activation, usually associated with conversion of prothrombin to thrombin. This results in platelet aggregates, due to platelet adhesion to each other, as well as platelet adhesion to endothelial cells. This precedes intravascular thrombosis, during which fibrin starts to deposit in and around aggregated platelets. Lastly, hemorrhage might also occur during an inflammatory response, due to the direct structural damage of the endothelial barrier.

All the previously mentioned inflammatory events are reversible. For instance, edema fluid is cleared together with inflammatory cells into the draining lymphatics [3]. Leukocytes can also be cleared from the tissues by apoptosis or phagocytosis by tissue-resident macrophages and thrombosis in the vessels can be avoided by activation of the fibrinolytic system.

The switch in lipid mediators from pro-inflammatory to anti-inflammatory eicosanoids is crucial for the resolution of inflammation. Lipoxins, which are originated through the LOX pathways, as mentioned above, inhibit the recruitment of neutrophils and promote the recruitment of monocytes, which remove dead cells and initiate tissue remodeling [9]. In parallel to the arachidonic acid cascade, omega-3 fatty acids which can be obtained by dietary intake, are also

released from the cellular membrane by phospholipases. Eicosapentaenoic acid (EPA) is metabolized to originate E series resolvins, while docosahexaenoic acid (DHA) is metabolized to produce D series resolvins and protectins [23]. Resolvins and protectins have a crucial role in the resolution of inflammation, including the initiation of tissue repair [24–25]

If the inflammatory stimuli is not eliminated by the acute inflammatory response, the resolution phase may not be effective and the inflammatory response can become exacerbated in magnitude and time, leading to chronic inflammation and tissue damage [8].

Chronic inflammation is a response of prolonged duration (weeks, months or years) in which inflammation, tissue injury, and efforts of tissue repair coexist. It may follow acute inflammation or begin without any sign of a preceding acute reaction [21]. The causes of chronic inflammation are not completely identified but can arise from: (1) persistent infections caused by microorganisms that are difficult to eradicate, such as mycobacteria and certain viruses, fungi, and parasites; (2) hypersensitivity diseases (asthma, rheumatoid arthritis), caused by excessive and disproportionate activation of the immune system; (3) prolonged exposure to potentially toxic agents [21]. The chronic inflammatory response can be systemic but is typically localized in the site where the inflammatory inducer is located and can be characterized by infiltration of mononuclear cells (e.g. macrophages and lymphocytes) and plasma cells (e.g. eosinophils, mast cells and neutrophils), and can lead to tissue destruction. The presence of these cells can be induced by the persistent presence of the inflammatory agent as well as by efforts to heal the damaged tissue by connective tissue replacement. Indeed, the tissue repair is accomplished by angiogenesis (proliferation of small blood vessels) and fibrosis. Frequently, acute and chronic inflammation coexist over long periods [26].

In summary, inflammation is essential and beneficial to human life, but can become detrimental when excessive or persistent, because of its tissue-damaging potential. Furthermore, non-resolving inflammation contributes significantly to the pathogenesis of several diseases, such as atherosclerosis, obesity, cancer, chronic obstructive pulmonary disease, asthma, inflammatory bowel disease and neurodegenerative diseases, making it a current medical burden for which new and effective therapeutic solutions are necessary and urgent [5, 26].

1.1.2 Current therapeutic solutions

Therapeutic interventions for inflammation-related diseases include the use of corticosteroids, nonsteroidal anti-inflammatory drugs (NSAIDs), and conventional, biologic and targeted synthetic disease-modifying antirheumatic drugs (DMARDs).

Corticosteroids are a class of steroid hormones, released by the adrenal cortex, such as glucocorticoids [27]. As all steroid hormones, corticosteroids are synthesized from cholesterol through a mitochondrial enzymatic process called steroidogenesis [28]. Corticosteroids have a role in the regulation of diverse cellular functions, including metabolism, development, cognition, homeostasis, and inflammation [29]. Synthetic corticosteroids are largely used for the treatment of inflammatory and autoimmune diseases, including allergy, septic shock, asthma, inflammatory bowel disease, rheumatoid arthritis and multiple sclerosis [27]. Corticosteroid therapy has a strong suppressive effect on the inflammatory response, which is predominantly due to the inhibition of the gene expression of NF- κ B and other pro-inflammatory transcription factors [21, 27]. Corticosteroids inhibit the expression of many pro-inflammatory cytokines, including IL-1 β , IL-2, IL-3, IL-4, IL-5, IL-6, IL-11, IL-12, IL-13, IL-16, IL-17, interferon-gamma (IFN γ), TNF- α and granulocyte-macrophage colony-stimulating factor, and have an important role during the resolution phase, namely in the clearance of cellular debris and in the production of anti-inflammatory factors [28]. However, the therapeutic use of corticosteroids is restricted due to their numerous side effects, such as hyperglycemia, osteoporosis, insulin resistance, hypertension, disturbed fat deposition and muscle atrophy [30]. Moreover, patients with long-term glucocorticoid therapy can develop tissue-specific glucocorticoid resistance [31]. For instance, glucocorticoid resistance is present in 4–10% of asthma patients, 30% of rheumatoid arthritis patients, and almost in all sepsis patients [32]. Therefore, corticosteroids are useful in short-term treatment of most patients, but the side effects of their long-term therapy result in the need to seek alternative therapies.

NSAIDs are the group of therapeutic agents most prescribed worldwide and present distinct structural and pharmacological features [33]. There are now at least 20 different NSAIDs from six major groups available in the clinic [34]. All of them are completely absorbed after oral administration, have negligible first-pass hepatic metabolism, and circulate tightly bound to albumin in the blood stream. In general, NSAIDs are hydrophobic and weak organic acids, which facilitate their binding to COX-2, an endoplasmic reticulum membrane protein with the active site located at the end of a hydrophobic channel [35]. Indeed, there is vast evidence indicating that the main mechanism for the anti-inflammatory properties of this group of drugs is related to the inhibition of the COX-2 enzyme [36]. The COX enzyme, also known as prostaglandin endoperoxide H synthase, exists in two well described isoforms: COX-1 and COX-2. A third isoform, COX-3, has been described, however its function and relevance in the NSAIDs mechanisms of action are still poorly understood and remain controversial, being, therefore, not herein described [37–38].

COX-1 is expressed in most mammalian cells and tissues, including the endothelium. Its functions are mostly regulatory, producing e.g. prostaglandins that are responsible for gastro and renal protection [39]. Conversely, COX-2 is an enzyme induced by tissue injury or other stimuli, such as LPS, IL-1 and TNF- α , mediating inflammatory responses. Previous studies revealed that COX-2 three-dimensional structure closely resembles COX-1 (Figure 1.6.) but includes an extra pocket in its catalytic site. This structural distinction is extremely relevant for the design of selective COX-2 inhibitors [40].

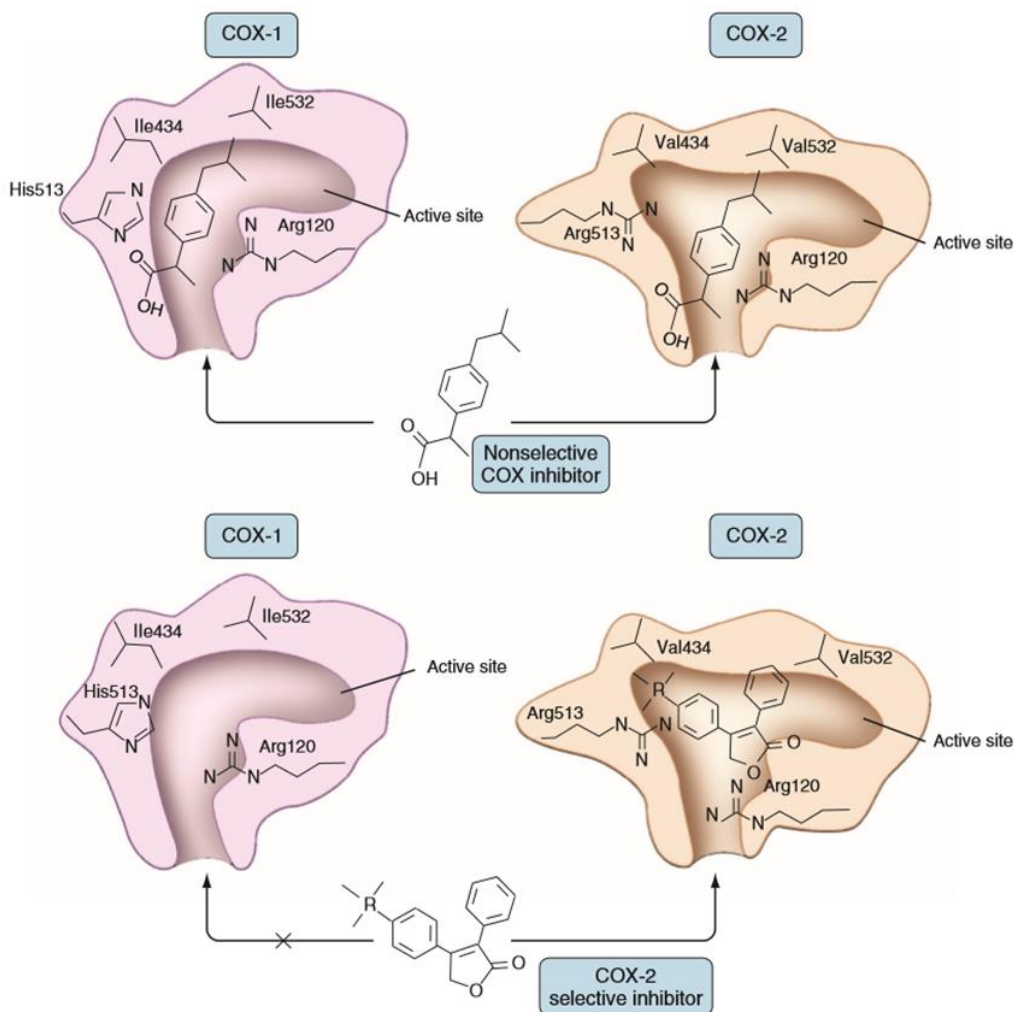


Figure 1.6. Differences between the active sites of COX-1 and COX-2. The amino acid residues Val434, Arg513, and Val523 form a side pocket in COX-2 that is absent in COX-1, making it a target for COX-2 selective drugs. Adapted from [41].

NSAIDs can be characterized by their selectivity to inhibit COX-1 and COX-2 (Figure 1.7.). The traditional NSAIDs inhibit both isoforms of COX, and consequently, their adverse effects, such as stomach pain are attributed to COX-1 inhibition [42]. Consequently, efforts have been made to design selective COX-2 inhibitors. The first selective COX-2 inhibitor in the clinical practice was celecoxib (Celebrex®), launched in 1999, by G.D. Searle and Pfizer.

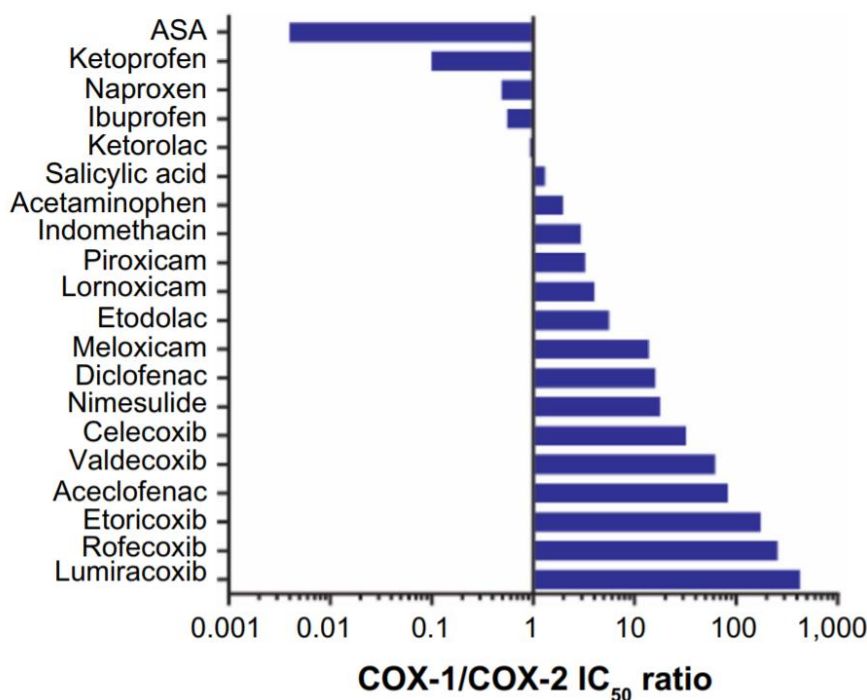


Figure 1.7. Relative COX-1/COX-2 selectivity of NSAIDs at their IC_{50} (half-maximal inhibitory concentration). Values higher than 1 indicate greater selectivity for COX-2, while lower values (<1) indicate greater selectivity for COX-1. Adapted from [43].

Despite the initial success of selective COX-2 inhibitors, concerns were raised regarding their adverse cardiovascular effects [44]. Indeed, several studies demonstrated that selective COX-2 inhibitors may alter the natural balance between prothrombotic thromboxane A₂ and antithrombotic prostacyclin, increasing the likelihood of a thrombotic cardiovascular event [45–46]. In April of 2005, the Food and Drug Administration (FDA) advisory committee overwhelmingly concluded that coxibs increase the risk of cardiovascular events and some formulations were removed from the market due to safety issues. However, traditional NSAIDs, which inhibit COX-2 to a greater extent than COX-1, can also be associated with an increased risk of cardiovascular events, specially at high doses [47–48]. Although novel compounds are being developed to improve drug safety and tolerability, an ideal NSAID that avoids all potential side effects has still to be discovered [49]. Therefore, the lowest effective dose of drug should be used for the shortest period of time to decrease the potential of cardiovascular and gastrointestinal side effects [43]. Moreover, new delivery strategies are necessary to reduce the risks associated with currently available NSAIDs.

DMARDs are a class of drugs indicated for the treatment of inflammatory arthritis but can also be used in the treatment of other inflammatory disorders [50–51]. There are two major classes of DMARDs: conventional and biological [50]. Commonly used conventional DMARDs

include methotrexate, leflunomide, hydroxychloroquine, and sulfasalazine. Methotrexate is the most frequently used DMARD in monotherapy as well as the cornerstone of combination therapy for rheumatoid arthritis [52]. The side effects of conventional DMARDs are variable and agent specific, including nausea, vomiting, skin rashes, gastrointestinal discomfort and general malaise [50]. Biologic DMARDs are usually prescribed after the failure of conventional DMARD therapy [51]. They are highly specific, targeting a particular pathway of the inflammatory cascade [50]. TNF- α , for example, is an attractive target for the treatment of inflammatory diseases, as it is the most rapidly released pro-inflammatory cytokine and its effects include up-regulation of other pro-inflammatory mediators [53]. For TNF- α targeting, four drugs were approved: adalimumab, certolizumab pegol, golimumab, and infliximab. For targeting of TNF- α receptor only one biological agent, etanercept, is available [54]. IL-6 is another primary regulator of both acute and chronic inflammation, showing potential as a target for the clinical treatment of chronic inflammatory diseases [53]. Blockage of IL-6 can be done using monoclonal antibodies against this cytokine or its receptor [54]. Tocilizumab and sarilumab are approved drugs to target the IL-6 receptor in the treatment of rheumatoid arthritis [54–56]. Furthermore, several IL-6 targeting biological drugs are currently in phase II or III clinical trials, including olokizumab, clazakizumab, and vobarilizumab. Despite being promising therapeutic approaches, biological DMARDs have several drawbacks that are due to the inherent properties of cytokines, which are pleiotropic (they can affect several processes in parallel) and redundant (the effects achieved by blocking one specific cytokine can be compensated by others) [57]. Moreover, as the cytokines network is a regulated and balanced system, its alteration can lead to impaired immune response, leading to an increased risk of infection of the patients [51–52].

Overall, though immense progress has been made in the treatment of inflammatory-related diseases, there is still a gap to be filled in order to guarantee patients safety and to improve clinical outcomes.

1.2 Drug delivery systems for inflammatory diseases

The field of drug delivery has grown tremendously in the past few decades by the development of a wide range of micro- and nano-sized advanced delivery systems for local and controlled drug delivery.

An ideal drug vehicle should be biocompatible, biodegradable and easily functionalized to target specific tissues/cells. Indeed, one of the main limitations in the drug delivery field is the

nonspecific uptake of the delivery devices by healthy tissues, causing unintended side effects. After drug delivery devices administration, they can be recognized by the immune system and removed from circulation or, if they pass the first immune screening, they can diffuse throughout the organism and accumulate in non-target organs, causing undesirable side effects and limiting the dose that reaches the target site [58]. Thus, their surface functionalization to sustain systemic circulation and target a specific diseased tissue/cell is essential.

A wide range of vehicles have been employed as controlled drug delivery systems, including nanoparticles [59], liposomes [60], micelles [61], fibers [62], hydrogels [63], films [64], and living cells [65]. Liposomes and cell-based strategies are discussed in greater detail in the next sections because of its relevance for this thesis.

1.2.1 Liposomes

Liposomes, whose structure mimic cellular membranes, are widely used to incorporate and deliver drugs [66]. Liposomes were first described in the 1960s by Bangham, but it was in the early 1970s that they were investigated as drug delivery systems [67–68]. Indeed, due to their versatility, biocompatibility and biodegradability, liposomes have been thoroughly studied as drug carriers. Currently, there are several liposomal drug formulations in the clinic for the treatment of different diseases (Table 1.3.), including hepatitis A, metastatic breast cancer and acute lymphoblastic leukemia [69–71]. Moreover, there are several liposome-based formulations in clinical trials that can reach the clinic in the near future[72–73].

Table 1.3. Clinically approved liposome-based formulations. Adapted from [60].

Product (approval year)	Administration	Active agent	Indication	Company
Epaxal® (1993)	i.m.	Inactivated hepatitis A virus	Hepatitis A	Crucell, Berna Biotech
Doxil® (1995)	i.v.	Doxorubicin	Ovarian, breast cancer, Kaposi's sarcoma	Sequus Pharmaceuticals
Abelcet® (1995)	i.v.	Amphotericin B	Invasive severe fungal infections	Sigma-Tau Pharmaceuticals
Amphotec® (1996)	i.v.	Amphotericin B	Severe fungal infections	Ben Venue Laboratories Inc.
DaunoXome® (1996)	i.v.	Daunorubicin	AIDS-related Kaposi's sarcoma	NeXstar Pharmaceuticals
Ambisome® (1997)	i.v.	Amphotericin B	Presumed fungal infections	Astellas Pharma
Inflexal® V (1997)	i.m.	Inactivated hemagglutinine of influenza virus strains A and B	Influenza	Crucell, Berna Biotech
Depocyt® (1999)	Spinal	Cytarabine/Ara-C	Neoplastic meningitis	SkyPharma Inc.
Myocet® (2000)	i.v.	Doxorubicin	Combination therapy for metastatic breast cancer	Ellan Pharmaceuticals
Visudyne® (2000)	i.v.	Verteporfin	Chorioidal neovascularization	Novartis
Mepact® (2004)	i.v.	Mifamurtide	High-grade, resectable, non-metastatic osteosarcoma	Takeda Pharmaceutical Limited
DepoDur™ (2004)	Epidural	Morphine sulfate	Pain management	SkyPharma Inc
Exparel® (2011)	i.v.	Bupivacaine	Pain management	Pacira Pharmaceuticals, Inc.
Marqibo® (2012)	i.v.	Vincristine	Acute lymphoblastic leukemia	Talon Therapies, Inc.
Onivyde™ (2015)	i.v.	Irinotecan	Combination therapy for metastatic adenocarcinoma of the pancreas	Merrimack Pharmaceuticals Inc.

Abbreviations: i.m. – intramuscular; i.v. – intravascular.

Liposomes are composed of phospholipids, which self-assemble in an aqueous medium to form spheres of lipid bilayers enclosing an aqueous core. Different phospholipids, such as phosphatidylcholine (PC), phosphatidylethanolamine (PE), phosphatidylserine and phosphatidylglycerol, can be used in their composition. Besides phospholipids, other lipids can be incorporated in the phospholipid bilayer. For instance, cholesterol is generally added to increase the liposomes stability. Indeed, the addition of this steroid can increase the packing of phospholipid molecules [74], reduce bilayer permeability to non-electrolyte and electrolyte solutes [75], improve LUVs resistance to aggregation [76] and change the fluidity of the LUVs to allow them to sustain severe shear stresses [77].

Phospholipids are amphiphilic, having hydrophilic headgroups and hydrophobic acyl chains, and in aqueous solutions they will organize to protect the hydrophobic moieties from the aqueous environment [78]. Their organization in a bilayer is thermodynamically favorable and strengthened by hydrogen bonding, van der Waals forces, and electrostatic interactions [79]. Since the liposomes present an aqueous core and a lipid bilayer, they can incorporate both hydrophilic and hydrophobic molecules within the aqueous core and lipid bilayer, respectively (Figure 1.8.). Therefore, liposomes possess the ability to improve the solubility of hydrophobic drugs, to prevent the chemical and biological degradation of therapeutic agents after administration, and to prolong the circulation lifetime of the drugs [80].

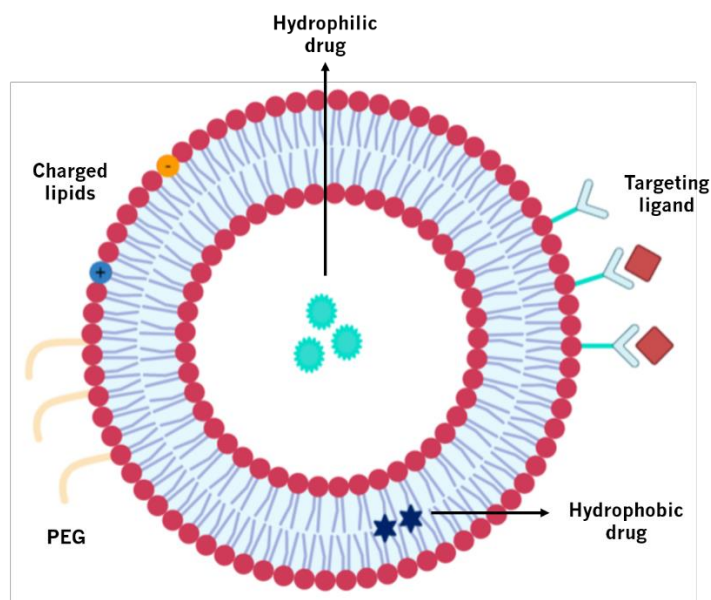


Figure 1.8. Schematic representation of the different types of liposomes functionalization. Conventional liposomes incorporating hydrophilic and hydrophobic molecules, liposomes functionalized with PEG, liposomes functionalized with target ligands.

The classification of liposomes can be done according to the number of bilayers in: unilamellar vesicles, multilamellar vesicles and multivesicular vesicles (Table 1.4.) [81]. Unilamellar vesicles can also be classified into three categories considering their size (Table 1.4.): (1) giant unilamellar vesicles (GUVs), (2) large unilamellar vesicles (LUVs) and (3) small unilamellar vesicles (SUVs).

Table 1.4. Classification of liposomes according to their lamellarity and size, and respective characteristics. Adapted from [81–82].

Classification	Size	Characteristics
<u>Lamellarity</u>		
Unilamellar vesicles	All size range	Single lipid bilayer; large aqueous core; usually used for the entrapment of hydrophilic drugs; sustained release profile of the encapsulated material.
Multilamellar vesicles	>500 nm	Several concentric lipid bilayers; high proportion of lipid material; usually used for the encapsulation of lipophilic compounds; sustained release profile of the encapsulated material.
Multivesicular vesicles	>1000 nm	Small vesicles entrapped within a single lipid bilayer; large aqueous phase to lipid ratio; very efficient at entrapping large volume of hydrophilic material; sustained release profile of the encapsulated material.
<u>Size</u>		
Small unilamellar vesicle (SUVs)	20–100 nm	Low aqueous core volume to lipid ratio; useful for entrapping lipophilic active materials.
Large unilamellar vesicle (LUVs)	>100 nm	Large aqueous phase to lipid ratio; very efficient at entrapping large volume of hydrophilic agents.
Giant unilamellar vesicle (GUVs)	>1 μm	Ideal models of cell membranes and can be used as microscale bioreactors

The circulation features of liposomes can be tailored by adjusting the liposomes composition and size. Indeed, small liposomes avoid the reticuloendothelial system (RES) more efficiently than their larger counterparts. To improve their carrier properties, liposomes have been functionalized with different ligands (polymers, carbohydrates, peptides, antibodies or proteins), including surface modification with hydrophilic polymers, such as polyethylene glycol (PEG) [83–84]. The addition

of PEG to liposomes creates a steric boundary, preventing the binding of plasma proteins and, consequently, their uptake by the reticuloendothelial system (RES) [85]. Indeed, when particles move through the blood stream, they are signaled for phagocytic removal by the adsorption of opsonins, such as antibodies and serum proteins. When the liposomes are functionalized with PEG, they become shielded by the dense coating, which creates a hydration layer that prevents the nonspecific adsorption of opsonins and reduces cell adhesion [86]. Though PEGylation has been widely used in the design of therapeutic particles, with improved results, this strategy also presents important limitations. To obtain a dense protective layer against opsonization, long PEG polymers are often needed, which may conceal the targeting ligands that are attached to their distal ends and hinder their binding to the cell surface receptors [87]. Moreover, PEGylation strongly hinders endosomal escape of nano-vehicles, leading to significant loss of activity of the encapsulated drugs [88]. Accelerated blood clearance by the immune system also occurs after repeated injections of PEGylated nanoparticles, including liposomes [89–90].

One of the main aims of any drug delivery device is to increase the therapeutic effect of the drug while minimizing its side effects. Therefore, as previously referred, efforts have been made to obtain passive, but also active targeting. Different approaches have been made to achieve selective delivery to the target area. Among the several ligands used to functionalize liposomes, folic acid, also known as folate or vitamin B9, has attracted attention to target activated macrophages, due to its selectivity, in imaging and therapeutic approaches [91–92].

Despite having been extensively and successfully used, liposomes still present unique and appealing features for drug delivery and their full potential as carriers has still to be met, maintaining the interest for future research.

1.2.2. Cell-based approaches

To improve the pharmacokinetic profile of drugs, cell or cell-derived vesicles can be used as drug carriers. For instance, the whole cell, extracellular vesicles and cell membrane-coated particles have been used for drug delivery [93, 97]. These strategies seek to improve the pharmacokinetic profile and targeting of the drugs toward pathological conditions, by mimicking the versatility and complexity of the cellular membrane, which has naturally evolved to successfully perform specific functions [98]. Many different cell types have been used, including erythrocytes, platelets, white blood cells, stem cells, cancer cells and even bacteria, presenting each its own set of unique features [97, 99, 103]. Table 1.5 presents the properties, advantages and limitations of the different cell-based strategies for drug delivery.

Table 1.5. Comparative analysis of different cell-based strategies. Adapted from [104–105].

	Erythrocytes	Platelets	Leukocytes	Stem Cells
Amount/mL blood	$4.2\text{--}6.0\times 10^6$	$\sim 1.5\text{--}4.5\times 10^8$	$4\times 10^3\text{--}1\times 10^3$	Unknown
Diameter (μm)	~ 7	$\sim 1\text{--}4$	7–15	30–40
Location	Blood circulation	Bone marrow, blood circulation	Circulation, tissues and organs	Circulation, tissues
Life Span	~ 120 days	$\sim 7\text{--}10$ days	A few days; years for memory lymphocytes	Depends on cell type
Functions	Transport oxygen and carbon dioxide	Coagulation, vascular regeneration, inflammation,	Immune defense	Repair of tissues and organs
Advantages as DDS	Large encapsulating volume; large surface areas; longer life span; reversible deformation; RES targeting.	Readily available; interaction with vascular injury sites specifically	Capable of cross biological membrane tumor-homing; immune response.	Potency; homing to cancer and injured cells, tissues and organs
Disadvantages as DDS	Rapid RES elimination; drug released off-site	Highly reactive (risk of thrombosis or bleeding); storage and contamination issues	Short lifespan; hard to handle.	Hard to maintain potency <i>in vitro</i> ; may promote tumor growth

1.2.2.1. Red blood cells

The use of red blood cells or erythrocytes as drug delivery systems was first described in the 1970s and recently resurfaced as an alternative to polymer-based drug vehicles [106]. Erythrocytes have several characteristics that make them advantageous carriers when compared to polymeric drug delivery systems, such as long circulation-time, high drug-loading capacity and inherent biocompatibility [98].

Erythrocytes have two main functions: to carry oxygen from the lung to the tissues and carbon dioxide, produced by tissues, to the lungs, maintaining the pH of the blood. The structure and composition of these cells are, therefore, tailored to allow the maximum efficiency of gas exchange. Indeed, erythrocyte's surface-to-volume ratio and shape enable optimal gas exchange. These cells are non-nuclear biconcave discs with a diameter of $\sim 7\ \mu\text{m}$, a thickness of $\sim 2\ \mu\text{m}$ and a plasma membrane surface area of $\sim 160\ \mu\text{m}^2$. If they were spherical, hemoglobin would be at the center of the cell, being relatively distant from the membrane, being not readily oxygenated and deoxygenated. Therefore, as erythrocytes have a biconcave shape, hemoglobins that are toward the center of the cell are not distant from the membrane and are able to exchange oxygen. This surface-to-volume ratio also renders them deformability, being able to stretch 2.5 times their resting diameter during their passage through narrow capillaries and splenic pores [107].

Erythrocytes are the most abundant type of blood cells in the human body, existing ≈ 5 million per microliter of blood and 30 trillion erythrocyte in the whole human body [108]. On the erythrocytes surface there are crucial surface-markers that allow these cells to circulate in the blood for a long period of time (approximately 120 days in humans) without being removed by macrophages [108–109].

Erythrocytes are completely biodegradable without producing toxic by-products. Moreover, as mature erythrocytes do not contain any genetic material, the safety risks are lower than with other gene or cell therapies [110]. The RES recognizes old or defective erythrocytes and rapidly removes them from the circulation. For this reason, several strategies took advantage of the clearance pathways of erythrocytes to target the RES of the liver, spleen and bone marrow [104]. However, this can pose a problem when non-RES targeting is desired. Therefore, erythrocyte-based carriers are usually modified morphologically and functionally to improve their pharmacokinetic properties.

Erythrocytes can be easily processed, isolated, frozen, and stored for at least ten years [111]. Another advantage of erythrocytes is to allow personalized devices because the patient's own blood can be used as a source [112].

To encapsulate drugs in erythrocytes, several methods are used [113–114]. Osmosis-based methods developed in the 1970s were considered standard methods due to the ability of erythrocytes to act as osmometers. In a hypotonic solution, erythrocytes swell and form temporary pores ranging from 200 Å to 500 Å in the membrane, through which substances can enter. If the erythrocytes are then placed on an isotonic solution, their shape is recovered, and their pores close, keeping the desired substances encapsulated in their interior [113]. Another encapsulation method that can be used for drugs loading in erythrocytes is electroporation or electro-insertion. In this method, a voltage is applied to the membrane, causing local disruptions of the bilayer structure that results in pore formation and enhanced permeability to macromolecules [114].

Various compounds, such as drugs and enzymes, were already encapsulated and sustained released from erythrocytes [115–118]. For instance, erythrocytes were able to encapsulate and protect L-asparaginase from degradation [116]. Moreover, the incorporated enzyme exhibited a longer half-life and lower incidence and severity of side effects than the free L-asparaginase. Another study demonstrated that when carboxylated polystyrene nanoparticles are attached to the erythrocytes membrane through non-covalent interactions, a prolonged circulation time of the nanoparticles in the blood, increased accumulation in lung and diminished uptake by liver and spleen are obtained [119].

Besides using directly erythrocytes, other strategies were employed using the erythrocytes membrane. The cells membrane can be used to produce erythrocyte mimicking nanoparticles or nanoerythrosomes (nanovesicles obtained by the serial extrusion of erythrocytes ghosts) [120–121]. In a reported study, injections of a fluorophore loaded in erythrocyte membrane-camouflaged polymeric nanoparticles revealed superior circulation half-life in mice compared to control (particles coated with PEG) [103]. Moreover, biodegradable doxorubicin-loaded polymeric nanoparticles coated with erythrocyte membranes were nonimmunogenic in a murine model of lymphoma and delivered doxorubicin into the tumor site, with fewer toxic effects than free drug [122]. Recently, nanoerythrosomes loaded with tumor antigens were used for cancer immunotherapy, being able to inhibit tumor growth in B16F10 and 4T1 mice tumor models [123].

1.2.2.2. Platelets

Platelets are enucleated, discoid shaped blood cells, produced by megakaryocytes, and are engaged in several physiological and pathological processes, such as maintenance of vascular integrity, wound healing and inflammation [124]. Platelets are stored in the spleen, and their release is regulated by the sympathetic nervous system. For instance, when blood vessels are injured, platelets are recruited and activated around the wounded site. Platelets and coagulation factors can repair the vessel damage by clumping and clotting the interrupted endothelium. Coagulation consists in a four-stage process of adhesion, activation, aggregation and wound repair [125]. The concentration of platelets in the blood is between 150×10^9 platelets/L to 350×10^9 platelets/L and their average life span is 7–10 days, both significantly lower than erythrocytes [126]. After this period, platelets are removed by RES of the liver and spleen [127, 128]. They are the smallest components of the blood, with an average diameter of 2–3 μm .

To take advantage of their natural carrier features, platelets have been studied for drug delivery. As platelets represent a small portion of blood components, they cannot be isolated effectively just by blood centrifugation. Generally, blood is centrifuged at different speeds to obtain platelet rich plasma (PRP) and platelet poor plasma (PPP). The platelets are separated from PRP using a sepharose column [136]. All steps must be carried out under sterile conditions and quickly to avoid undesirable activation of the platelets. Drugs can then be encapsulated within platelets by high voltage electroporation [137]. However, there are alternative methods that attaches drugs/nanoparticles to the surface of circulating platelets rather than their isolation and load.

Platelets targets are well defined, being mostly sites with high density of proliferating cells or injured sites. Thus, side effects caused by nonspecific targeting are decreased. Another advantage of using platelets as well as other cells types-derived from patients, as previously referred for erythrocytes, is obtaining personalized vehicles because the patient's own platelets, cells can be used to deliver drugs [112]. Nevertheless, this approach still present significant drawbacks, such as the risk of thrombogenesis, short shelf-life, challenging storage and possible contamination [105]. Indeed, platelets are highly reactive blood components and, consequently, platelet-mediated drug delivery can lead to functional alterations resulting in thrombosis or bleeding.

A study demonstrated the ability of platelets to load and release doxorubicin hydrochloride, a potent anti-cancer drug [112]. The efficiency of drug-loaded platelets in inducing cytotoxicity of the cancer cells was significantly higher in both *in vitro* (adenocarcinoma cell line) and *in vivo* (Ehrlich ascites carcinoma bearing mice model), compared to the free drug [112, 129]. Another

example of using platelets as vehicles for tumor targeting include to load kabiramide and antitumor proteins, such as transferrin, into these cells. The presence of kabiramide prevents platelets activation and the antitumor proteins allow myeloma tumors targeting [130]. Platelets successfully loaded and released the drugs as well as accumulated at the site of myeloma xenotransplant in mice. Another study reported, fucoidan nanoparticles loaded with multiple drugs including a chemotherapeutic and imaging agent were targeted to P-selectin [131]. The fucoidan-platelet system was able to deliver the therapeutics locally, compared to delivery systems not targeting P-selectin. Besides cancer, platelets have also been effectively exploited as carriers for antithrombotic agents, especially for arterial clots [132–133].

1.2.2.3. Leukocytes

Leukocytes are cells of the immune system that can be used for the encapsulation of drugs. These cells possess several features that confer them desirable properties as carriers, such as long blood circulation time, easy crossing of biological barriers, identification of diseased or inflamed tissues and natural tumor tropic nature [134–137].

There are five major types of leukocytes, namely neutrophils (40%-75%), lymphocytes (20%-45%), monocytes and macrophages (2%-10%), eosinophils (1%-6%) and basophils (less than 1%) [104]. Leukocytes are usually separated and purified from the whole blood by centrifugation and their different types can be separated by immunomagnetic cell separation [138]. If necessary, the leukocyte's membrane can be isolated through a discontinuous sucrose gradient [139]. Consequently, drugs can be bound to the leukocyte's membrane or encapsulated inside the cell. Several techniques were described for binding drugs to leukocytes' membranes, including receptor-mediated adhesion, covalent binding and selectin-mediated adhesion [126–127]. For drug encapsulation into the leukocytes, hypotonic and resealing methods have been used [125].

Neutrophils, lymphocytes, monocytes and macrophages have been studied as potential carriers of therapeutics for the treatment of various diseases [139, 142–149]. In particular, neutrophils present several advantages to deliver nanotherapeutics. Firstly, neutrophils are the first cells to arrive at the sites of infection or inflammation. Secondly, neutrophils are the most abundant leukocyte in the human body and even though neutrophils lifespan is short in circulation, circa 5.4 days (and only a few hours after their isolation from blood), the number of neutrophils can be increased by tens-hundreds of folds in a short period of time in the presence of an inflammatory scenario, which would quickly increase the drug delivery [142, 150]. Therefore, several studies investigated neutrophils application in drug delivery. For example, microvesicles produced by

neutrophils were able to enter cartilage and to protect the joint in inflammatory arthritis [143]. More recently, neutrophil membrane-coated poly(lactic-co-glycolic acid) nanoparticles presented potential to neutralize proinflammatory cytokines, suppress synovial inflammation and provide strong chondroprotection against joint damage [144].

As mentioned before, monocytes and macrophages have also been investigated for drug delivery. Monocytes are the largest leukocytes, with a diameter of 50–80 μm , and are progenitor cells of macrophages and dendritic cells. Monocytes have unilobed nuclei and granulated cytoplasm. Monocytes have the ability to migrate toward pathological sites, such as infections, inflammation and tumors, which are important features for drug delivery [151]. During an inflammatory response, monocytes can differentiate into macrophages. Macrophages have a diameter of 5–50 μm and generally contain a large kidney-shaped nuclear lobe [152]. The cytoplasm is abundant and contains many large and small granules, responsible for killing and digesting invading pathogens. Multiple studies have reported the use of macrophages to carry antiretroviral drugs for sites of active viral replication and anti-cancer drugs, since tumors have the natural ability to recruit macrophages [153–155]. Macrophage membrane-coated pH-sensitive emtansine-loaded liposomes, developed to suppress the lung metastasis of breast cancer, presented higher cancer cells toxicity when compared with the uncoated liposomes [114, 125]. Moreover, monocytes/macrophages have been employed as “Trojan Horses” to deliver gold nanoshells to the hypoxic regions of cancer. The results showed that malignant cells were killed in areas where nanoshells alone could not access [149]

Despite being a promising strategy, macrophage-based drug delivery systems still presents drawbacks that involve the risk of free drug loading into macrophages causing cytotoxicity and impairment of macrophage function, as well as premature drug release or degradation due to the natural enzymes contained in macrophages [156].

Lastly, lymphocytes potential in cancer therapy has also been explored owing to their intrinsic ability to migrate to tumor and inflammation sites [157]. Lymphocytes are primarily found in the circulation and central lymphoid organs, such as tonsils, spleen and lymph nodes [158]. Lymphocytes have a large nucleus surrounded by a thin layer of cytoplasm, and their average diameter is 7–15 μm [104]. Both T and B cells are involved in defense mechanisms and represent a potential platform to deliver drugs [104]. Lymphocyte membrane-camouflaged nanoparticles have been studied and showed, e.g. potential to exhibit enhanced localization at the tumor site after low-dose irradiation [159].

Although leukocyte membrane-coated formulations are a promising strategy, there are still some limitations that need to be considered for their application. For instance, leukocyte membranes are frequently obtained from immortal cell lines, which may not be as biocompatible as autologous membranes. Moreover, leukocytes express specific major histocompatibility complex molecules on their surface. Consequently, their immunogenicity should be considered.

1.2.2.4. Stem Cells

Stem cells are self-renewable and have potential to differentiate into various cell types, being essential in tissue repair and regeneration. They are broadly classified into two categories according to their source and plasticity: embryonic stem cells and adult stem cells [160]. Embryonic stem cells originate from the inner cell mass of a blastocyst in an early stage embryo and are pluripotent, being able to differentiate into cells of the three germ layers [160]. Adult stem cells are tissue-specific stem cells that can differentiate into limited specialized cells [160].

Stem cells in drug delivery applications have versatile advantages, including their natural targeting capability, immunomodulatory ability, potential of migrating towards tumor and inflammatory microenvironments, easy harvesting and *in vitro* culture, low immunogenicity, and differentiability into specialized cells [104, 151]. These properties make stem cells promising candidates for targeted drug delivery [160].

Several types of stem cells have been studied as carriers for drug delivery, including mesenchymal stem cells (MSCs) [159] and neural stem cells (NSCs) [161–164]. The use of MSCs to deliver therapeutic agents is widely investigated for cancer treatment. Unmodified MSCs have been shown to release factors that have anti-tumor properties, inhibiting the proliferation of several tumor types [165]. In addition, therapeutic genes have been introduced into MSCs for cancer treatment, including immunomodulatory factors [166–167], which can also be used to treat multiple inflammatory diseases [151]. NSCs also presented ability to migrate toward intracranial gliomas and deliver an oncolytic drug, 5-fluorouracil, leading to the reduction of about 80% of the tumor mass within 2 weeks [161].

Despite this promising progress with stem cells, they also present disadvantages, such as the difficulty to maintain the cells' potency *in vitro* and concerns related with their ability to promote the tumor growth or even differentiate into cancer cells [168–171]. Thus, it is necessary to carefully select and characterize the stem cell type when designing the stem cell-based delivery system [172].

Overall drug delivery with living cells is a promising strategy, with each cell having their advantages and disadvantages depending on the target conditions (Table 1.5.). However, there is still space for improvement, particularly regarding patient safety. One aspect that affects directly the safety of the therapies is the source of the cells used, which can be autologous or allogeneic [173]. Autologous therapies have the advantage of the host immune system recognizing the engineered cells as 'self', resulting in minimal immunogenic responses. However, maintenance of autologous cells is usually difficult. Conversely, when allogeneic cell types are used questions regarding the immune responses from the host arise. Indeed, the repeated administration in a clinical setting could be complicated, because of the development of neutralizing antibodies or severe infusion reactions.

1.3 Erythrocytes as a lipidic source for drug delivery

As described previously, erythrocytes are promising drug carriers due to their ability to increase drug circulation and excellent bioavailability. Erythrocytes advantageous characteristics are a consequence of their plasma membrane, which is their structural component responsible for all their antigenic, transport, and mechanical characteristics. As a result, it is essential to understand the structural properties and composition of the erythrocytes membrane to better comprehend its full potentialities.

1.3.1 Membrane structure, composition and function

In general, any cell membrane has four basic functions: (1) to provide a physical but flexible barrier to protect cell components from the extracellular environment, (2) to regulate and facilitate the exchange of substances, (3) to establish electrochemical gradients between the intra- and extracellular milieus, and (4) to present receptors to allow the cell to answer signaling molecules through signal transduction pathways [146–147]. The first insights about the structure of the erythrocytes membrane were provided by Gorter and Grendel in 1925, who inferred that there are “bimolecular layers of lipids on the chromocytes of blood” [176]. Since then, the continuous evolution of analytic methods allowed for further unveil these cells membrane' characteristics.

The erythrocytes plasma membrane, presenting 5 nm of thickness, is 100 times more elastic than a comparable latex membrane and has a tensile strength greater than steel. The erythrocytes membrane consists of approximately 52% proteins, 40% lipids and 8% carbohydrates [107]. The lipid bilayer, composed of cholesterol and phospholipids, is universal to all animal cells

and is anchored to a 2-dimensional elastic network of skeletal proteins through tethering sites on cytoplasmatic domains of transmembrane proteins embedded in the lipid bilayer [177].

Cholesterol and phospholipids are in the membrane in the same ratio. The phosphate end of the phospholipid (head) and the hydroxyl group of cholesterol have hydrophilic properties, being oriented towards the extracellular and intracellular environment of the cell membrane. Conversely, the fatty acid chains of the phospholipids (tails) and the steroid nucleus of cholesterol are hydrophobic, and, therefore, are directed to each other in the center of the bilayer to avoid the contact with the aqueous environment [178]. It is assumed that cholesterol is distributed equally between the 2 leaflets, conferring tensile strength to the lipid bilayer [179]. However, as cholesterol concentration increases the membrane increases its strength but loses elasticity.

The four major phospholipids of the erythrocyte's membranes, namely phosphatidylcholine, sphingomyelin, phosphatidylethanolamine and phosphatidylserine, are asymmetrically disposed. Phosphatidylcholine and sphingomyelin are predominantly located in the outer monolayer, while the majority of phosphatidylethanolamine and all phosphatidylserine, together with the minor phosphoinositide constituents, are present in the inner monolayer [180–181]. The distribution of the four phospholipids is energy dependent, relying on membrane-associated enzymes, namely flippases, floppases, and scramblases, to maintain their positions [182]. If phospholipids distribution is disrupted, as observed in sickle cell anemia or in erythrocytes that have reached their 120-day life span, phosphatidylserine, the only negatively charged phospholipid, flips to the outer layer. Splenic macrophages possess receptors that bind to the displaced phosphatidylserine and destroy senescent and damaged erythrocytes [183].

Erythrocyte membranes are rich in major classes of fatty acids: saturated fatty acids, monounsaturated fatty acids and polyunsaturated fatty acids (PUFAs) [184]. Among the PUFAs present in the erythrocytes membrane, the omega-3 fatty acids EPA and DHA have been widely reported for the health benefits of the dietary intake of these fatty acids, including a reduced risk for cardiac arrest, sudden cardiac death and fatal ischemic heart disease [185–187]. Moreover, the omega-3 index, termed the measurement of EPA and DHA in erythrocyte membranes, is used to assess when the intake of omega-3 fatty acids is suboptimal and is used to predict the risk to develop coronary heart disease [184, 188]. In addition to their cardioprotective effects, EPA and DHA have also been reported to have anti-inflammatory, immunoregulatory, antioxidant and anti-tumor activities [13, 189]. The anti-inflammatory effects reported include reduction of leukocyte chemotaxis, reduction of the expression of CAMs, decreased production of

eicosanoids from arachidonic acid and of inflammatory cytokines, and increased production of pro-resolution resolvins and protectins [13, 189].

In the erythrocyte membrane outer layer, carbohydrates are covalently linked to membrane proteins and phospholipids, forming glycoproteins and glycolipids, respectively [174]. The glycocalyx, also known as pericellular matrix, is a layer of carbohydrates whose net negative charge prevents microbial attack and protects erythrocytes from mechanical damage caused by adhesion to neighbor erythrocytes or to the endothelium [174].

Transmembrane and cytoskeletal proteins represent 52% of weight of the membrane structure [190]. A proteomic study revealed at least 300 different proteins, including 105 transmembrane proteins [190]. Some of the transmembrane proteins define the various blood group antigens [191]. As previously referred, through glycosylation they also support surface carbohydrates, which join with glycolipids to build the protective glycocalyx [192]. These proteins function as molecule membrane transport and signaling receptors [174]. Signaling receptors bind plasma ligands and trigger activation of intracellular signaling proteins, which then initiate various energy-dependent cellular activities, a process called signal transduction.

The principal cytoskeletal proteins are the filamentous α -spectrin and β -spectrin [174]. The spectrins form a hexagonal lattice that is immediately adjacent to the cytoplasmic membrane lipid layer and provides lateral or horizontal membrane stability [193].

1.4 Purpose of this work

In this work, a novel drug carrier was developed by using erythrocytes membranes as a lipidic source for the preparation of liposomes. Indeed, liposomes resemble the cell membranes, being consequently also widely used as membrane models [194–195]. These vesicles are valuable carriers due to their several advantageous features mentioned above. As previously mentioned, omega-3 fatty acids play a crucial role during the resolution stage of inflammation, having anti-inflammatory activity. It is intended that by preparing liposomes from erythrocytes membranes, they will be rich in omega-3 fatty acids, thus having an intrinsic anti-inflammatory action.

Folic acid, has been widely used for the selective targeting of activated macrophages [91–92]. Indeed, macrophages play an active role in the pro-inflammatory stages of inflammation and, therefore, represent an important target for anti-inflammatory strategies. By functionalizing liposomes with folic acid, it is aimed to obtain a specific delivery of their cargo into active macrophages.

To demonstrate their carrier ability, diclofenac was loaded into the liposomes. Diclofenac is a widely prescribed worldwide NSAID [196]. As other NSAIDs, diclofenac is associated with severe dose-dependent cardiovascular, gastrointestinal and renal injurious effects. Because of this, new improved methods of encapsulating this drug are paramount, making it an appealing drug to validate the efficacy of the novel liposomes to reduce the side effects and increase therapeutic efficacy.

1.5 References

- [1] World Health Organization, *Noncommunicable Diseases Country Profiles 2018*. 2018.
- [2] R. H. Straub and C. Schradin, "Chronic inflammatory systemic diseases – an evolutionary trade-off between acutely beneficial but chronically harmful programs," *Evol. Med. Public Heal.*, vol. 2016 (1), pp. 37–51, 2016.
- [3] C. N. Serhan, D. W. Gilroy, and P. A. Ward, Eds., "The inflammatory response - an overview," in *Fundamentals of Inflammation*, Cambridge: Cambridge University Press, 2010, pp. 1–38.
- [4] V. Kumar, A. K. Abbas, and J. C. Aster, Eds., "Chapter 5. Diseases of the Immune System," in *Robbins Basic Pathology*, 10th ed., Philadelphia: Elsevier, 2018, pp. 121–189.
- [5] P. Libby, "Inflammatory Mechanisms: The Molecular Basis of Inflammation and Disease," *Nutr. Rev.*, vol. 65(12 Pt 2), pp. S140–S146, 2007.
- [6] R. Medzhitov, "Inflammation 2010: New Adventures of an Old Flame," *Cell*, vol. 140, no. 6, pp. 771–776, 2010.
- [7] L. Chen *et al.*, "Inflammatory responses and inflammation-associated diseases in organs," *Oncotarget*, vol. 9, no. 6, pp. 7204–7218, 2018.
- [8] D. Okin and R. Medzhitov, "Evolution of inflammatory diseases," *Curr. Biol.*, vol. 22, no. 17, pp. R733–R740, 2012.
- [9] R. Medzhitov, "Origin and physiological roles of inflammation," *Nature*, vol. 454, no. 7203, pp. 428–435, 2008.
- [10] R. Medzhitov and C. A. Janeway, "Innate immunity: The virtues of a nonclonal system of recognition," *Cell*, vol. 91, no. 3, pp. P295-298, 1997.
- [11] O. Takeuchi and S. Akira, "Pattern Recognition Receptors and Inflammation," *Cell*, vol. 140, no. 6, pp. 805–820, 2010.
- [12] C. A. Janeway Jr. and R. Medzhitov, "Innate immune recognition," *Annu Rev Immunol*, vol. 20, pp. 197–216, 2002.

- [13] P. C. Calder, “n-3 Polyunsaturated fatty acids, inflammation, and inflammatory diseases,” *Am. J. Clin. Nutr.*, vol. 83, no. 6 Suppl, pp. 1505S-1519S, 2006.
- [14] J. M. Kyriakis and J. Avruch, “Mammalian mitogen-activated protein kinase signal transduction pathways activated by stress and inflammation,” *Physiol. Rev.*, vol. 81, no. 2, pp. 807–869, 2001.
- [15] B. Kaminska, “MAPK signalling pathways as molecular targets for anti-inflammatory therapy - From molecular mechanisms to therapeutic benefits,” *Biochim. Biophys. Acta - Proteins Proteomics*, vol. 1754, no. 1–2, pp. 253–262, 2005.
- [16] G. Pearson *et al.*, “Mitogen-activated protein (MAP) kinase pathways: Regulation and physiological functions,” *Endocr. Rev.*, vol. 22, no. 2, pp. 153–183, 2001.
- [17] J. Raingeaud, A. J. Whitmarsh, T. Barrett, B. Dérjard, and R. J. Davis, “MKK3- and MKK6-regulated gene expression is mediated by the p38 mitogen-activated protein kinase signal transduction pathway,” *Mol. Cell. Biol.*, vol. 16, no. 3, pp. 1247–1255, 1996.
- [18] T. Lawrence, “The nuclear factor NF-kappaB pathway in inflammation,” *Cold Spring Harb. Perspect. Biol.*, vol. 1, no. 6, p. a001651, 2009.
- [19] S. H. Venkatesha, B. Acharya, and K. D. Moudgil, “Natural Products as Source of Anti-Inflammatory Drugs,” in *Inflammation: From Molecular and Cellular Mechanisms to the Clinic*, Wiley-VCH, 2017, pp. 1661–1690.
- [20] K. Shuai and B. Liu, “Regulation of JAK-STAT signalling in the immune system,” *Nat. Rev. Immunol.*, vol. 3, pp. 900–911, 2003.
- [21] V. Kumar, A. K. Abbas, and J. C. Aster, Eds., “Chapter 3. Inflammation and Repair,” in *Robbins Basic Pathology*, 10th ed., Philadelphia: Elsevier, 2018, pp. 57–96.
- [22] T. Liu, L. Zhang, D. Joo, and S. C. Sun, “NF-κB signaling in inflammation,” *Signal Transduct. Target. Ther.*, vol. 2, p. 17023, 2017.
- [23] C. N. Serhan and J. Z. Haeggström, “Lipid Mediators in Acute Inflammation and Resolution: Eicosanoids, PAF, Resolvins, and Protectins,” in *Fundamentals of Inflammation*, C. N. Serhan, D. W. Gilroy, and P. A. Ward, Eds. Cambridge: Cambridge University Press, 2010, pp. 153–174.
- [24] C. N. Serhan and J. Savill, “Resolution of inflammation: the beginning programs the end,” *Nat. Immunol.*, vol. 6, no. 12, pp. 1191–1197, 2005.
- [25] C. N. Serhan, “Resolution phase of inflammation: Novel endogenous anti-inflammatory and proresolving lipid mediators and pathways,” *Annu. Rev. Immunol.*, vol. 25, pp. 101–137,

- 2007.
- [26] C. Nathan and A. Ding, "Nonresolving Inflammation," *Cell*, vol. 140, no. 6, pp. P871-882, 2010.
 - [27] S. Ramamoorthy and J. A. Cidlowski, "Corticosteroids. Mechanisms of Action in Health and Disease," *Rheum. Dis. Clin. North Am.*, vol. 42, no. 1, pp. 15–31, 2016.
 - [28] D. W. Cain and J. A. Cidlowski, "Immune regulation by glucocorticoids," *Nat. Rev. Immunol.*, vol. 17, pp. 233–247, 2017.
 - [29] T. Rhen and J. A. Cidlowski, "Antiinflammatory action of glucocorticoids - New mechanisms for old drugs," *N. Engl. J. Med.*, vol. 353, pp. 1711–1723, 2005.
 - [30] J. Vandewalle, A. Luybaert, K. De Bosscher, and C. Libert, "Therapeutic Mechanisms of Glucocorticoids," *Trends Endocrinol. Metab.*, vol. 29, no. 1, pp. 42–54, 2018.
 - [31] P. J. Barnes, "Mechanisms and resistance in glucocorticoid control of inflammation," *J. Steroid Biochem. Mol. Biol.*, vol. 120, no. 2–3, pp. 76–85, 2010.
 - [32] P. J. Barnes and I. M. Adcock, "Glucocorticoid resistance in inflammatory diseases," *Lancet*, vol. 373, no. 9678, pp. P1905-1917, 2009.
 - [33] G. García-Rayado, M. Navarro, and A. Lanás, "NSAID induced gastrointestinal damage and designing GI-sparing NSAIDs," *Expert Rev. Clin. Pharmacol.*, vol. 11, no. 10, pp. 1031–1043, 2018.
 - [34] F. Díaz-González and F. Sánchez-Madrid, "NSAIDs: Learning new tricks from old drugs," *Eur. J. Immunol.*, vol. 45, no. 3, pp. 679–86, 2015.
 - [35] D. L. Simmons, R. M. Botting, and T. Hla, "Cyclooxygenase isozymes: The biology of prostaglandin synthesis and inhibition," *Pharmacol. Rev.*, vol. 56, no. 3, pp. 387–437, 2004.
 - [36] N. Osafo, C. Agyare, D. D. Obiri, and A. O. Antwi, "Mechanism of Action of Nonsteroidal Anti-Inflammatory Drugs," in *Nonsteroidal Anti-Inflammatory Drugs*, InTech, 2017, p. 13.
 - [37] N. V. Chandrasekharan *et al.*, "COX-3, a cyclooxygenase-1 variant inhibited by acetaminophen and other analgesic/antipyretic drugs: Cloning, structure, and expression," *Proc. Natl. Acad. Sci. U. S. A.*, vol. 99, no. 21, pp. 13926–13931, 2002.
 - [38] B. Kis, J. A. Snipes, and D. W. Busija, "Acetaminophen and the cyclooxygenase-3 puzzle: Sorting out facts, fictions, and uncertainties," *J. Pharmacol. Exp. Ther.*, vol. 315, no. 1, pp. 1–7, 2005.
 - [39] W. L. Smith, D. L. DeWitt, and R. M. Garavito, "Cyclooxygenases: Structural, Cellular, and

- Molecular Biology," *Annu. Rev. Biochem.*, vol. 69, pp. 145–182, 2000.
- [40] R. G. Kurumbail *et al.*, "Structural basis for selective inhibition of cyclooxygenase-2 by anti-inflammatory agents," *Nature*, vol. 384, no. 6610, pp. 644–648, 1996.
 - [41] L. J. Crofford, "Biology and Therapeutic Targeting of Prostanoids," in *Kelley and Firestein's Textbook of Rheumatology*, 10th ed., Philadelphia: Elsevier, 2017, pp. 908–931.
 - [42] P. N. Praveen Rao and E. E. Knaus, "Evolution of nonsteroidal anti-inflammatory drugs (NSAIDs): Cyclooxygenase (COX) inhibition and beyond," *J. Pharm. Pharm. Sci.*, vol. 11, no. 2, pp. 81s–110s, 2008.
 - [43] K. Brune and P. Patrignani, "New insights into the use of currently available non-steroidal anti-inflammatory drugs," *J. Pain Res.*, vol. 8, pp. 105–118, 2015.
 - [44] D. Mukherjee, S. E. Nissen, and E. J. Topol, "Risk of cardiovascular events associated with selective COX-2 inhibitors," *J. Am. Med. Assoc.*, vol. 286, no. 8, pp. 954–959, 2001.
 - [45] D. H. Solomon *et al.*, "Relationship between Selective Cyclooxygenase-2 Inhibitors and Acute Myocardial Infarction in Older Adults," *Circulation*, vol. 109, no. 17, pp. 2068–2073, 2004.
 - [46] R. S. Bresalier *et al.*, "Cardiovascular events associated with rofecoxib in a colorectal adenoma chemoprevention trial," *N. Engl. J. Med.*, vol. 352, pp. 1092–1102, 2005.
 - [47] L. A. García Rodríguez, S. Tacconelli, and P. Patrignani, "Role of Dose Potency in the Prediction of Risk of Myocardial Infarction Associated With Nonsteroidal Anti-Inflammatory Drugs in the General Population," *J. Am. Coll. Cardiol.*, vol. 52, no. 20, pp. 1628–36, 2008.
 - [48] C. Baigent *et al.*, "Vascular and upper gastrointestinal effects of non-steroidal anti-inflammatory drugs: Meta-analyses of individual participant data from randomised trials," *Lancet*, vol. 382, no. 9894, pp. P769–779, 2013.
 - [49] J. W. Atchison, C. M. Herndon, and E. Rusie, "NSAIDs for musculoskeletal pain management: current perspectives and novel strategies to improve safety," *J. Manag. Care Pharm.*, vol. 19, no. 9 Suppl A, pp. S3–19, 2013.
 - [50] D. G. Lambert, "Disease-modifying antirheumatic drugs," *Anaesth. Intensive Care Med.*, vol. 13, no. 3, pp. 128–130, 2012.
 - [51] I. Padjen, "Drugs Used in Rheumatic Disease," in *Handbook of Systemic Autoimmune Diseases*, vol. 15, Elsevier, 2018, pp. 39–76.
 - [52] A. C. Cannella, "Traditional DMARDs: Methotrexate, Leflunomide, Sulfasalazine, Hydroxychloroquine, and Combination Therapies," in *Kelley and Firestein's Textbook of*

Rheumatology, 10th ed., Philadelphia: Elsevier, 2017, pp. 958-982.e7.

- [53] T. Yoshimoto and T. Yoshimoto, *Cytokine frontiers: Regulation of immune responses in health and disease*. Springer, 2014.
- [54] T. Takeuchi, J. S. Smolen, E. H. Choy, D. Aletaha, I. McInnes, and S. A. Jones, "Considering new lessons about the use of IL-6 inhibitors in arthritis," *Considerations Med.*, vol. 2, no. 1, 2018.
- [55] A. Ogata *et al.*, "Phase III study of the efficacy and safety of subcutaneous versus intravenous tocilizumab monotherapy in patients with rheumatoid arthritis," *Arthritis Care Res.*, vol. 66, no. 3, pp. 344–354, 2014.
- [56] Y. Yoshida and T. Tanaka, "Interleukin 6 and rheumatoid arthritis," *Biomed Res. Int.*, vol. 2014, p. 698313, 2014.
- [57] P. Rider, Y. Carmi, and I. Cohen, "Biologics for Targeting Inflammatory Cytokines, Clinical Uses, and Limitations," *Int. J. Cell Biol.*, vol. 2016, p. 9259646, 2016.
- [58] C. Ross *et al.*, "Principles of nanoparticle design for overcoming biological barriers to drug delivery," *Nat. Biotechnol.*, vol. 33, no. 9, pp. 1–8, 2015.
- [59] S. Parveen, R. Misra, and S. K. Sahoo, "Nanoparticles: A boon to drug delivery, therapeutics, diagnostics and imaging," *Nanomedicine Nanotechnology, Biol. Med.*, vol. 8, no. 2, pp. 147–166, 2012.
- [60] U. Bulbake, S. Doppalapudi, N. Kommineni, and W. Khan, "Liposomal formulations in clinical use: An updated review," *Pharmaceutics*, vol. 9, no. 2, p. 12, 2017.
- [61] U. Kedar, P. Phutane, S. Shidhaye, and V. Kadam, "Advances in polymeric micelles for drug delivery and tumor targeting," *Nanomedicine Nanotechnology, Biol. Med.*, vol. 6, no. 6, pp. 714–729, 2010.
- [62] W. Cui, Y. Zhou, and J. Chang, "Electrospun nanofibrous materials for tissue engineering and drug delivery," *Sci. Technol. Adv. Mater.*, vol. 11, no. 1, p. 014108, 2010.
- [63] G. W. Ashley, J. Henise, R. Reid, and D. V. Santi, "Hydrogel drug delivery system with predictable and tunable drug release and degradation rates," *Proc. Natl. Acad. Sci. U. S. A.*, vol. 110, no. 6, pp. 2318–2323, 2013.
- [64] M. R. Prausnitz and R. Langer, "Transdermal drug delivery," *Nat. Biotechnol.*, vol. 26, no. 11, pp. 1261–1268, 2008.
- [65] Q. Jiang *et al.*, "Erythrocyte-cancer hybrid membrane-camouflaged melanin nanoparticles for enhancing photothermal therapy efficacy in tumors," *Biomaterials*, vol. 192, no. 2019,

- pp. 292–308, 2019.
- [66] B. S. Pattni, V. V. Chupin, and V. P. Torchilin, “New Developments in Liposomal Drug Delivery,” *Chem. Rev.*, vol. 115, no. 19, pp. 10938–10966, 2015.
 - [67] A. D. Bangham, M. M. Standish, and J. C. Watkins, “Diffusion of univalent ions across the lamellae of swollen phospholipids,” *J. Mol. Biol.*, vol. 13, no. 1, pp. 238–252, 1965.
 - [68] G. Sessa and G. Weissmann, “Incorporation of lysozyme into liposomes. A model for structure-linked latency,” *J. Biol. Chem.*, vol. 245, no. 13, pp. 3295–3301, 1970.
 - [69] K. Gardikis, C. Tsimplouli, K. Dimas, M. Micha-Screttas, and C. Demetzos, “New chimeric advanced Drug Delivery nano Systems (chi-aDDnSs) as doxorubicin carriers,” *Int. J. Pharm.*, vol. 402, no. 1–2, pp. 231–237, 2010.
 - [70] J. A. Silverman and S. R. Deitcher, “Marqibo® (vincristine sulfate liposome injection) improves the pharmacokinetics and pharmacodynamics of vincristine,” *Cancer Chemother. Pharmacol.*, vol. 71, no. 3, pp. 555–564, 2013.
 - [71] V. Usonis and V. Bakasénas, “Antibody titres after primary and booster vaccination of infants and young children with a virosomal hepatitis A vaccine (Epaxal®),” *Vaccine*, vol. 21, no. 31, pp. 4588–4592, 2003.
 - [72] A. Iacono *et al.*, “A randomised single-centre trial of inhaled liposomal cyclosporine for bronchiolitis obliterans syndrome post-lung transplantation,” *ERJ Open Res.*, vol. 5, no. 4, pp. 167–2019, 2019.
 - [73] E. C. Tampaki and A. Tampakis, “Efficacy and Safety of Neoadjuvant Treatment with Bevacizumab, Liposomal Doxorubicin, Cyclophosphamide and Paclitaxel Combination in Locally/Regionally Advanced, HER2-Negative, Grade III at Premenopausal Status Breast Cancer: A Phase II Study,” *Clin. Drug Investig.*, vol. 38, no. 7, pp. 639–648, 2018.
 - [74] R. A. Demel and B. De Kruffy, “The function of sterols in membranes,” *Biochim. Biophys. Acta*, vol. 457, no. 2, pp. 109–32, 1976.
 - [75] D. Papahadjopoulos, K. Jacobson, S. Nir, and I. Isac, “Phase transitions in phospholipid vesicles Fluorescence polarization and permeability measurements concerning the effect of temperature and cholesterol,” *BBA - Biomembr.*, vol. 311, no. 3, pp. 330–348, 1973.
 - [76] J. W. Virden and J. C. Berg, “NaCl-induced Aggregation of Dipalmitoylphosphatidylglycerol Small Unilamellar Vesicles with Varying Amounts of Incorporated Cholesterol,” *Langmuir*, vol. 8, no. 6, pp. 1532–1537, 1992.
 - [77] A. R. Mohammed, N. Weston, A. G. A. Coombes, M. Fitzgerald, and Y. Perrie, “Liposome

- formulation of poorly water soluble drugs: Optimisation of drug loading and ESEM analysis of stability," *Int. J. Pharm.*, vol. 258, no. 1–2, pp. 23–34, 2004.
- [78] A. Akbarzadeh *et al.*, "Liposome: classification, preparation, and applications," *Nanoscale Res. Lett.*, vol. 8, no. 1, p. 102, 2013.
- [79] J. N. Israelachvili, S. Marcelja, R. G. Horn, and J. N. Israelachvili, "Physical principles of membrane organization," *Q. Rev. Biophys.*, vol. 13, no. 2, pp. 121–200, 1980.
- [80] G. Bozzuto and A. Molinari, "Liposomes as nanomedical devices," *Int. J. Nanomedicine*, vol. 10, pp. 975–999, 2015.
- [81] S. Emami, S. Azadmard-Damirchi, S. H. Peighambaroust, H. Valizadeh, and J. Hesari, "Liposomes as carrier vehicles for functional compounds in food sector," *J. Exp. Nanosci.*, vol. 11, no. 9, pp. 737–759, 2016.
- [82] R. Nisini, N. Poerio, S. Mariotti, F. De Santis, and M. Fraziano, "The Multirole of Liposomes in Therapy and Prevention of Infectious Diseases," *Front. Immunol.*, vol. 9, p. 155, 2018.
- [83] K. Maruyama, T. Yuda, A. Okamoto, S. Kojima, A. Suganaka, and M. Iwatsuru, "Prolonged circulation time in vivo of large unilamellar liposomes composed of distearoyl phosphatidylcholine and cholesterol containing amphipathic poly(ethylene glycol)," *Biochim. Biophys. Acta*, vol. 1128, no. 1, pp. 44–49, 1992.
- [84] A. L. Klibanov, K. Maruyama, V. P. Torchilin, and L. Huang, "Amphipathic polyethyleneglycols effectively prolong the circulation time of liposomes," *FEBS Lett.*, vol. 268, no. 1, pp. 235–237, 1990.
- [85] M. I. Papisov, "Theoretical considerations of RES-avoiding liposomes: Molecular mechanics and chemistry of liposome interactions," *Adv. Drug Deliv. Rev.*, vol. 32, no. 1–2, pp. 119–138, 1998.
- [86] M. L. Immordino, F. Dosio, and L. Cattel, "Stealth liposomes: Review of the basic science, rationale, and clinical applications, existing and potential," *Int. J. Nanomedicine*, vol. 1, no. 3, pp. 297–315, 2006.
- [87] H. Hatakeyama, H. Akita, and H. Harashima, "The Polyethyleneglycol Dilemma: Advantage and Disadvantage of PEGylation of Liposomes for Systemic Genes and Nucleic Acids Delivery to Tumors," *Biol. Pharm. Bull.*, vol. 36, no. 6, pp. 892–899, 2013.
- [88] A. D. Tagalakakis *et al.*, "PEGylation improves the receptor-mediated transfection efficiency of peptide-targeted, self-assembling, anionic nanocomplexes," *J. Control. Release*, vol. 174, pp. 177–187, 2014.

- [89] H. Xu *et al.*, "Influence of phospholipid types and animal models on the accelerated blood clearance phenomenon of PEGylated liposomes upon repeated injection," *Drug Deliv.*, vol. 22, no. 5, pp. 598–607, 2015.
- [90] P. H. Kierstead *et al.*, "The effect of polymer backbone chemistry on the induction of the accelerated blood clearance in polymer modified liposomes," *J. Control. Release*, vol. 213, pp. 1–9, 2015.
- [91] P. S. Low, W. A. Henne, and D. D. Doorneweerd, "Discovery and development of folic-acid-based receptor targeting for imaging and therapy of cancer and inflammatory diseases," *Acc. Chem. Res.*, vol. 41, no. 1, pp. 120–9, 2008.
- [92] A. C. Lima, H. Ferreira, R. L. Reis, and N. M. Neves, "Biodegradable polymers: an update on drug delivery in bone and cartilage diseases," *Expert Opin. Drug Deliv.*, vol. 16, no. 8, pp. 795–813, 2019.
- [93] A. V. Kroll, R. H. Fang, and L. Zhang, "Biointerfacing and applications of cell membrane-coated nanoparticles," *Bioconjug. Chem.*, vol. 28, no. 1, pp. 23–32, 2017.
- [94] B. T. Luk and L. Zhang, "Cell membrane-camouflaged nanoparticles for drug delivery," *J. Control. Release*, vol. 220, no. Pt B, pp. 600–607, 2015.
- [95] P. Zhang, G. Liu, and X. Chen, "Nanobiotechnology: Cell membrane-based delivery systems," *Nano Today*, vol. 13, pp. 7–9, 2017.
- [96] H. A. Cole, M. Yuasa, G. Hawley, J. M. M. Cates, J. S. Nyman, and J. G. Schoenecker, "Differential development of the distal and proximal femoral epiphysis and physis in mice," *Bone*, vol. 52, no. 1, pp. 337–346, 2013.
- [97] C. M. J. Hu *et al.*, "Nanoparticle biointerfacing by platelet membrane cloaking," *Nature*, vol. 526, pp. 118–121, 2015.
- [98] M. Magnani and L. Rossi, "Approaches to erythrocyte-mediated drug delivery," *Expert Opin. Drug Deliv.*, vol. 11, no. 5, pp. 677–687, 2014.
- [99] R. H. Fang *et al.*, "Cancer cell membrane-coated nanoparticles for anticancer vaccination and drug delivery," *Nano Lett.*, vol. 14, no. 4, pp. 2181–2188, 2014.
- [100] C. Gao, Z. Lin, B. Jurado-Sánchez, X. Lin, Z. Wu, and Q. He, "Stem Cell Membrane-Coated Nanogels for Highly Efficient In Vivo Tumor Targeted Drug Delivery," *Small*, vol. 12, no. 30, pp. 4056–4062, 2016.
- [101] A. Parodi *et al.*, "Biomimetic functionalization with leukocyte membranes imparts cell like functions to synthetic particles," *Nat. Nanotechnol.*, vol. 8, no. 1, pp. 61–68, 2013.

- [102] W. Gao *et al.*, "Modulating antibacterial immunity via bacterial membrane-coated nanoparticles," *Nano Lett.*, vol. 15, no. 2, pp. 1403–1409, 2015.
- [103] C. M. J. Hu, L. Zhang, S. Aryal, C. Cheung, R. H. Fang, and L. Zhang, "Erythrocyte membrane-camouflaged polymeric nanoparticles as a biomimetic delivery platform," *Proc. Natl. Acad. Sci. U. S. A.*, vol. 108, no. 27, pp. 10980–10985, 2011.
- [104] Y. Su, Z. Xie, G. B. Kim, C. Dong, and J. Yang, "Design Strategies and Applications of Circulating Cell-Mediated Drug Delivery Systems," *ACS Biomater. Sci. Eng.*, vol. 1, no. 4, pp. 201–217, 2015.
- [105] V. Agrahari, V. Agrahari, and A. K. Mitra, "Next generation drug delivery: circulatory cells-mediated nanotherapeutic approaches," *Expert Opin. Drug Deliv.*, vol. 14, no. 3, pp. 285–289, 2017.
- [106] G. M. Ihler, R. H. Glew, and F. W. Schnure, "Enzyme loading of erythrocytes," *Proc. Natl. Acad. Sci. U. S. A.*, vol. 70, no. 9, pp. 2663–2666, 1973.
- [107] R. A. Cooper, "Lipids of human red cell membrane: normal composition and variability in disease.," *Semin. Hematol.*, vol. 7, no. 3, pp. 296–322, 1970.
- [108] V. R. Muzykantov, "Drug delivery by red blood cells: Vascular carriers designed by mother nature," *Expert Opin. Drug Deliv.*, vol. 7, no. 4, pp. 403–427, 2010.
- [109] P. A. Oldenburg, A. Zheleznyak, Y. F. Fang, C. F. Lagenaur, H. D. Gresham, and F. P. Lindberg, "Role of CD47 as a marker of self on red blood cells," *Science (80-.).*, vol. 288, no. 5473, pp. 2051–2054, 2000.
- [110] M. Hamidi, A. Zarrin, M. Foroozesh, and S. Mohammadi-Samani, "Applications of carrier erythrocytes in delivery of biopharmaceuticals," *J. Control. Release*, vol. 118, no. 2, pp. 145–160, 2007.
- [111] S. Biagiotti, M. F. Paoletti, A. Fraternale, L. Rossi, and M. Magnani, "Drug delivery by red blood cells," *IUBMB Life*, vol. 63, no. 8, pp. 621–631, 2011.
- [112] S. Sarkar, M. A. Alam, J. Shaw, and A. K. Dasgupta, "Drug delivery using platelet cancer cell interaction," *Pharm. Res.*, vol. 30, no. 11, pp. 2785–2794, 2013.
- [113] W. O. Kwant and P. Seeman, "The erythrocyte ghost is a perfect osmometer," *J. Gen. Physiol.*, vol. 55, no. 2, pp. 208–219, 1970.
- [114] Q. Dong and W. Jin, "Monitoring diclofenac sodium in single human erythrocytes introduced by electroporation using capillary zone electrophoresis with electrochemical detection," *Electrophoresis*, vol. 22, no. 13, pp. 2786–2792, 2001.

- [115] X. Zhang, M. Qiu, P. Guo, Y. Lian, E. Xu, and J. Su, "Autologous red blood cell delivery of betamethasone phosphate sodium for long anti-inflammation," *Pharmaceutics*, vol. 10, no. 4, p. 286, 2018.
- [116] V. Agrawal, J. Hee Woo, G. Borthakur, H. Kantarjian, and A. E. Frankel, "Red Blood Cell-Encapsulated L-Asparaginase: Potential Therapy of Patients with Asparagine Synthetase Deficient Acute Myeloid Leukemia," *Protein Pept. Lett.*, vol. 20, no. 4, pp. 392–402, 2013.
- [117] L. A. Lotero, G. Olmos, and J. C. Diez, "Delivery to macrophages and toxic action of etoposide carried in mouse red blood cells," *Biochim. Biophys. Acta - Gen. Subj.*, vol. 1620, no. 1–3, pp. 160–166, 2003.
- [118] G. E. din I. Harisa, M. F. Ibrahim, and F. K. Alanazi, "Characterization of human erythrocytes as potential carrier for pravastatin: An in vitro study," *Int. J. Med. Sci.*, vol. 8, no. 3, pp. 222–230, 2011.
- [119] A. C. Anselmo *et al.*, "Delivering nanoparticles to lungs while avoiding liver and spleen through adsorption on red blood cells," *ACS Nano*, vol. 7, no. 12, pp. 11129–11137, 2013.
- [120] K. A. Nangare, S. D. Powar, and S. A. Payghan, "Nanoerythrocytes: Engineered erythrocytes as a novel carrier for the targeted drug delivery," *Asian J. Pharm.*, vol. 10, no. 3, pp. S223-233, 2016.
- [121] X. Dong *et al.*, "Formulation and Drug Loading Features of Nano-Erythrocytes," *Nanoscale Res. Lett.*, vol. 12, no. 1, p. 202, Dec. 2017.
- [122] B. T. Luk *et al.*, "Safe and immunocompatible nanocarriers cloaked in RBC membranes for drug delivery to treat solid tumors," *Theranostics*, vol. 6, no. 7, pp. 1004–1011, 2016.
- [123] X. Han *et al.*, "Red blood cell-derived nanoerythrocyte for antigen delivery with enhanced cancer immunotherapy," *Sci. Adv.*, vol. 5, no. 10, p. eaaw6870, 2019.
- [124] P. Münzer *et al.*, "Acid sphingomyelinase regulates platelet cell membrane scrambling, secretion, and thrombus formation," *Arterioscler. Thromb. Vasc. Biol.*, vol. 34, pp. 61–71, 2014.
- [125] T. Li, H. Dong, C. Zhang, and R. Mo, "Cell-based drug delivery systems for biomedical applications," *Nano Res.*, vol. 11, no. 10, pp. 5240–5257, 2018.
- [126] P. Xu, R. Wang, X. Wang, and J. Ouyang, "Recent advancements in erythrocytes, platelets, and albumin as delivery systems," *Onco. Targets. Ther.*, vol. 9, pp. 2873–2884, 2016.
- [127] A. K. Tsun Wong, "Platelet biology: The role of shear," *Expert Rev. Hematol.*, vol. 6, no. 2, pp. 205–212, 2013.

- [128] T. G. Walsh, P. Metharom, and M. C. Berndt, "The functional role of platelets in the regulation of angiogenesis," *Platelets*, vol. 26, no. 3, 2015.
- [129] P. Xu *et al.*, "Doxorubicin-loaded platelets as a smart drug delivery system: An improved therapy for lymphoma," *Sci. Rep.*, vol. 7, p. 42632, 2017.
- [130] L. Dai, N. Gu, B. A. Chen, and G. Marriott, "Human platelets repurposed as vehicles for in vivo imaging of myeloma xenotransplants," *Oncotarget*, vol. 7, no. 16, pp. 21076–21090, 2016.
- [131] Y. Shamay *et al.*, "P-selectin is a nanotherapeutic delivery target in the tumor microenvironment," *Sci. Transl. Med.*, vol. 8, no. 345, p. 345ra87, 2016.
- [132] C. F. Greineder, M. D. Howard, R. Carnemolla, D. B. Cines, and V. R. Muzykantov, "Advanced drug delivery systems for antithrombotic agents," *Blood*, vol. 122, no. 9, pp. 1565–1575, 2013.
- [133] H. Chen, W. Mo, H. Su, Y. Zhang, and H. Song, "Characterization of a novel bifunctional mutant of staphylokinase with platelet-targeted thrombolysis and antiplatelet aggregation activities," *BMC Mol. Biol.*, vol. 8, p. 88, 2007.
- [134] Z. Wang, J. Li, J. Cho, and A. B. Malik, "Prevention of vascular inflammation by nanoparticle targeting of adherent neutrophils," *Nat. Nanotechnol.*, vol. 9, pp. 204–210, 2014.
- [135] F. Sallusto and M. Baggiolini, "Chemokines and leukocyte traffic," *Nat. Immunol.*, vol. 392, no. 6676, pp. 565–568, 2008.
- [136] T. A. Springer, "Traffic signals for lymphocyte recirculation and leukocyte emigration: The multistep paradigm," *Cell*, vol. 76, no. 2, pp. 301–314, 1994.
- [137] A. Narain, S. Asawa, V. Chhabria, and Y. Patil-Sen, "Cell membrane coated nanoparticles: Next-generation therapeutics," *Nanomedicine*, vol. 76, no. 2, pp. 301–314, 2017.
- [138] Y. Sun *et al.*, "Advances of blood cell-based drug delivery systems," *Eur. J. Pharm. Sci.*, vol. 96, pp. 115–128, 2017.
- [139] A. Parodi *et al.*, "Synthetic nanoparticles functionalized with biomimetic leukocyte membranes possess cell-like functions," *Nat. Nanotechnol.*, vol. 8, pp. 61–68, 2013.
- [140] N. Doshi *et al.*, "Cell-based drug delivery devices using phagocytosis-resistant backpacks," *Adv. Mater.*, vol. 23, no. 12, pp. H105-109, 2011.
- [141] F. C. Vasconcellos, A. J. Swiston, M. M. Beppu, R. E. Cohen, and M. F. Rubner, "Bioactive polyelectrolyte multilayers: Hyaluronic acid mediated B lymphocyte adhesion," *Biomacromolecules*, vol. 11, no. 9, pp. 2407–2414, 2010.

- [142] Y. Huang, X. Gao, and J. Chen, "Leukocyte-derived biomimetic nanoparticulate drug delivery systems for cancer therapy," *Acta Pharm. Sin. B*, vol. 8, no. 1, pp. 4–13, 2018.
- [143] S. E. Headland *et al.*, "Neutrophil-derived microvesicles enter cartilage and protect the joint in inflammatory arthritis," *Sci. Transl. Med.*, vol. 7, no. 315, p. 315ra190, 2015.
- [144] Q. Zhang *et al.*, "Neutrophil membrane-coated nanoparticles inhibit synovial inflammation and alleviate joint damage in inflammatory arthritis," *Nat. Nanotechnol.*, vol. 13, pp. 1182–1190, 2018.
- [145] M. Xuan, J. Shao, L. Dai, Q. He, and J. Li, "Macrophage Cell Membrane Camouflaged Mesoporous Silica Nanocapsules for In Vivo Cancer Therapy," *Adv. Healthc. Mater.*, vol. 4, no. 11, pp. 1645–1652, 2015.
- [146] M. Xuan, J. Shao, L. Dai, J. Li, and Q. He, "Macrophage Cell Membrane Camouflaged Au Nanoshells for in Vivo Prolonged Circulation Life and Enhanced Cancer Photothermal Therapy," *ACS Appl. Mater. Interfaces*, vol. 8, no. 15, pp. 9610–9618, 2016.
- [147] B. Huang, W. D. Abraham, Y. Zheng, S. C. Bustamante López, S. S. Luo, and D. J. Irvine, "Active targeting of chemotherapy to disseminated tumors using nanoparticle-carrying T cells," *Sci. Transl. Med.*, vol. 7, no. 291, p. 291ra94, 2015.
- [148] A. S. Nowacek *et al.*, "NanoART synthesis, characterization, uptake, release and toxicology for human monocyte-macrophage drug delivery," *Nanomedicine*, vol. 4, no. 8, pp. 903–917, 2009.
- [149] M. R. Choi *et al.*, "A cellular trojan horse for delivery of therapeutic nanoparticles into tumors," *Nano Lett.*, vol. 7, no. 12, pp. 3759–3765, 2007.
- [150] E. Kolaczkowska and P. Kubes, "Neutrophil recruitment and function in health and inflammation," *Nat. Rev. Immunol.*, vol. 13, pp. 159–175, 2013.
- [151] L. A. L. Fliervoet and E. Mastrobattista, "Drug delivery with living cells," *Adv. Drug Deliv. Rev.*, vol. 106, pp. 63–72, 2016.
- [152] S. Fox, A. G. Rossi, and S. S. Ayoub, "Macrophages," in *Fundamentals of Inflammation*, C. N. Serhan, P. A. Ward, and D. W. Gilroy, Eds. Cambridge: Cambridge University Press, 2010, pp. 96–106.
- [153] H. Dou *et al.*, "Macrophage Delivery of Nanoformulated Antiretroviral Drug to the Brain in a Murine Model of NeuroAIDS," *J. Immunol.*, vol. 183, no. 1, pp. 661–669, 2009.
- [154] H. Dou *et al.*, "Development of a macrophage-based nanoparticle platform for antiretroviral drug delivery," *Blood*, vol. 108, no. 8, pp. 2827–2835, 2006.

- [155] A. S. Nowacek *et al.*, "Analyses of nanoformulated antiretroviral drug charge, size, shape and content for uptake, drug release and antiviral activities in human monocyte-derived macrophages," *J. Control. Release*, vol. 150, no. 2, pp. 204–211, 2011.
- [156] A. C. Anselmo and S. Mitragotri, "Cell-mediated delivery of nanoparticles: Taking advantage of circulatory cells to target nanoparticles," *J. Control. Release*, vol. 190, pp. 531–541, 2014.
- [157] A. Wieczorek and L. Uharek, "Genetically modified T cells for the treatment of malignant disease," *Transfus. Med. Hemotherapy*, vol. 40, no. 6, pp. 388–402, 2013.
- [158] E. J. Kunkel and E. C. Butcher, "Chemokines and the tissue-specific migration of lymphocytes," *Immunity*, vol. 16, no. 1, pp. 1–4, 2002.
- [159] J. Ankrum and J. M. Karp, "Mesenchymal stem cell therapy: Two steps forward, one step back," *Trends Mol. Med.*, vol. 15, no. 3, pp. 203–209, 2010.
- [160] A. J. Wagers and I. L. Weissman, "Plasticity of adult stem cells," *Cell*, vol. 116, no. 5, pp. 639–648, 2004.
- [161] K. S. Aboody *et al.*, "Neural stem cells display extensive tropism for pathology in adult brain: Evidence from intracranial gliomas," *Proc. Natl. Acad. Sci. U. S. A.*, vol. 97, no. 23, pp. 12846–12851, 2000.
- [162] K. I. Park, B. T. Himes, P. E. Stieg, A. Tessler, I. Fischer, and E. Y. Snyder, "Neural stem cells may be uniquely suited for combined gene therapy and cell replacement: Evidence from engraftment of Neurotrophin-3-expressing stem cells in hypoxic-ischemic brain injury," *Exp. Neurol.*, vol. 199, no. 1, pp. 179–190, 2006.
- [163] M. Alieva *et al.*, "Glioblastoma therapy with cytotoxic mesenchymal stromal cells optimized by bioluminescence imaging of tumor and therapeutic cell response," *PLoS One*, vol. 7, no. 4, p. e35148, 2012.
- [164] J. R. Bagó, K. T. Sheets, and S. D. Hingtgen, "Neural stem cell therapy for cancer," *Methods*, vol. 99, pp. 37–43, 2016.
- [165] M. F. Corsten and K. Shah, "Therapeutic stem-cells for cancer treatment: hopes and hurdles in tactical warfare," *Lancet Oncol.*, vol. 9, no. 4, pp. 376–384, 2008.
- [166] L. Elzaouk, K. Moelling, and J. Pavlovic, "Anti-tumor activity of mesenchymal stem cells producing IL-12 in a mouse melanoma model," *Exp. Dermatol.*, vol. 15, no. 11, pp. 865–874, 2006.
- [167] O. Levy *et al.*, "MRNA-engineered mesenchymal stem cells for targeted delivery of

- interleukin-10 to sites of inflammation," *Blood*, vol. 122, no. 14, pp. e23-32, 2013.
- [168] D. W. Stuckey and K. Shah, "Stem cell-based therapies for cancer treatment: Separating hope from hype," *Nat. Rev. Cancer*, vol. 14, no. 10, pp. 683–691, 2014.
- [169] B. Ljubic *et al.*, "Human mesenchymal stem cells creating an immunosuppressive environment and promote breast cancer in mice," *Sci. Rep.*, vol. 3, p. 2298, 2013.
- [170] A. E. Karnoub *et al.*, "Mesenchymal stem cells within tumour stroma promote breast cancer metastasis," *Nature*, vol. 449, no. 7162, pp. 557–563, 2007.
- [171] G. V. Røslund *et al.*, "Long-term cultures of bone marrow-derived human mesenchymal stem cells frequently undergo spontaneous malignant transformation," *Cancer Res.*, vol. 69, no. 13, pp. 5331–5339, 2009.
- [172] S. Tan, T. Wu, D. Zhang, and Z. Zhang, "Cell or cell membrane-based drug delivery systems," *Theranostics*, vol. 5, no. 8, pp. 863–881, 2015.
- [173] A. Dove, "Cell-based therapies go live," *Nat. Biotechnol.*, vol. 20, pp. 339–343, 2002.
- [174] G. Fritsma, "Erythrocyte Metabolism and Membrane Structure and Function," in *Rodak's Hematology: Clinical Principles and Applications*, 5th: Elsevier Inc, 2015, pp. 112–123.
- [175] B. S. B. P. C. Herrmann, "Morphology of the Erythron," in *Williams Hematology*, Eighth Edi., McGraw-Hill Professional, 2011.
- [176] E. Gorter and F. Grendel, "On bimolecular layers of lipoids on the chromocytes of the blood," *J. Exp. Med.*, vol. 41, no. 4, pp. 439–443, 1925.
- [177] N. Mohandas and E. Evans, "Mechanical properties of the red cell membrane in relation to molecular structure and genetic defects," *Annu. Rev. Biophys. Biomol. Struct.*, vol. 23, pp. 787–818, 1994.
- [178] S. J. Singer and G. L. Nicolson, "The fluid mosaic model of the structure of cell membranes," *Science (80-)*, vol. 175, no. 4023, pp. 720–731, 1972.
- [179] R. A. Cooper, "Influence of increased membrane cholesterol on membrane fluidity and cell function in human red blood cells," *J. Supramol. Cell. Biochem.*, vol. 8, no. 4, pp. 413–430, 1978.
- [180] A. J. Verkleij, R. F. A. Zwaal, B. Roelofsen, P. Comfurius, D. Kastelijn, and L. L. M. van Deenen, "The asymmetric distribution of phospholipids in the human red cell membrane. A combined study using phospholipases and freeze-etch electron microscopy," *BBA - Biomembr.*, vol. 323, no. 2, pp. 178–193, 1973.
- [181] R. F. A. Zwaal and A. J. Schroit, "Pathophysiologic implications of membrane phospholipid

- asymmetry in blood cells," *Blood*, vol. 89, no. 4, pp. 1121–1132, 1997.
- [182] Q. Zhou, J. Zhao, J. G. Stout, R. A. Luhm, P. J. Sims, and T. Wiedmer, "Molecular cloning of erythrocyte membrane phospholipid scramblase," *FASEB J.*, vol. 272, no. 29, pp. 18240–18244, 1997.
- [183] B. N. Yamaja Setty, S. Kulkarni, and M. J. Stuart, "Role of erythrocyte phosphatidylserine in sickle red cell-endothelial adhesion," *Blood*, vol. 99, no. 5, pp. 1564–1571, 2002.
- [184] K. D. Stark, M. E. Van Elswyk, M. R. Higgins, C. A. Weatherford, and N. Salem, "Global survey of the omega-3 fatty acids, docosahexaenoic acid and eicosapentaenoic acid in the blood stream of healthy adults," *Prog. Lipid Res.*, vol. 63, pp. 132–152, 2016.
- [185] D. S. Siscovick, "Dietary intake and cell membrane levels of long-chain n-3 polyunsaturated fatty acids and the risk of primary cardiac arrest," *JAMA J. Am. Med. Assoc.*, vol. 274, no. 17, pp. 1363–1367, 2003.
- [186] C. M. Albert *et al.*, "Blood Levels of Long-Chain n-3 Fatty Acids and the Risk of Sudden Death," *N. Engl. J. Med.*, vol. 346, no. 15, pp. 1113–1118, 2002.
- [187] R. N. Lemaitre, I. B. King, D. Mozaffarian, L. H. Kuller, R. P. Tracy, and D. S. Siscovick, "n-3 polyunsaturated fatty acids, fatal ischemic heart disease, and nonfatal myocardial infarction in older adults: The Cardiovascular Health Study," *Am. J. Clin. Nutr.*, vol. 77, no. 2, pp. 319–25, 2003.
- [188] M. Madjid and O. Fatemi, "Components of the complete blood count as risk predictors for coronary heart disease: In-depth review and update," *Texas Hear. Inst. J.*, vol. 40, no. 1, pp. 17–29, 2013.
- [189] P. C. Calder, "n-3 fatty acids, inflammation, and immunity - Relevance to postsurgical and critically ill patients," *Lipids*, vol. 39, no. 12, pp. 1147–1161, 2004.
- [190] T. L. Steck, "The organization of proteins in the human red blood cell membrane: A review," *J. Cell Biol.*, vol. 62, no. 1, pp. 1–19, 1974.
- [191] M. E. Reid and N. Mohandas, "Red Blood Cell Blood Group Antigens: Structure and Function," *Semin. Hematol.*, vol. 41, no. 2, pp. 93–117, 2004.
- [192] H. Furthmayr, "Glycophorins A, B, and C: A family of sialoglycoproteins. Isolation and preliminary characterization of trypsin derived peptides," *Prog. Clin. Biol. Res.*, vol. 9, no. 1, pp. 79–95, 1979.
- [193] D. W. Speicher and V. T. Marchesi, "Erythrocyte spectrin is comprised of many homologous triple helical segments," *Nature*, vol. 311, no. 5982, pp. 177–180, 1984.

- [194] H. Ferreira, M. Lúcio, J. L. F. C. Lima, C. Matos, and S. Reis, "Effects of diclofenac on EPC liposome membrane properties," *Anal. Bioanal. Chem.*, vol. 382, no. 5, pp. 1256–1264, 2005.
- [195] H. Ferreira, M. Lúcio, J. L. F. C. Lima, C. Matos, and S. Reis, "Interaction of clonixin with EPC liposomes used as membrane models," *J. Pharm. Sci.*, vol. 94, no. 6, pp. 1277–1287, 2005.
- [196] P. McGettigan and D. Henry, "Use of Non-Steroidal Anti-Inflammatory Drugs That Elevate Cardiovascular Risk: An Examination of Sales and Essential Medicines Lists in Low-, Middle-, and High-Income Countries," *PLoS Med.*, vol. 10, no. 2, p. e1001388, 2013.

CHAPTER II

Materials and Methods

CHAPTER II. Materials and Methods

In this chapter, the materials selected and the techniques that were used to produce and evaluate the efficacy of erythrocyte-based liposomes are discussed with enough detail to allow the future reproduction of this work. A brief description of each method is also included to facilitate the comprehension of the procedures performed.

2.1. Materials

Phosphatidylcholine (PC) from egg yolk, HEPES hemisodium salt ($C_8H_{18}N_2O_4S \cdot 0.5Na$, $\geq 99.5\%$), Fiske-subbarow reducer, perchloric acid ($HClO_4$, 70%), stearic acid ($C_{18}H_{36}O_2$, 95%), eicosapentaenoic acid ($C_{20}H_{38}O_2$, analytical standard), docosahexaenoic acid ($C_{22}H_{42}O_2$, $\geq 98\%$) and tricosanoic acid ($C_{23}H_{46}O_2$, $\geq 99\%$) were purchased from Sigma. N-hexane (C_6H_{14} , $\geq 97.0\%$) was purchased from VWR and potassium chloride (KCl) was purchased from JMGS. Human TNF- α DuoSet ELISA and Human IL-6 DuoSet ELISA were purchased from Citomed. Roswell Park Memorial Institute (RPMI)-1640 culture medium with 2 mM stable glutamine ($C_5H_{10}N_2O_3$) and 2 g/L sodium bicarbonate ($NaHCO_3$) was purchased from Alfacene. BD Vacutainer K2E (EDTA) 10 mL tubes were purchased from BD Diagnostics – PreAnalytical Systems, PD-10 desalting columns and all other reagents were purchased from Laborspirit.

2.1.1. Phosphatidylcholine from egg yolk

Phosphatidylcholines are not only an essential constituent of the human cellular membrane, but can also be found in chicken egg yolk, representing almost three quarters of the total phospholipids [1]. PC from egg yolk (Figure 2.3.) has a choline head group and glycerophosphoric acid linked to different fatty acids, including saturated (e.g. palmitic acid -16:0, and stearic acid -18:0), as well as unsaturated fatty acids (e.g. palmitoleic acid -16:1, oleic acid -18:1, linoleic acid -18:2 and arachidonic acid -20:4) [1].

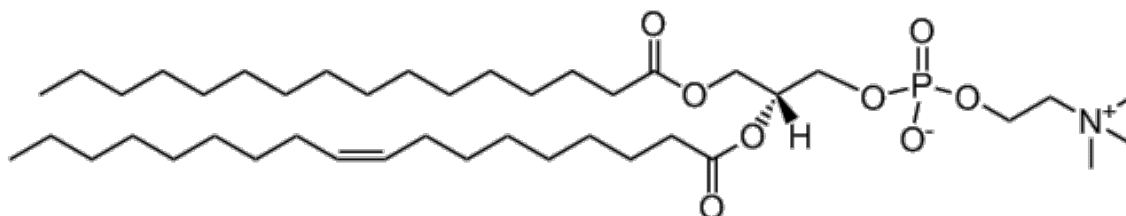


Figure 2.1. Chemical structure of phosphatidylcholine (16:0/18:1) from egg. Adapted from [1].

PC from egg yolk has been extensively used for the preparation of natural liposomes [2–3]. PC liposomes are well established as drug vehicles and some formulations are clinically used in

the treatment of different diseases, such as breast cancer or serious life-threatening fungal infections [2–3].

2.1.2. Erythrocytes

As discussed in Chapter 1, erythrocytes are cells of the circulatory system, with a biconcave disk shape and a mean diameter of 7-8 μm (Figure 2.1.) [4].

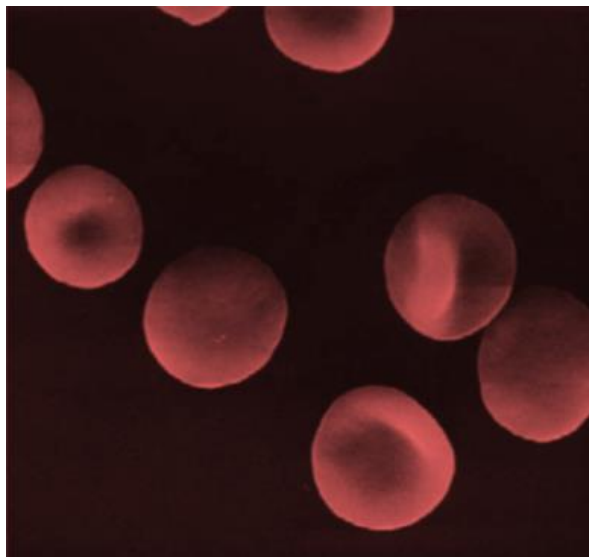


Figure 2.2. Scanning electron micrograph of erythrocytes (colored, $\times 2500$). Adapted from [5].

Erythrocytes mature in the red bone marrow and are produced at a rate of more than 2 million cells per second. They are the most abundant cellular constituent of the blood, circulating in the bloodstream up to 120 days [4, 6]. Their primary functions are to carry oxygen from the lungs to the tissues and carbon dioxide from the tissues to the lungs [4]. To perform these functions, erythrocytes need to be able to change their shape and squeeze through capillaries, which is enabled by their structural membrane, rich in phospholipids and cholesterol (Figure 2.2.a.) [6]. Phospholipids are formed by a three-carbon glycerol backbone with two fatty acid molecules attached to carbons 1 and 2, and a phosphate-containing group attached to the third carbon (Figure 2.2.b.) [6].

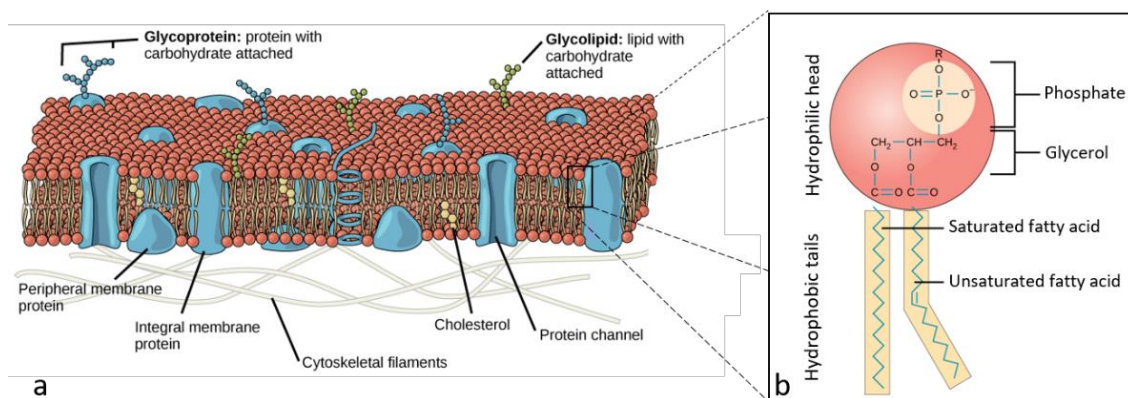


Figure 2.3. Model of the erythrocyte membrane (a) composed of phospholipids, cholesterol, proteins, and carbohydrates. Membrane phospholipids (b), composed of a hydrophilic head and two hydrophobic tails. The hydrophilic head consists of a phosphate group attached to a glycerol molecule. The hydrophobic tails are long hydrocarbon chains, each containing either a saturated or an unsaturated fatty acid. Adapted from [7].

In human red cells, phosphatidylcholine (PC), phosphatidylethanolamine (PE), sphingomyelin, and phosphatidylserine are predominant, being present in a percentage (w/w) approximately of 31%, 29%, 26% and 13%, respectively [6, 8]. Among the different phospholipids, some fatty acids are more common than others [9]. In human red cells, the fatty acid (16:0) is predominant, but there are also other fatty acids (18:0, 18:1, 18:2, and 20:4) that are present at almost the same levels (Table 2.1.) [9–10].

Table 2.1. Fatty acids occurrence (%) in the erythrocyte membrane lipids. Adapted from [6].

Fatty acids	Total lipids	Phosphatidyl- choline	Sphingo- myelin	Phosphatidyl- ethanolamine	Phosphatidyl- serine
16:0	21.8 ± 1.2	34.9 ± 0.8	26.2 ± 1.1	16.0 ± 0.5	3.8 ± 0.7
18:0	14.3 ± 0.4	12.2 ± 0.4	7.1 ± 0.5	8.7 ± 0.2	46.7 ± 2.8
18:1	13.4 ± 1.0	17.2 ± 0.6	2.4 ± 0.6	17.0 ± 0.8	8.5 ± 0.7
18:2	10.8 ± 1.0	22.6 ± 1.0	2.2 ± 0.8	6.6 ± 1.2	2.3 ± 0.2
20:4	12.0 ± 0.8	4.6 ± 0.6		16.4 ± 0.9	18.2 ± 0.7
20:5	1.5 ± 0.5	1.6 ± 0.4		3.0 ± 0.7	0.9 ± 0.4
22:0			7.0 ± 0.4		
22:4				3.4 ± 0.5	2.0 ± 0.3
22:5	2.8 ± 0.3		4.4 ± 0.5	3.8 ± 0.4	3.2 ± 0.4
22:6	7.2 ± 0.9	2.9 ± 0.4		9.5 ± 0.9	10.8 ± 0.9
24:0	4.9 ± 0.7		19.1 ± 0.8		
24:1	4.4 ± 0.9		26.6 ± 1.5		

16:0- Palmitic acid, 18:0 , Stearic acid, 18:1 , ω -9 oleic acid, 18:2 , ω -6 Linoleic acid, 20:4 , ω -6 Arachidonic acid, 20:5 , ω -3 Eicosapentaenoic acid, 22:0 , Behenic acid, 22:4 , ω -6 Docosatetraenoic acid, 22:5 , Docosapentaenoic acid, 22:6 , ω -3 Docosahexaenoic acid, 24:0 , Lignoceric acid, 24:1 , ω -9 Nervonic acid.

2.1.3. Diclofenac

Diclofenac was the drug selected to demonstrate the carrier ability of the liposomes prepared in this work.

Diclofenac is a NSAID of the phenylacetic acid class that is widely prescribed worldwide [11] due to its anti-inflammatory, analgesic, and antipyretic properties [12]. Diclofenac's structure contains a phenylacetic acid group and a phenyl ring with two chlorine atoms (Figure 2.4). This configuration results in a maximal twisting of the phenyl ring that confers a good fit to the substrate-binding pocket of the COX-2 enzyme (Figure 2.4) [13].

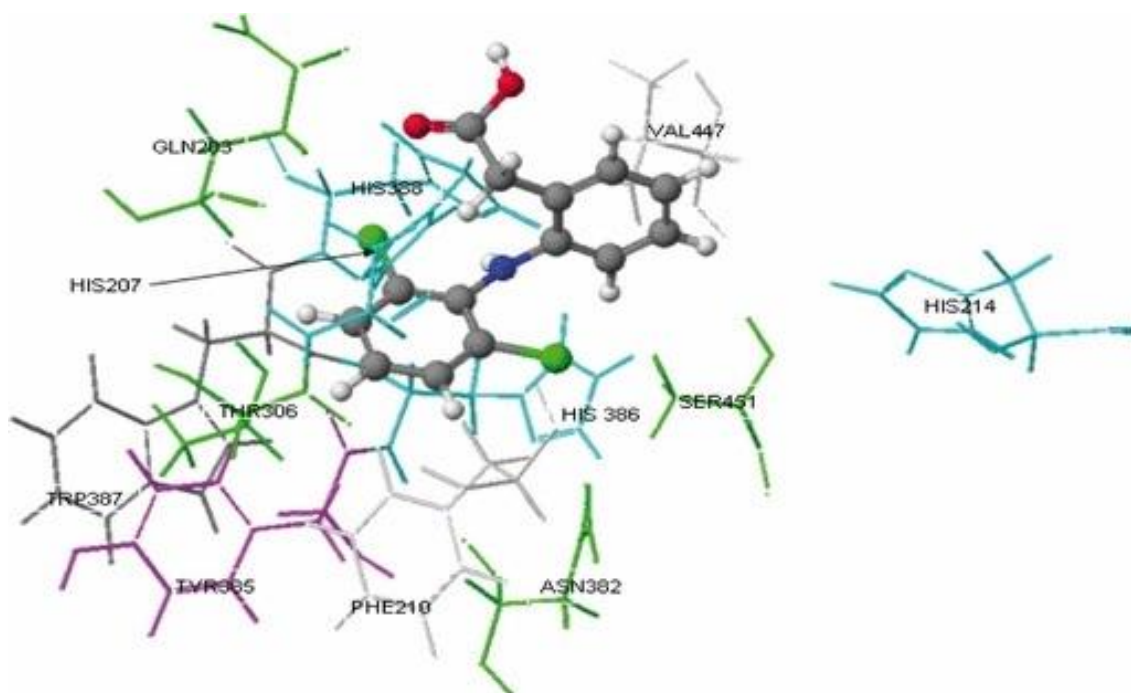


Figure 2.4. Chemical structure of diclofenac enclosed on COX-2 receptor. HIS - Histidine, VAL - Valine, THR - Threonine, SER - Serine, PHE -Phenylalanine. Adapted from [14].

The anti-inflammatory and analgesic efficacy of NSAIDs results from the inhibition of the enzymatic activity of COX-2, which convert arachidonic acid to prostaglandins (PGs) [15–16]. Conversely to the most traditional NSAIDs, diclofenac has a higher selectivity for COX-2 than for COX-1, being associated with a relatively lower level of gastrointestinal toxicity, compared with other non-specific NSAIDs [17]. Nevertheless, because of its short biological half-life (2 h) and fast elimination rate (1.2 ± 1.8 h), it is necessary to frequently administrate diclofenac to maintain therapeutic levels. This can contribute to increase the risk of adverse events, including severe dose-dependent gastrointestinal, cardiovascular, and renal side effects. Therefore, new strategies for the encapsulation of this drug are paramount.

2.1.4. Folic acid

Folic acid (FA; Figure 2.5), also known as folate or vitamin B9, is a vitamin of the B group that has been used as a targeting ligand for the specific delivery of imaging and therapeutic agents to activated macrophages [18–19].

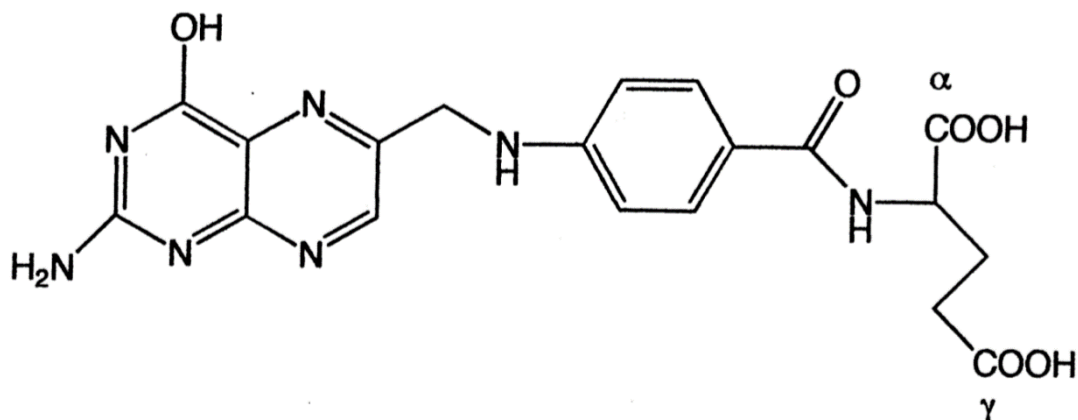


Figure 2.5. Chemical structure of FA, with α and γ carboxyl groups labelled. Adapted from [20].

FA present properties that make it an attractive ligand for use in drug targeting, namely (1) high affinity to its target, even after it's conjugation with delivery devices; (2) small size, which allows good tissue penetration; (3) availability; (4) low molecular weight; (5) easy conjugation chemistry; (6) lack of immunogenicity; (7) water solubility; and (8) stability in diverse solvents, pH and temperature [18–19]. Moreover, healthy cells have a very low or undetectable expression of FA receptors, while a high expression is observed on cancer cells and activated macrophages [18, 21]. Therefore, folate linked to a spacer, namely 1,2-distearoyl-sn-glycero-3-phosphoethanolamine-N-[folate(polyethylene glycol)-2000], was used to functionalize the erythrocyte-based liposomes to obtain a specific therapeutic action on activated macrophages.

2.2. Methods

2.2.1. Extraction of lipids from erythrocytes

The blood samples were collected in the CEF Taipás Saúde using BD Vacutainer K2E (EDTA) 10 mL tubes, after donor consentment.

The lipid extraction was done as previously described [22] on the same day of blood collection. Briefly, the fresh blood was centrifuged at 3000×g for 5 min at 4 °C, using a 5810R centrifuge (Eppendorf), and the plasma and buffy coat removed by suction. For cells wash, they were mixed by inversion with 150 mM of sodium chloride (NaCl) and centrifuged again at 500×g for 5 min at 4°C. The washing procedure was repeated twice. Then, the erythrocytes were counted, using a Neubauer Chamber. Several solvents were added to the packed erythrocytes (PER). First, after addition of 1 vol of sterile water, the mixture was vortexed and then left to stand for 15 min. Next, isopropanol (C₃H₈O, 11 mL/mL of PER) was added slowly and with mixing. This mixture was

stired for 1 h, at room temperature. Finally, chloroform (CHCl_3 , 7 mL/mL of PER) was added and the mixture was incubated for another 1 h, with mixing.

To separate the lipidic extract from iron and other erythrocytes constituents, the mixture was centrifuged at 500xg for 10 min. The extract was then transferred to chloroform-methanol (2:1; v/v) and washed with 0.2 vol of 0.05 M sodium chloride (KCl). After organic phase separation, the water containing methanol were removed by aspiration. Magnesium sulphate (MgSO_4) was added to absorb remaining water and after filtration through a cotton filter, the chloroformic solution of lipids was obtained.

2.2.2. Fatty acids profile

The lipidic profile of the lipidic extracts was evaluated by gas chromatography.

Analytical gas chromatography is a technique of separation of components present in a mixture to obtain information about their amounts and, if coupled with a mass spectrometer (GC-MS), of molecular compositions. It is based on the different partitioning behavior of the components between a gas phase and a stationary phase [23–24].

Gas chromatography is performed in long columns, where the sample is injected, and a carrier gas acts as the mobile phase (Figure 2.6.). The gas should be chemically inert and is continuously pumped to push the solutes along the column [24]. When a molecule partitions into the stationary phase, it does not move along the column, but when the molecule enters the gas phase, it is carried down the column by the flowing carrier gas. The carried molecules are in contact with a new portion of the stationary phase and reestablish an equilibrium between the stationary and mobile phases, reentering the stationary phase some distance down the column. Solute that have high affinity to the stationary phase will be retained for longer periods of time in this phase than in the mobile phase. Therefore, these solutes will be carried to the end of the column slower than solutes with weaker interactions with the stationary phase, allowing the complete separation of the mixture components.

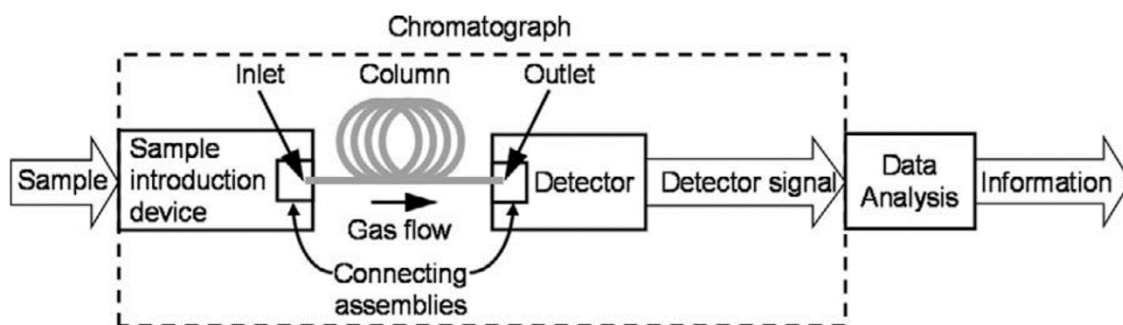


Figure 2.6. Schematics of a GC system. Adapted from [24].

Standard solutions of stearic acid (18:0), EPA (20:5) and DHA (22:6), were prepared in the concentrations of 250, 500, 1000 and 1500 mg/L in chloroform. Tricosanoic acid (23:0) was used as internal standard in the concentration of 500 µg/ mL in chloroform. To each digestive tube it were added 50 µL of standard solution or sample, 1 mL of methanol/sulfuric acid (9:1) and 100 µL of internal standard solution. The tubes were tightly closed and incubated at 100°C for 2h. Afterwards, 2 mL of hexane were added to the cooled tubes and they were vortexed for 20 seconds. The upper phase was transferred to a glass vial and magnesium sulphate was added. Then, 100 µL of sample was transferred to a GC injection vial.

The procedure was carried out in the Centre of Biological Engineering of University of Minho. A Scion 436-GC chromatograph (Bruker Daltonics) coupled with a SQ1 Bruker Mass spectrometer, equipped with a Restek Rxi-5Sil MS Column, 30 m x 0.25 x 0.25 mm, was used. The sample injection was performed in a split mode at 250 °C with a 1:10 split ratio. Helium was used as the carrier gas at 1 mL/min flow. The temperature was initially programmed at 70 °C and held for 1 min, followed by an increase to 250 °C at 5 °C/min and held for 5 min. The temperature was again increased to 300 °C at 5°C/min and held for 5 min.

The identification and quantification of the fatty acids was achieved using the standards solutions with different concentrations, the Supelco® 37 Component FAME Mix and the OpenChrom® software.

2.2.3. Preparation of erythrocyte-based LUVs incorporating or not diclofenac

The Bangham method or thin lipid film hydration method was the first method described to prepare liposomes [25]. This is a simple method that consists in creating a thin film of lipids in a round-bottom glass flask by complete evaporation of the organic solvents. The MLVs are formed after rehydration and vigorous shaking of the dried lipid film with aqueous solvents.

In this work, the lipid film was obtained through organic solvents evaporation in a RV10 AUTO Rotary Evaporator (IKA). The system was first cleaned by evaporating 100 mL of acetone (C_3H_6O) and then the samples organic solvents was evaporated. The pressure was carefully reduced to a pressure (50-100 mbar) below chloroform vapor pressure (260 mbar, at 25 °C [26]) and the water bath was adjusted to 25 °C. After organic solvent evaporation, the extracts were placed under nitrogen flow for up to 4 h, to guarantee the complete chloroform evaporation. The lipid film were kept protected from light with aluminum foil during the whole procedure, as unsaturated phospholipids are light-sensitive. 2% (v/v) folic acid-linked to a lipid was added to the lipidic film to functionalize the liposomes. Afterwards, the dried lipid film was hydrated with a 10 mM solution of HEPES hemisodium salt (pH 7.4) and strongly vortexed to produce MLVs. To obtain diclofenac-loaded liposomes, a buffered solution of this NSAID at 10 mM was used to hydrate the lipidic film.

LUVs were prepared by extrusion of the MLV suspensions through Nucleopore® polycarbonate filters of 400 nm and then 100 nm of pore diameter. During the extrusion, the system was maintained between 37-39 °C. Between the preparation of different formulations of liposomes, the extruder was carefully cleaned with water and ethanol to avoid contamination.

After the preparation of the liposomes, the non-entrapped diclofenac was removed by size exclusion chromatography through a PD-10 Desalting column containing 8.3 mL of Sephadex™ G-25 medium. First, the column storage solution was discarded and, then, 25 mL of 10 mM HEPES buffer was added to the column and discarded. Next, the liposome suspension was added, and the volume completed with 10 mM HEPES to make 2.5 mL. The sample and buffer were left to enter the packed bed completely and the flow-through was again discarded. Finally, 3.5 mL of buffer was added, and the liposomes were collected.

2.2.4. Preparation of phosphatidylcholine liposomes

PC liposomes, which are well established, were used for comparison. The PC liposomes were prepared as previously described for the erythrocyte-based liposomes, with and without diclofenac, but instead of using erythrocytes as the lipidic source, PC from egg yolk was used and the extrusion was done at room temperature.

2.2.5. Characterization of LUVs

2.2.5.1. Phosphorus concentration

The Bartlett method was used to determine the concentration of the phospholipids through the colorimetric determination of inorganic phosphate [27]. The phosphorus content of liposomes

was determined after digestion of the phospholipids with perchloric acid. Then, the inorganic phosphate was converted to phospho-molybdic acid by the addition of ammonium molybdate, which was reduced to a blue coloured complex by 4-amino-2-naphthyl-4-sulfonic acid (Fiske-Subbarow) at 100 °C. This compound can be quantified by measuring the absorbance at 830 nm followed by interpolation of that value on a calibration curve [27].

The liposome formulations were assayed by mixing 50 µL of sample with 150 µL of ultra-pure water in glass tubes. The standards were prepared from a monopotassium phosphate (KH_2PO_4) 0.83 mM solution at concentrations of 0, 12.5, 25, 50, 100 and 300 mM. To each sample and standard, 500 µL of 70% perchloric acid (HClO_4) was added and the tubes were incubated at 180-200 °C for 30 min.

After tubes cooling to room temperature, 5 mL of 0.22% ammonium molybdate ($(\text{NH}_4)_2\text{MoO}_4$) and 200 µL of 0.5% Fiske-Subbarow reducer were added to each standard and sample. Following solutions vortex, the tubes were incubated at 100 °C for 30 min. The tubes were left to cool to room temperature and, then, the absorbance was read at 830 nm, using a SYNERGY HT microplate reader (BIO-TEK). Each sample and standard were read in triplicate, being the volume of 300 µL/well. The concentration of free phosphate was interpolated from the standard curve relating phosphate concentration and absorbance intensity.

2.2.5.2. Cholesterol content

The cholesterol content in the erythrocyte-based liposomes was determined using Cell Biolabs's Total Cholesterol Assay Kit, according to manufacturer's instructions. The assay is based on an enzymatic reaction that quantifies both cholesterol esters and free cholesterol. Cholesterol esters are hydrolyzed via cholesterol esterase into cholesterol, which is then oxidized by cholesterol oxidase into the ketone cholest-4-en-3-one with the formation of hydrogen peroxide (H_2O_2). Then, the hydrogen peroxide is detected with a highly specific colorimetric probe. Horseradish peroxidase catalyzes the reaction between the probe and hydrogen peroxide, which binds in a 1:1 ratio. Samples and standards were incubated for 45 min and then the absorbance was read in a standard 96-well plate reader, in the 540-570 nm range. The concentration of cholesterol was interpolated using a standard curve relating the cholesterol concentration and absorbance intensity.

2.2.5.3. Diclofenac concentration into liposomes

To determine the concentration of diclofenac into the liposomes, High Performance Liquid Chromatography (HPLC) was performed, in collaboration with CESPU (Polytechnic and University Higher Education Cooperative).

HPLC equipment is typically composed by nine basic components (Figure 2.7.): mobile phase/solvent reservoir, solvent delivery system, sample introduction device, column, post-column apparatus, detector, data collection and output system, post-detector eluent processing, and connective tubing and fittings [28].

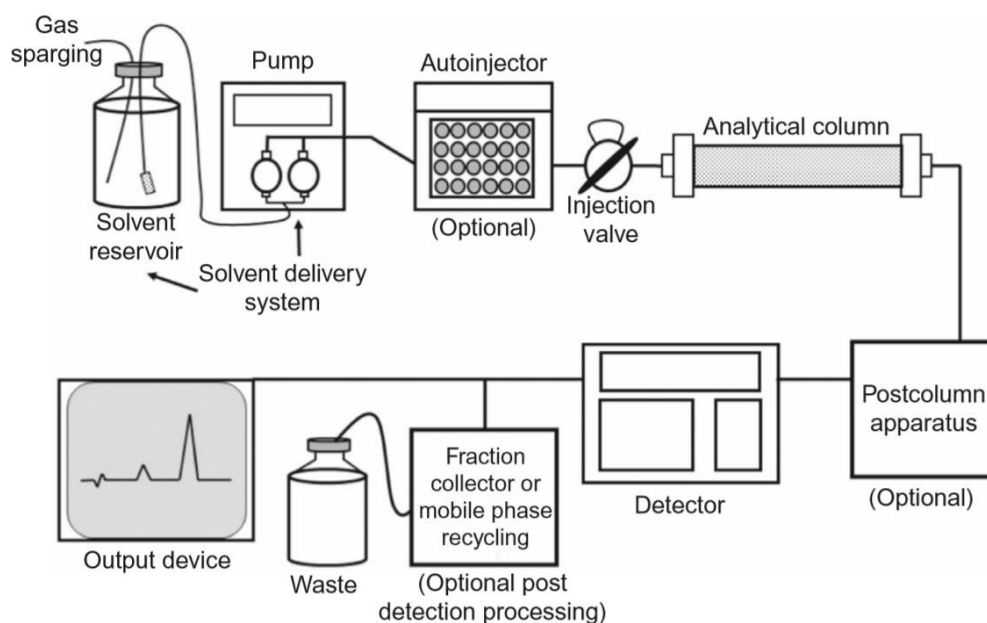


Figure 2.7. General schematics of a HPLC system [28].

Detection and quantification of diclofenac were done using a Shimadzu UFLC Prominence system equipped with two pumps LC-20 AD, an autosampler SIL-20 AC, a column oven CTO-20 AC, a degasser DGU-20A5, a system controller CBM-20A and a LC solution, version 1.24 SP1 (Shimadzu Corporation). A Shimadzu SPD-20A UV/Vis detector, coupled to the LC system, had the wavelength set at 270 nm. HPLC analysis was performed at 15 °C using a LiChrocart Lichrosphere RP-18 (5 µm) (250x4.6 mm) column. The mobile phase consisted of 0.1% triethylamine ($C_6H_{15}N$) in water, at pH 2.3, adjusted with trifluoroacetic acid ($C_2HF_3O_2$) and acetonitrile (C_2H_3N , 30:70, v/v). The mobile phase was injected at a flow rate of 1 mL/min. Previously to the analysis, the samples were diluted in ethanol (C_2H_5OH) at 1:5 and 1:10. Diclofenac standards were prepared in the concentrations of 0, 1.25, 2.5, 5, 10, 20, 40, 60, 80 and 100 µM.

2.2.5.4. Size distribution and zeta potential measurements

Dynamic light scattering (DLS), also known as photon correlation spectroscopy, is a method used to determine the size distribution of particles in suspension through the Brownian motion and Doppler shift induced by a laser beam [29–30]. DLS has numerous advantages for measuring the size of the nanoparticles, such as fast analysis, no requirement of calibration and high sensitivity [30]. DLS also allows to determine the polydispersity index (PDI), which represents the size distribution of particles measured [31].

When a suspension of particles in Brownian motion is excited with a monochromatic laser beam the wavelength of the incoming light is altered after contacting with the particles in motion. This creates a Doppler shift, which is a small frequency modification of the scattered light compared to the unscattered light [29–30]. This change provides information about the size and PDI of the samples. The light scattered by small particles has a quick fluctuation with a small Doppler shift, while light scattered from large particles is propagated slowly with a large Doppler shift.

For zeta potential measurements, the sample is placed into a chamber containing two electrodes and an electric field is applied, causing the charged nanoparticles moving with a velocity proportional to its zeta potential to the electrode presenting a opposite charge [32]. In solution, different electrical layers surround a nanoparticle (Figure 2.8.). The layer of ions with an opposite charge strongly bounded to the nanoparticle's surface is the Stern layer [33]. This layer together with the diffuse outer layer of loosely associated ions constitutes the electrical double layer. When particles move due to Brownian diffusion or applied force, the ions in the diffuse layer move with the nanoparticles. The electrostatic potential at this plane is called the zeta potential (Figure 2.8.) and is associated with the surface charge of the nanoparticle [33]. Nanoparticles with a zeta potential between -10 and $+10$ mV are considered neutral, while nanoparticles with zeta potentials higher than $+30$ mV or lower than -30 mV are considered strongly cationic or anionic, respectively [33].

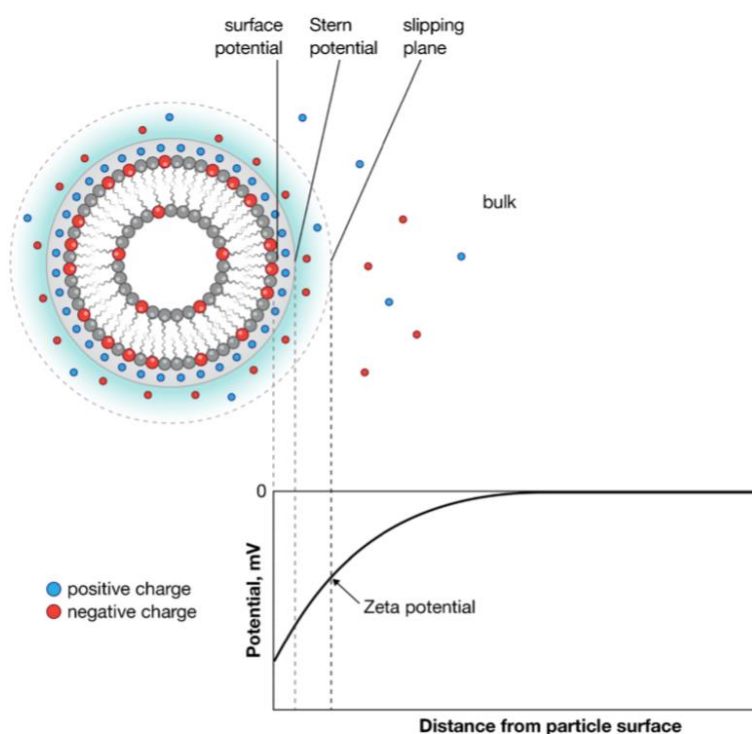


Figure 2.8. Schematics of charge distribution around a nanoparticle in solution. Adapted from [32].

LUVs size and PDI were determined using DLS and their surface electric charge was assessed by laser Doppler micro-electrophoresis, using a Zetasizer Nanoseries ZS equipment (Malvern Instruments). The measurements were performed at 37 °C using samples diluted in HEPES (1:20; v/v).

2.2.5.5. LUVs morphology

Morphological analysis of LUVs was performed by scanning transmission electron microscopy (STEM).

Although it was Baron Manfred von Ardenne who first developed the scanning transmission electron microscope in 1938, it is Crewe who is considered the father of STEM due to the development of the first high brightness cold field emission gun (FEG) that achieves sufficient beam current in a small spot or probe [34–35]. A STEM microscope uses a FEG to generate high-brightness electron probes [36–37]. To form a small electron probe on the specimen, at least two condenser lenses and an objective lens are necessary (Figure 2.9.) To control the convergent angle of the incident probe, a condenser aperture is placed between the condenser lens and the objective lens. This allows to keep outside the electron waves with large phase variation.

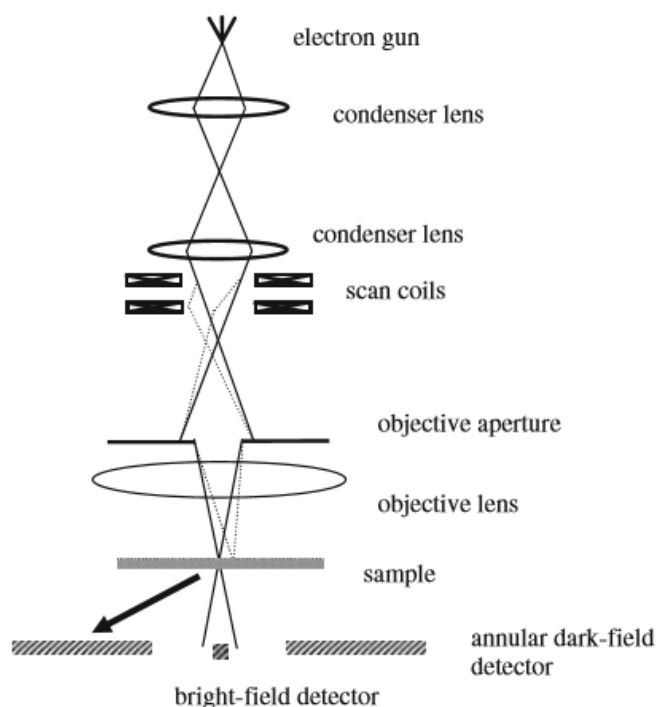


Figure 2.9. Schematics of a STEM system. Adapted from [37].

STEM combines the principles of transmission electron microscopy (TEM) and scanning electron microscopy (SEM). The electron beam is finely focused and scans the sample area, similar to SEM, but the image is generated by the electrons passing through the necessarily thin sample, like in TEM [36, 37]. Its primary advantage over conventional SEM imaging is the improvement in spatial resolution [36, 37]. STEM has also advantages over conventional TEM, including allowing to collect both bright and dark field images simultaneously [36–37].

Prior to analysis, the LUVs were diluted in HEPES (1:20; v/v), left to dry for at least 24 h, and analyzed using a High-Resolution Field Emission Scanning Electron Microscope with Focused Ion Beam (Auriga Compact, Zeiss).

2.2.5.6. Differential scanning calorimetry

Differential scanning calorimetry (DSC) is the most frequent technique that is used to thermally characterize materials, pinpointing important events of enthalpy change that may be biologically relevant [38].

If thermal energy is added, phospholipids change from the ordered gel to the disordered fluid lamella state, due to the decrease of the hydrophobic van der Waals interactions between lipid acyl chains [38]. The amount of energy needed for phase transition is associated with the phase and conformation properties of phospholipids and affects the stability of the system [38].

In a basic DSC experiment, energy is introduced simultaneously into a sample cell and a reference cell and the temperature of both cells is raised identically over time [39]. The difference in the input energy required to match the temperature of the sample to that of the reference would be the amount of heat absorbed or released by the molecules in the sample.

DSC has several characteristic temperatures relevant for the thermal analysis (Figure 2.10.).

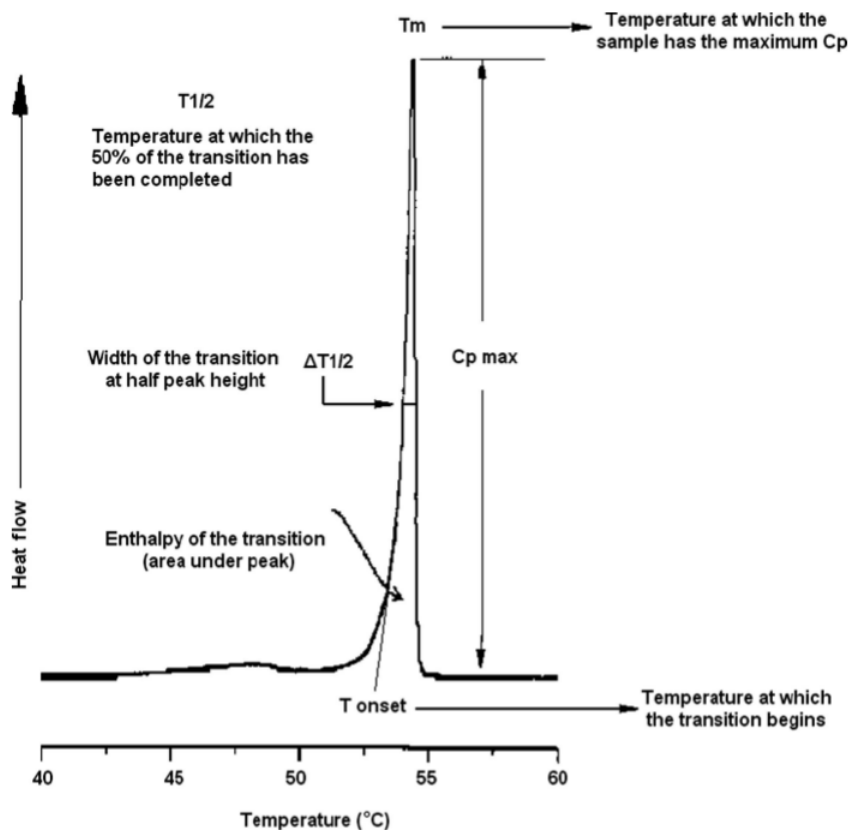


Figure 2.10. Characteristic thermodynamic parameters of a DSC curve. Adapted from [38].

Preceding the analysis, the samples were freeze-dried using the Lyoquest -85°C Plus Eco (Telstar). The thermal stability of the erythrocyte-derived LUVs was studied by DSC, using a DSC Q100 (TA Instruments). The freeze-dried samples were weighed and sealed into aluminum pans. An empty pan was used as reference. Samples were scanned from -10 °C to 240 °C, at a constant heating rate of 5 °C/min.

Biological characterization

2.2.5.7. THP-1 cell culture

The metabolic activity and anti-inflammatory activity of the developed liposomes were evaluated using the human peripheral blood monocyte cell line THP-1, according to the procedure previously described [40]. (10^6 cells/mL) in RPMI-1640 culture medium supplemented with 2 mM

L-glutamine, 100 units/mL of penicillin, 100 µg/mL of streptomycin, 10 mM HEPES buffer, and 10 % FBS, were seeded into 24-wells culture plates. The monocytes were differentiated into macrophages by stimulation with 100 nM of phorbol 12-myristate-13-acetate (PMA) for 24 h. Then, non-attached cells were removed by aspiration, and the adherent cells washed three times with RPMI. To ensure the reversion of cells to a resting macrophage phenotype before stimulation, the cells were incubated for an additional 48 h in RPMI without PMA. For macrophages stimulation, cells were further incubated for 2 h with 100 ng/mL of LPS in fresh media. Then, 50 µL of each sample, previously filtered with a 0.45 µm filter, was added to the LPS-stimulated macrophages and incubated for 22 h. After the incubation, the culture media was collected, centrifuged to remove cell debris, and stored at -80 °C until the determination of pro-inflammatory cytokines IL-6 and TNF-α concentration. The cells were washed with warm and sterile PBS and the cells metabolic activity and DNA were quantified. Cell morphology was also analyzed with SEM (Axiovert 40, Zeiss).

LPS-stimulated macrophages cultured only with culture medium were used as negative control and macrophages cultured with LPS were used as positive control. Diclofenac dissolved in Hepes, in similar concentrations of the drug encapsulated in the liposomes, and free dexamethasone were used as positive controls of cytokines production inhibition.

2.2.5.8. Metabolic activity assessment

The metabolic activity of LPS-stimulated or not macrophages incubated or not with liposomes was determined by the reduction of the resazurin (blue) to resorufin (pink) by living macrophages using the alamarBlue assay. RPMI medium containing 10% alamarBlue was added to each well. A blank was also made (10% alamarBlue without cells). The plates were incubated at 37 °C for 4 h in a humidified atmosphere containing 5% CO₂. Thereafter, the absorbance of the alamarBlue reduction from each sample was recorded in triplicate at 600 and 570 nm on a microplate reader (Synergy HT, Bio-Tek). The results are expressed in percentage related to the control.

2.2.5.9. DNA quantification

DNA quantification was performed using a fluorimetric dsDNA quantification kit (Quant-iT, PicoGreen, Molecular Probes, Invitrogen), according to the manufacturer's instructions. After metabolic activity determination, the macrophages were gently washed with warm and sterile PBS. Then, 1 mL of ultrapure water was added to each well and the samples were frozen at -80 °C until further analysis.

Prior to DNA quantification, the samples were thawed and sonicated for 15 min. DNA standards were prepared at concentrations ranging from 0 to 3.5 $\mu\text{g/mL}$ in ultrapure water. To each well of a white opaque 96-well plate were added 28.7 μL of sample or standard, 71.3 μL of PicoGreen solution and 100 μL of Tris-EDTA buffer. The plate was incubated for 10 min in the dark and the fluorescence of each sample was measured in a microplate reader (Synergy HT, Bio-Tek) using an excitation wavelength of 485 nm and an emission wavelength of 528 nm. The DNA concentration ($\mu\text{g/mL}$) of each sample was calculated using the standard curve relating the DNA concentration and the fluorescence intensity. The results are expressed in relative DNA concentration to the control.

2.2.5.10. SEM analysis of cell morphology

The morphological characterization of the cells was performed using SEM. In SEM, the images are reconstructed from the information of the scattered electrons, and not from the ones transmitted as in STEM. A scanning electron microscope comprises an electron optical system, a vacuum system, an electronics system, a computer and a software [41]. The electron optical system includes the electron gun, the demagnification system, the scanning unit, and the focusing system. This system is responsible for the formation of the electron probe. When the electron beam reaches the sample, the incident electrons are randomly scattered and some of them will escape from the sample and be collected by the detector. This interaction between the electron beam and specimen originates different signals, including secondary electrons (SE), backscattered electrons (BSE), Auger electrons, X-rays and cathodoluminescence (Figure 2.11). Each signal carries some information of the specimen, for the morphological characterization. However, the SEs are the most widely utilized signals because they can offer very high-resolution images, while BSEs are more used to obtain compositional information.

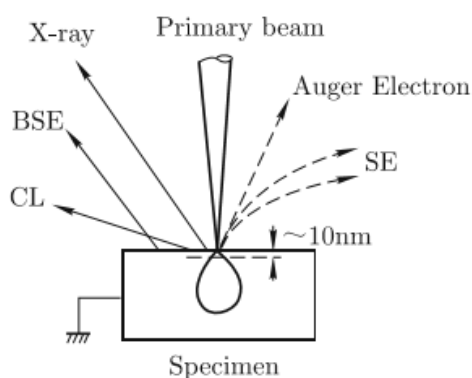


Figure 2.11. Types of signals resulting from the interaction between the electron beam and the specimen. Adapted from [28].

After the removal of the alamarBlue reagent, the samples were dehydrated for SEM analysis. The dehydration procedure was done as previously described [42]. First, cells seeded in the 24-well plate were washed with 500 μ L of PBS. After that, 500 μ L of 2.5% glutaraldehyde was added to each well to fixate the cells. The plate was closed with Parafilm M® and incubated at 4 °C for at least 5 h. On the day before the SEM analysis, the glutaraldehyde was removed, and the cells were washed twice with 500 μ L of PBS. Afterward, 500 μ L of 10% ethanol was added to each well, left to incubate for 30 min and removed. This was repeated with 20%, 30%, 40%, 50%, 60%, 70%, 80%, 90% and 100% of ethanol. The last 500 μ L of 100% ethanol was left in the wells overnight.

On the day of the SEM analysis, the bottom of each well was cut using a soldering iron and placed on SEM supports. To improve conductivity before the analysis, the samples were coated with 3 nm of platinum, using a Sputter coater from Cressington. The samples were analyzed using a High-Resolution Field Emission Scanning Electron Microscope (Auriga Compact, ZEISS) and microphotographs were recorded at 5 kV with magnifications of 200 and 1000 x.

2.2.5.11. Evaluation of the liposomes anti-inflammatory activity

Cytokines concentration in the culture medium was evaluated using enzyme-linked immunosorbent assay (ELISA) kits for IL-6 and TNF- α , according to manufacturer's instructions (R&D Systems). The standards were prepared in RPMI medium, at 0, 9.38, 18.8, 37.5, 75, 150, 300 and 600 pg/mL. Briefly, the capture antibody was incubated overnight in a high-binding, flat-bottom polystyrene 96-well plate and then blocked by adding 1% bovine serum albumin for 1 h. 100 μ L of sample or standards were added to each well and incubated for 2 h. Afterward, 100 μ L of detection antibody was added to each well and left for 2 h. Next, 100 μ L of streptavidin-HRP was added to each well and incubated for 20 min at room temperature, carefully protected from light with aluminum foil. Finally, 100 μ L of substrate solution (1:1 mixture of H₂O₂ and tetramethylbenzidine -C₁₆H₂₀N₂) was added and incubated for 20 min, at room temperature. After the incubation period, the reaction was stopped by adding 50 μ L of 2 N sulfuric acid (H₂SO₄). The plate was read immediately at 450 nm, with correction at 540 nm and 570 nm. The cytokines concentration of each sample was determined according to the standard curve relating to the respective cytokine concentrations and the absorbance intensity. The results were normalized using the respective DNA concentration and are expressed in percentage related to the control.

2.2.5.12. Statistical Analysis

Results are shown as arithmetic means \pm standard deviation of at least three independent measurements. Statistical analyses were performed using GraphPad Prism software version 7.00 (GraphPad Software, La Jolla California USA). The data from the LUVs size, PDI and zeta potential followed a normal distribution, thus a D'Agostino & Pearson omnibus normality test was applied.

The rest of the data did not follow a normal distribution, the Dunnet's multiple comparison test was applied to evaluate the statistical significance of the difference between the conditions tested. Differences were considered statistically significant when $p < 0.05$.

2.3. References

- [1] C. N. Blesso, "Egg phospholipids and cardiovascular health," *Nutrients*, vol. 7, no. 4, pp. 2731–2747, 2015.
- [2] R. Nisini, N. Poerio, S. Mariotti, F. De Santis, and M. Fraziano, "The Multirole of Liposomes in Therapy and Prevention of Infectious Diseases," *Front. Immunol.*, vol. 9, p. 155, 2018.
- [3] C. Ross *et al.*, "Principles of nanoparticle design for overcoming biological barriers to drug delivery," *Nat. Biotechnol.*, vol. 33, no. 9, pp. 1–8, 2015.
- [4] G. Fritsma, "Erythrocyte Metabolism and Membrane Structure and Function," in *Rodak's Hematology: Clinical Principles and Applications*, 5th: Elsevier Inc, 2015, pp. 112–123.
- [5] B. F. Rodak and J. H. Carr, "Hematopoiesis," in *Clinical Hematology Atlas*, Elsevier Health Sciences, 2012, pp. 11–88.
- [6] Y. Yawata, "Composition of Normal Red Cell Membranes," in *Cell Membrane: The Red Blood Cell as a Model*, Wiley-VCH, 2003, pp. 27–46.
- [7] C. OpenStax, "Chapter 19: The Cardiovascular System: The Heart," in *Anatomy & Physiology*, 2013.
- [8] L. L. M. van Deenen and J. De Gier, "Lipids of the Red Cell Membrane," in *The Red Blood Cell*, New York: Academic Press, 1974, pp. 147–211.
- [9] Y. Yawata, "Composition of Normal Red Cell Membranes," in *Cell Membrane*, 2004, pp. 27–46.
- [10] J. Fan, Y. Cui, M. Wan, W. Wang, and Y. Li, "Lipid accumulation and biosynthesis genes response of the oleaginous *Chlorella pyrenoidosa* under three nutrition stressors," *Biotechnol. Biofuels*, vol. 7, p. 17, 2014.
- [11] N. M. Davies and K. E. Andersen, "Clinical pharmacokinetics of diclofenac. Therapeutic insights and pitfalls," *Clin. Pharmacokinet.*, vol. 33, no. 3, pp. 184–213, 1997.
- [12] P. McGettigan and D. Henry, "Use of Non-Steroidal Anti-Inflammatory Drugs That Elevate Cardiovascular Risk: An Examination of Sales and Essential Medicines Lists in Low-, Middle-, and High-Income Countries," *PLoS Med.*, vol. 10, no. 2, p. e1001388, 2013.
- [13] R. Altman, B. Bosch, K. Brune, P. Patrignani, and C. Young, "Advances in NSAID development: Evolution of diclofenac products using pharmaceutical technology," *Drugs*, vol. 75, no. 8, pp. 859–877, 2015.
- [14] A. Meena, D. K. Yadav, A. Srivastava, F. Khan, D. Chanda, and S. K. Chattopadhyay, "In Silico Exploration of Anti-Inflammatory Activity of Natural Coumarinolignoids," *Chem. Biol.*

- Drug Des.*, vol. 78, no. 4, pp. 567–579, 2011.
- [15] I. Tegeder, J. Pfeilschifter, and G. Geisslinger, “Cyclooxygenase-independent actions of cyclooxygenase inhibitors,” *FASEB J.*, vol. 15, no. 12, pp. 2057–2072, 2001.
 - [16] J. R. Vane, “Inhibition of prostaglandin synthesis as a mechanism of action for aspirin-like drugs,” *Nat. New Biol.*, vol. 231, pp. 232–235, 1971.
 - [17] T. J. Gan, “Diclofenac: An update on its mechanism of action and safety profile,” *Curr. Med. Res. Opin.*, vol. 26, no. 7, pp. 1715–31, 2010.
 - [18] P. S. Low, W. A. Henne, and D. D. Doorneweerd, “Discovery and development of folic-acid-based receptor targeting for imaging and therapy of cancer and inflammatory diseases,” *Acc. Chem. Res.*, vol. 41, no. 1, pp. 120–9, 2008.
 - [19] A. C. Lima, H. Ferreira, R. L. Reis, and N. M. Neves, “Biodegradable polymers: an update on drug delivery in bone and cartilage diseases,” *Expert Opin. Drug Deliv.*, vol. 16, no. 8, pp. 795–813, 2019.
 - [20] J. Sudimack and R. J. Lee, “Targeted drug delivery via the folate receptor,” *Adv. Drug Deliv. Rev.*, vol. 41, no. 2, pp. 147–162, 2000.
 - [21] M. D. A. Salazar and M. Ratnam, “The folate receptor: What does it promise in tissue-targeted therapeutics?,” *Cancer Metastasis Rev.*, vol. 26, no. 1, pp. 141–152, 2007.
 - [22] H. G. Rose and M. Oklander, “Improved Procedure for the Extraction of Lipids From Human Erythrocytes,” *J. Lipid Res.*, vol. 6, pp. 428–431, 1965.
 - [23] C. F. Poole, “Mark F. Vitha: Chromatography: Principles and Instrumentation,” *Chromatographia*, vol. 81, pp. 727–728, 2018.
 - [24] L. M. Blumberg, “Theory of Gas Chromatography,” in *Gas Chromatography*, Elsevier, 2012, pp. 19–78.
 - [25] A. D. Bangham, J. De Gier, and G. D. Greville, “Osmotic properties and water permeability of phospholipid liquid crystals,” *Chem. Phys. Lipids*, vol. 1, no. 3, pp. 225–246, May 1967.
 - [26] C. R. Mueller and E. R. Kearns, “Thermodynamic Studies of the System: Acetone + Chloroform,” *J. Phys. Chem.*, vol. 62, no. 11, pp. 1441–1445, Nov. 1958.
 - [27] G. R. Bartlett, “Phosphorus assay in column chromatography,” *J. Biol. Chem.*, vol. 234, no. 3, pp. 466–8, Mar. 1959.
 - [28] M. E. LaCourse and W. R. LaCourse, “General instrumentation in HPLC *,” in *Liquid Chromatography*, Elsevier, 2017, pp. 417–429.
 - [29] E. H. M. Sakho, E. Allahyari, O. S. Oluwafemi, S. Thomas, and N. Kalarikkal, “Dynamic

- Light Scattering (DLS),” in *Thermal and Rheological Measurement Techniques for Nanomaterials Characterization*, Elsevier, 2017, pp. 37–49.
- [30] R. Xu, “Light scattering: A review of particle characterization applications,” *Particuology*, vol. 18, pp. 11–21, Feb. 2015.
- [31] H. Kato, “Size Determination of Nanoparticles by Dynamic Light Scattering,” in *Nanomaterials*, Weinheim, Germany: Wiley-VCH Verlag GmbH & Co. KGaA, 2012, pp. 535–554.
- [32] M. C. Smith, R. M. Crist, J. D. Clogston, and S. E. McNeil, “Zeta potential: a case study of cationic, anionic, and neutral liposomes,” *Anal. Bioanal. Chem.*, vol. 409, no. 24, pp. 5779–5787, 2017.
- [33] T. Glawdel and C. L. Ren, “Zeta Potential Measurement,” in *Encyclopedia of Microfluidics and Nanofluidics*, Boston, MA: Springer US, 2014, pp. 1–12.
- [34] A. V. Crewe, D. N. Eggenberger, J. Wall, and L. M. Welter, “Electron Gun Using a Field Emission Source,” *Rev. Sci. Instrum.*, vol. 39, no. 4, pp. 576–583, Apr. 1968.
- [35] M. von Ardenne, “Das Elektronen-Rastermikroskop,” *Zeitschrift für Phys.*, vol. 109, no. 9–10, pp. 553–572, Sep. 1938.
- [36] B. Ge, “Scanning Transmission Electron Microscopy (STEM),” in *Springer Tracts in Modern Physics*, 2018, pp. 205–254.
- [37] P. D. Nellist, “The Principles of STEM Imaging,” in *Scanning Transmission Electron Microscopy*, New York, NY: Springer New York, 2011, pp. 91–115.
- [38] C. Demetzos, “Differential Scanning Calorimetry (DSC): A Tool to Study the Thermal Behavior of Lipid Bilayers and Liposomal Stability,” *J. Liposome Res.*, vol. 18, no. 3, pp. 159–173, 2008.
- [39] P. Gill, T. T. Moghadam, and B. Ranjbar, “Differential scanning calorimetry techniques: applications in biology and nanoscience,” *J. Biomol. Tech.*, vol. 21, no. 4, pp. 167–93, Dec. 2010, [Online]. Available: <http://www.ncbi.nlm.nih.gov/pubmed/21119929>.
- [40] D. R. P. Loureiro *et al.*, “Yicathins B and C and Analogues: Total Synthesis, Lipophilicity and Biological Activities,” *ChemMedChem*, vol. 15, no. 9, pp. 749–755, 2020.
- [41] W. Han, H. Jiao, and D. Fox, “Scanning Electron Microscopy,” in *Springer Tracts in Modern Physics*, 2018, pp. 35–68.
- [42] A. C. Lima, C. Cunha, A. Carvalho, H. Ferreira, and N. M. Neves, “Interleukin-6 Neutralization by Antibodies Immobilized at the Surface of Polymeric Nanoparticles as a

Therapeutic Strategy for Arthritic Diseases," *ACS Appl. Mater. Interfaces*, vol. 10, no. 16, pp. 13839–13850, 2018.

CHAPTER III

Erythrocyte-derived liposomes for the
treatment of inflammatory diseases

CHAPTER III. Erythrocyte-derived liposomes for the treatment of inflammatory diseases

Ana Olival^{1,2}, Sara F. Vieira^{1,2}, Virgínia Gonçalves³, Cristina Cunha^{2,4}, Maria Elizabeth Tiritan^{3,5,6}, Agostinho Carvalho^{2,4}, Helena Ferreira^{1,2}, Nuno M. Neves^{1,2}

¹3B's Research Group, I3Bs – Research Institute on Biomaterials, Biodegradables and Biomimetics, University of Minho, Headquarters of the European Institute of Excellence on Tissue Engineering and Regenerative Medicine, AvePark, Parque de Ciência e Tecnologia, Zona Industrial da Gandra, 4805-017 Barco, Guimarães, Portugal

²ICVS/3B's - PT Government Associate Laboratory, Braga/Guimarães, Portugal

³CESPU, Instituto de Investigação e Formação Avançada em Ciências e Tecnologias da Saúde, Rua Central de Gandra, 1317, 4585-116 Gandra PRD, Paredes, Portugal

⁴Life and Health Sciences Research Institute, School of Health Sciences, University of Minho, Campus de Gualtar, 4710-057 Braga, Portugal

⁵Laboratório de Química Orgânica e Farmacêutica, Departamento de Ciências Químicas, Faculdade de Farmácia, Universidade do Porto, Rua Jorge Viterbo Ferreira, 228, 4050-313 Porto, Portugal

⁶Centro Interdisciplinar de Investigação Marinha e Ambiental (CIIMAR/CIMAR), Universidade do Porto, Rua dos Bragas 289, 4050-123 Porto, Portugal

Abstract

Chronic inflammation-related diseases are the main cause of morbidity and mortality worldwide. Consequently, there is an urgent demand for the development of new and effective approaches to counteract persistent inflammation. Here, a novel anti-inflammatory erythrocyte-based liposome was developed. Erythrocyte membranes present the major classes of fatty acids, including omega-3 fatty acids that have several health benefits throughout human life. Consequently, erythrocytes membranes were used as a lipidic source for the preparation of liposomes with intrinsic anti-inflammatory activity. Diclofenac, a widely used nonsteroidal anti-inflammatory drug (NSAID), was incorporated into the liposomes to demonstrate their potential as drug delivery devices for inflammatory diseases treatment. The erythrocyte-derived liposomes were also functionalized with folic acid to target active macrophages since they are key inflammatory mediators. The size of the large unilamellar liposomes (LUVs) was approximately 222 nm and 297 nm in the absence and after incorporating diclofenac, respectively. Relevant therapeutic concentrations of the NSAID were encapsulated into liposomes (≈ 193). *In vitro* assays demonstrated that the developed liposomes do not alter the metabolic activity and proliferation of monocyte-differentiated macrophages. In the presence of lipopolysaccharide (LPS)-stimulated macrophages, liposomes incorporating or not diclofenac presented ability to reduce the IL-6 concentration in a percentage of 77% and 85% as well as 72% and 64% of the TNF- α amount, respectively. Moreover, the anti-inflammatory performance of the prepared erythrocyte-derived LUVs was superior to established and commonly used phosphatidylcholine liposomes, as well as

to free diclofenac. Strikingly, cytocompatible concentrations of erythrocyte-derived LUVs presented similar effects to dexamethasone, a potent corticosteroid anti-inflammatory drug, in reducing IL-6 and TNF- α concentration. This demonstrates the potential of the developed LUVs to be used as bioactive carriers in the treatment of inflammatory diseases.

Keywords: Erythrocytes, inflammatory diseases, liposomes, active targeting, drug delivery, anti-inflammatory

3.1. Introduction

Chronic inflammatory diseases, such as rheumatoid arthritis and osteoarthritis, are important debilitating illnesses, often associated with extremely high societal and economic burdens [1]. Indeed, according to World Health Organization, chronic inflammation-related diseases are the main causes of death globally [2].

Inflammation is a fundamental and complex response of the immune system triggered by exogenous pathogens or damaged tissue [3–4]. Therefore, an orchestrated inflammatory response is a vital defense mechanism to ensure the return to homeostasis. However, when uncontrolled, this biological response can become excessive in magnitude and persistence, damaging the tissue and, if not resolved, leading to chronic inflammation [3, 5]. Therapeutic interventions for inflammation-related diseases include the use of corticosteroids, nonsteroidal anti-inflammatory drugs (NSAIDs) and conventional or biological disease-modifying antirheumatic drugs (DMARDs). Corticosteroids have powerful suppressive effects on the inflammatory response but also result in serious side effects, such as hyperglycemia, osteoporosis, insulin resistance and hypertension [6] [22]. NSAIDs have in addition to anti-inflammatory activity, analgesic and antipyretic effects, which are mainly due to the inhibition of COX-2 enzyme [7]. However, NSAIDs are also associated with severe cardiovascular, gastrointestinal and renal injurious effects [8, 9]. Biological DMARDs have shown therapeutic benefits by targeting TNF- α and IL-6 in the treatment of e.g. rheumatoid arthritis [10–12]. Nevertheless, they also present several drawbacks as alteration of cytokine cascades can lead to impaired immune response, leading, for instance, to an increased risk of infection of the patients [13–14].

Liposomes have been widely used to incorporate and deliver drugs to overcome the conventional therapy drawbacks (e.g. severe side-effects) [15–16]. Liposomes are biocompatible and biodegradable carriers that can incorporate therapeutic agents regardless of their solubility and molecular weight, preventing their chemical and biological degradation after patient

administration [17–19]. Liposomes have been successfully translated, existing several formulations in the clinic for the treatment of different diseases, including hepatitis A, metastatic breast cancer and acute lymphoblastic leukemia [20–22]. As these drug delivery devices are composed by a lipid bilayer that resembles the structure of the cell membrane, in this work, lipids of erythrocyte membranes were extracted to prepare autologous and immunologically compatible liposomes to treat inflammatory conditions. Erythrocytes, and other blood cells, have recently been used as vehicles, as an alternative to polymer-based drug vehicles [23–24], since they have the capacity to load clinically relevant concentrations of drugs [25–26]. For instance, Erydel® and Erycaps® are examples of erythrocytes products commercially available for clinical use. The use of erythrocytes presents advantages, since they are the most abundant blood component ($4.2\text{--}6.0 \times 10^6/\text{mL}$ of blood) and present long circulation-time (approximately 120 days) [27]. Moreover, the human erythrocyte membrane has important lipids, such as omega-3 long-chain polyunsaturated fatty acids (PUFA), namely eicosapentaenoic acid (EPA, 20:5n-3) and docosahexaenoic acid (DHA, 22:6n-3), which have been widely associated with anti-inflammatory, immunoregulatory, antioxidant and anti-tumor activities [28–29]. In addition to their anti-inflammatory activity, EPA and DHA have also been reported to have other health benefits, including a reduced risk for cardiac arrest, sudden cardiac death and fatal ischemic heart disease [30–32].

Diclofenac, a strong NSAID widely prescribed worldwide, was the drug selected to demonstrate the carrier ability of the prepared liposome [9]. Indeed, it shares the side effects previously referred for NSAIDs in general, being, therefore, the search of new improved methods of encapsulating this drug paramount.

To assess the anti-inflammatory activity of the developed formulations THP-1 monocytes differentiated into macrophages and stimulated with lipopolysaccharide (LPS) were used. Activated (M1) macrophages are central players of the inflammatory response, producing an array of inflammatory mediators, such as pro-inflammatory cytokines (e.g. interleukin-6 - IL-6- and tumor necrosis factor- α -TNF- α). Moreover, to obtain a specific targeting of activated macrophages, the erythrocyte-derived liposomes were tethered to folic acid via a polyethylene glycol (PEG) spacer. Indeed, folic acid has been widely used for the selective targeting of activated macrophages in an inflammatory scenario [33–34].

3.2. Materials and Methods

3.2.1. Materials

Phosphatidylcholine (PC) from egg yolk, HEPES hemisodium salt ($C_8H_{18}N_2O_4S \cdot 0.5 Na$, $\geq 99.5\%$), Fiske-subbarow reducer, perchloric acid ($HClO_4$, 70%), stearic acid ($C_{18}H_{36}O_2$, 95%), eicosapentaenoic acid ($C_{18}H_{36}O_2$, analytical standard), docosahexaenoic acid ($C_{22}H_{32}O_2$, $\geq 98\%$) and tricosanoic acid ($C_{23}H_{46}O_2$, $\geq 99\%$) were purchased from Sigma. N-hexane (C_6H_{14} , $\geq 97.0\%$) was purchased from VWR and potassium chloride (KCl) was purchased from JMGS. Human TNF-alpha DuoSet ELISA and Human IL-6 DuoSet ELISA were purchased from Citomed. RPMI-1640 culture medium with 2 mM stable glutamine ($C_5H_{10}N_2O_3$) and 2 g/L sodium bicarbonate ($NaHCO_3$) was purchased from Alfagene. BD Vacutainer K2E (EDTA) 10 mL tubes were purchased from BD Diagnostics – PreAnalytical Systems. PD-10 desalting columns and all other reagents were purchased from Laborspirit.

3.2.2. Extraction of lipids from erythrocytes membranes and evaluation of their profile

The lipids were extracted from the erythrocytes as described previously [35]. Briefly, the blood was centrifuged at $3000\times g$ for 5 min at $4^\circ C$, using a 5810R centrifuge, and the plasma and buffy coat were removed by suction. For cells wash, they were mixed by inversion with 150 mM of sodium chloride (NaCl) and centrifuged again at $500\times g$ for 5 min at $4^\circ C$. The washing procedure was repeated twice. Then, several solvents were added to the packed erythrocytes (PE). First, after addition of 1 vol of sterile water, the mixture was vortexed and then left to stand for 15 min. Next, isopropanol (C_3H_8O , 11 mL/mL of PE) was added slowly and with mixing. This mixture was incubated for 1 h at room temperature, with agitation. Finally, chloroform ($CHCl_3$, 7 mL/mL of PE) was added and the mixture was incubated for another 1 h, with mixing.

To separate the lipidic extract from iron and other erythrocytes constituents, the mixture was centrifuged at $500\times g$ for 10 min. The extract was then transferred to chloroform-methanol (2:1; v/v) and washed with 0.2 vol of 0.05 M sodium chloride (KCl). After organic phase separation, the water containing methanol were removed by aspiration. Magnesium sulphate ($MgSO_4$) was added to absorb the remaining water and after filtration through a cotton filter, the chloroformic solution of lipids was obtained.

The lipid profile of the lipidic extracts was evaluated by gas chromatography and mass spectrometry (GC-MS). Standard solutions of stearic acid (18:0), EPA (20:5) and DHA (22:6), were

prepared in the concentrations of 250, 500, 1000 and 1500 mg/L in chloroform. Tricosanoic acid (23:0) was used as internal standard at the concentration of 500 µg/ mL in chloroform. To each digestive tube it was added 50 µL of standard solution or sample, 1 mL of methanol/sulfuric acid (9:1) and 100 µL of internal standard solution. The tubes were tightly closed and incubated at 100 °C for 2 h. Afterwards, 2 mL of hexane were added to the cooled tubes and they were vortexed for 20 sec. The upper phase was transferred to a glass vial and magnesium sulphate was added. Then, the dehydrated samples were transferred to a GC injection vial. A Scion 436-GC chromatograph (Bruker Daltonics) coupled with a SQ1 Bruker Mass spectrometer and equipped with a Restek Rxi-5Sil MS Column, 30 m x 0.25 x 0.25 mm, was used. The sample injection was performed in a split mode at 250 °C with a 1:10 split ratio. Helium was used as the carrier gas at a flow rate of 1 mL/min. The temperature was initially programmed at 70 °C and held for 1 min, followed by an increase to 250 °C at 5 °C/min and held for 5 min. Then, the temperature was again increased to 300 °C a 5°C/min and held for 5 min. The identification and quantification of the fatty acids was achieved using standards solutions with different concentrations (250, 500, 1000 and 1500 mg/L), the Supelco® 37 Component FAME Mix and the OpenChrom® software.

3.2.3. Preparation erythrocyte-based LUVs incorporating or not diclofenac

To produce erythrocyte-based large unilamellar vesicles (LUVs), the dried lipidic extracts obtained as previously referred were hydrated with HEPES buffer and strongly vortexed to produce multilamellar liposomes (MLVs). LUVs were prepared by extrusion of the MLVs suspensions through Nucleopore® polycarbonate filters of 100 nm of pore diameter, after 23 passages at 37 °C.

The liposomes loaded with diclofenac were prepared as just referred but using a buffered solution of this NSAID to hydrate the lipidic film. After LUVs preparation, the non-entrapped diclofenac was removed by size exclusion chromatography through a Sephadex G-25 M column.

3.2.3.1 Phospholipids and cholesterol concentration

The phosphorus content of the liposomes was determined through the Bartlett method [36] and the cholesterol concentration was determined by an enzymatic method, using the Cell BioLabs' Total Cholesterol Assay Kit according to manufacturer's instructions.

3.2.4. Preparation of PC liposomes

PC liposomes with and without diclofenac were prepared as previously described for the erythrocyte-based liposomes production, but instead of using erythrocytes as the lipidic source, PC from egg yolk was used and the extrusion was done at room temperature.

3.2.4.1 PC concentration

The PC content of LUVs was determined using the LabAssay™ Phospholipid, according to the instructions of the manufacturer.

3.2.5. Diclofenac concentration into liposomes

The concentration of diclofenac into LUVs was determined by High Performance Liquid Chromatography (HPLC). The detection and quantification of the NSAID were done using a Shimadzu UFLC Prominence system equipped with two pumps LC-20 AD, an autosampler SIL-20 AC, a column oven CTO-20 AC, a degasser DGU-20A5, a system controller CBM-20A and a LC solution, version 1.24 SP1 (Shimadzu Corporation). A Shimadzu SPD-20A UV/Vis detector, coupled to the LC system, had the wavelength set at 270 nm. HPLC analysis was performed at 15 °C using a LiChrocart Lichrosphere RP-18 (5 µm) (250x4.6 mm) column. The mobile phase consisted of 0.1% triethylamine in water at pH 2.3 (adjusted with trifluoroacetic acid) and acetonitrile (30:70, v/v). The mobile phase was injected at a flow rate of 1 mL/min. Previously to the analysis, the samples were diluted in ethanol at 1:5 and 1:10 ratios. Diclofenac standards were prepared in the concentrations of 0, 1.25, 2.5, 5, 10, 20, 40, 60, 80 and 100 µM.

3.2.6. Size distribution and zeta potential measurements

LUVs were characterized by their size and polydispersity index (PDI) using dynamic light scattering (DLS) and by their surface electric charge using laser Doppler micro-electrophoresis. The measurements were performed in a Zetasizer Nanoseries ZS equipment (Malvern Instruments), at 37 °C using samples diluted in HEPES (1:20; v/v).

3.2.7. LUVs morphology

Morphological analysis of erythrocyte-derived LUVs was performed by scanning transmission electron microscopy (STEM) using High-Resolution Field Emission Scanning Electron Microscope with Focused Ion Beam (Auriga Compact, Zeiss). Prior to analysis, the LUVs were diluted in HEPES (1:20; v/v) and left to dry overnight.

3.2.8. Differential scanning calorimetry

The thermal stability of the erythrocyte-derived LUVs was studied by differential scanning calorimetry, using a DSC Q100 (TA Instruments). Preceding the analysis, the samples were freeze-dried using the LYOQUEST -85 °C PLUS ECO (Telstar). Then, the freeze-dried samples were weighed and sealed into aluminium pans. Samples were scanned from -10 °C to 240 °C, at a constant heating rate of 5 °C/min, using an empty pan as reference.

3.2.9. THP-1 cell culture

The biological effects of the LUVs were evaluated using THP-1 monocytes. 10^6 cells/mL were seeded in cell culture plates, using Roswell Park Memorial Institute (RPMI)-1640 culture medium with 2 mM stable glutamine and 2 g/L NaHCO₃, supplemented with 10% human serum, 10 U/mL penicillin/streptomycin and 10 mM HEPES. The THP-1 monocytes were differentiated into macrophages as previously described[37]. First, they were incubated with 100 nM of phorbol 12-myristate-13-acetate (PMA) for 24 h. Then, non-attached cells were removed by aspiration, and the adherent cells were washed three times with the complemented RPMI (cRPMI). To ensure reversion of cells to a resting macrophage phenotype before stimulation, the cells were incubated for an additional 48 h in cRPMI without PMA. A preliminary study was performed to assess the toxicity of the liposomes in the presence of non-stimulated macrophages.

For cells stimulation, they were incubated for 2 h with 100 ng/mL of lipopolysaccharide (LPS) in fresh media. Then, 50 µL of either erythrocyte-derived liposomes, with and without diclofenac, PC liposomes, with and without diclofenac, free diclofenac and free dexamethasone, previously filtered with a 0.45 µm filter, were added to the LPS-stimulated macrophages and incubated for 22 h. After the incubation, the culture media was collected, centrifuged to remove cell debris, and stored at -80 °C until determination of pro-inflammatory cytokines concentration. LPS-stimulated macrophages cultured only with culture medium were used as a negative control and macrophages cultured with LPS-free medium were used as positive control.

3.2.10. Cell metabolic activity and proliferation assessment

The metabolic activity of macrophages incubated with either erythrocyte-derived and PC liposomes, with and without diclofenac, or free diclofenac) was determined using the alamarBlue assay (alamarBlue®, Bio-Rad). cRPMI medium containing 10% alamarBlue was added to each well. A blank was also made (10% alamarBlue without cells). The plates were incubated at 37 °C for 4 h in a humidified atmosphere containing 5% CO₂. Thereafter, the absorbance of the

AlamarBlue reduction from each sample was recorded in triplicate at 600 and 570 nm on a microplate reader (Synergy HT, Bio-Tek).

Cell proliferation was assessed using a fluorometric dsDNA quantification kit (Quant-iT, PicoGreen, Molecular Probes, Invitrogen). First, cell samples were transferred to eppendorf tubes containing 1 mL of ultrapure water and frozen at -80°C until further analysis. Prior to DNA quantification, samples were defrosted and sonicated for 15 min. DNA standards were prepared at concentrations ranging from 0 to 2 $\mu\text{g/mL}$ in ultrapure water. To each well of a white opaque 96-well plate (Falcon) were added 28.7 μL of sample or standard ($n=3$), 71.3 μL of PicoGreen solution, and 100 μL of Tris-EDTA buffer. The plate was incubated for 10 min in the dark, and the fluorescence of each sample was measured in a microplate reader (Synergie HT, Bio-Tek), using an excitation wavelength of 485 nm and an emission wavelength of 528 nm. DNA concentration of the samples was inferred from the standard curve.

3.2.11. Cell morphology analysis

After the removal of the AlamarBlue reagent, the samples were dehydrated for SEM analysis. The dehydration procedure was done according to a procedure previously described [38]. First, cells seeded in the 24-well plate were washed with 500 μL of PBS. After that, the cells were fixated by adding 500 μL of 2.5% glutaraldehyde to each well and incubated for at least 5 h. On the day before of the SEM analysis, the glutaraldehyde was removed, and the cells were washed twice with 500 μL of PBS. Afterward, 500 μL of 10% ethanol was added to each well, left to incubate for 30 min and removed. This procedure was repeated with 20%, 30%, 40%, 50%, 60%, 70%, 80%, 90% and 100% of ethanol. The last 500 μL of 100% ethanol was left in the wells overnight. On the day of the SEM analysis and after removing the ethanol, the bottom of each well was cut using a soldering iron and placed on SEM supports.

To improve conductivity before the analysis, the samples were coated with 3 nm of platinum, using a Sputter coater (Cressington). The samples were analyzed using a High-Resolution Field Emission Scanning Electron Microscope (Auriga Compact, ZEISS) and microphotographs were recorded at 5 kV with magnifications of 200 and 1000x.

3.2.12. Evaluation of anti-inflammatory activity

Cytokines concentration in the culture medium of each condition was evaluated using enzyme-linked immunosorbent assay (ELISA) kits, according to manufacturer's instructions (R&D Systems) for IL-6 and TNF- α . The standards were prepared in RPMI medium, at 0, 9.38, 18.8,

37.5, 75, 150, 300 and 600 pg/mL. Briefly, the capture antibody was incubated overnight in a high-binding, flat-bottom polystyrene 96-well plate and then blocked by adding 1% bovine serum albumin (BSA) for 1 h. Then, 100 μ L of each sample or standard were added to each well and incubated for 2 h. Afterward, 100 μ L of detection antibody was added to each well and left for 2 h. Next, 100 μ L of streptavidin-HRP was added to each well and incubated for 20 min at room temperature, carefully protected from light with aluminum foil. Finally, 100 μ L of substrate solution (1:1 mixture of H_2O_2 and tetramethylbenzidine - $\text{C}_{16}\text{H}_{20}\text{N}_2$) was added and incubated for 20 min, at room temperature. After the incubation period, the reaction was stopped by adding 50 μ L of 2 N sulfuric acid (H_2SO_4). The plate was read immediately at 450 nm, with corrections at 540 nm and 570 nm. The cytokines concentration of each sample was determined using the standard curve relating cytokine concentrations and the absorbance intensity. The results were normalized using the respective DNA concentration and are expressed in percentage related to the control.

3.3. Statistical analysis

Results are shown as arithmetic means \pm standard deviation (SD) of at least three independent measurements. Statistical analyses were performed using GraphPad Prism software version 7.00 (GraphPad Software, La Jolla California USA). The data from the LUVs size, PDI and zeta potential followed a normal distribution, thus a D'Agostino & Pearson omnibus normality test was applied. The rest of the data did not follow a normal distribution, being the Dunnett's multiple comparison test applied to evaluate the statistical significance of the difference between the tested conditions. Differences were considered statistically significant when $p < 0.05$.

3.4. Results

3.4.1. Fatty acids profile evaluation

The content of different fatty acids in the lipidic extracts was determined using GC-MS. The saturated fatty acid stearic acid (18:0) and the unsaturated fatty acids EPA (20:5 ω 3) and DHA (22:6 ω 3) were successfully identified and quantified (Table 3.1.). The higher fatty acids concentration obtained in LUVs is related to the use of concentrated extracts in their production. Other fatty acids, including palmitic acid (16:0), ω -9 oleic acid (18:1), ω -6 linoleic acid (18:2), ω -6 arachidonic acid (20:4) and lignoceric acid (24:0), as well as cholesterol esters were also identified.

Table 3.1. Concentration of stearic acid (18:0), EPA (20:5 ω 3) and DHA (22:6 ω 3) in the lipidic extracts and LUVs.

Fatty acids	Lipidic extracts (g/L)	LUVs (g/L)
Stearic acid	1.3 \pm 0.4	90.4 \pm 29.1
EPA	1.5 \pm 0.6	99.5 \pm 38.1
DHA	0.6 \pm 0.3	41.3 \pm 17.1

3.4.2. PC liposomes characterization

The size, PDI and zeta potential of the liposomes prepared from PC are present in Table 3.2. The size and PDI of the liposomes with and without diclofenac was similar, however, the addition of diclofenac to the LUVs increased significantly their zeta potential.

Table 3.2. Size, PDI and zeta potential of PC liposomes with and without diclofenac (DF).

LUVs	Size (nm)	PDI	Zeta potential (mV)
PC	123.6 \pm 4.44	0.05 \pm 0.02	-3.6 \pm 0.82
PC with DF	123.2 \pm 15.68	0.18 \pm 0.06	-33.0 \pm 2.86

3.4.3. Erythrocyte-derived liposomes characterization

The incorporation of diclofenac into liposomes resulted in an increase in size, PDI and zeta potential modulus, however this increase was not statistically significant (Table 3.3.).

Table 3.3. Size, PDI and zeta potential of erythrocyte-derived (ED) liposomes with and without diclofenac (DF).

LUVs	Size (nm)	PDI	Zeta potential (mV)
ED LUVs	221.8 \pm 55.2	0.35 \pm 0.10	-40.2 \pm 11.0
ED LUVs with DF	296.5 \pm 58.1	0.43 \pm 0.08	-51.6 \pm 12.2

The concentration of phospholipids and cholesterol present after LUVs preparation are present in Table 3.4. The ratio of cholesterol and phosphorus was approximately 0.9 (Table 3.4.). The amount of diclofenac incorporated into liposomes with a phospholipid concentration of 650.0 \pm 438.7 μ M and a cholesterol concentration of 534.4 \pm 50.28 μ M was of 192.7 \pm 30.8 μ M.

Table 3.4. Concentration of phosphorus, cholesterol and diclofenac in erythrocyte-derived (ED) liposomes.

LUVs	Phosphorus (μ M)	Cholesterol (μ M)	Cholesterol/ phosphorus ratio
ED LUVs	866.7 \pm 485.3	764.0 \pm 109.6	0.88

The morphology of the erythrocyte-based liposomes with and without diclofenac was assessed by STEM, revealing well defined structures with a characteristic circular shape (Figure 3.1.).

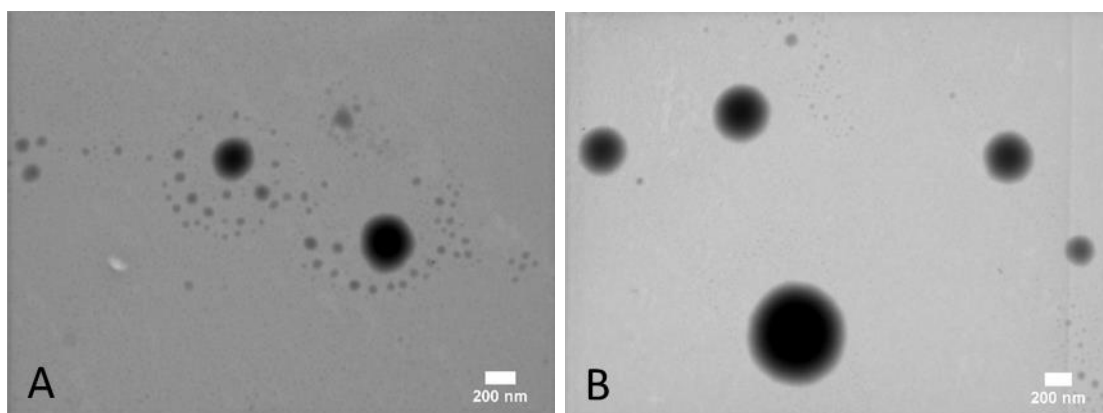


Figure 3.1. STEM images of erythrocyte-derived LUVs (A) and erythrocyte-derived LUVs incorporating diclofenac (B).

3.4.4. Thermal stability of erythrocyte-based liposomes

The thermal stability of the developed LUVs was assessed using DSC. The thermograms of the erythrocyte-based liposomes showed two distinct endothermic peaks at 58.8 ± 10.7 °C and 243.3 ± 0.2 °C and one exothermic peak at 295.7 ± 2.5 °C (Figure 3.2.). The thermograms of the erythrocyte-based liposomes incorporating diclofenac presented four endothermic peaks at 67.6 ± 2.3 , 110.8 ± 0.6 , 245.2 ± 4.6 and 264.5 ± 3.2 °C, and one exothermic peak, at 296.4 ± 3.1 °C (Figure 3.2.). The onset temperature of the first peak, indicating the temperature at which the sample started to transition to the fluid state, and the enthalpy of the transition was 17.5 ± 3.6 °C and 109.4 ± 12.4 J/g for the empty erythrocyte-derived liposomes and 23.8 ± 3.4 °C and 76.6 ± 16.6 J/g for the liposomes with diclofenac, respectively.

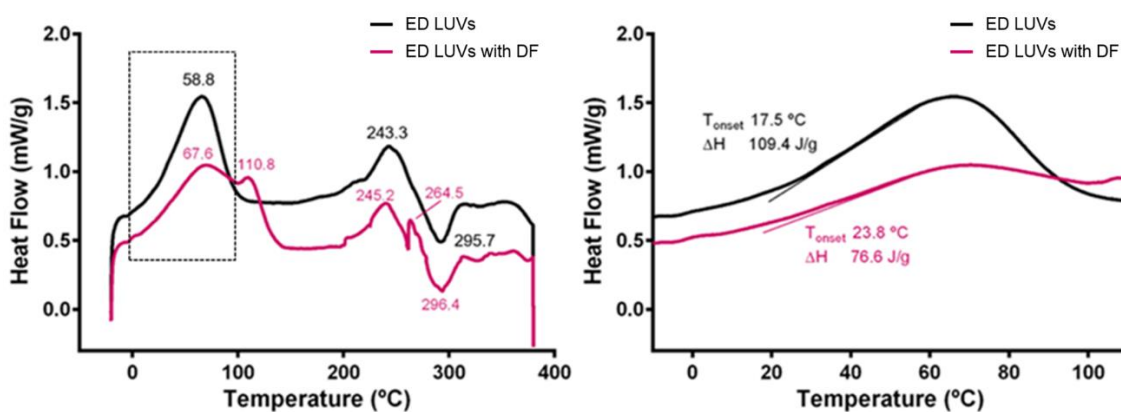


Figure 3.2. DSC Thermograms of the erythrocyte-derived (ED) liposomes encapsulating or not diclofenac (DF).

3.4.5. Biological assays

Different biological assays were conducted to assess cell metabolic activity (Alamar Blue assay), proliferation (DNA quantification) and morphology (SEM) after exposure to erythrocyte-based liposomes with and without diclofenac as well as free drug.

The study of the effect of liposomes prepared with lipids extracted from erythrocyte membranes or PC on non-stimulated macrophages, revealed that the metabolic activity and cell proliferation was similar to the control and that there were no significant differences between the all the tested conditions (Figure 3.3.).

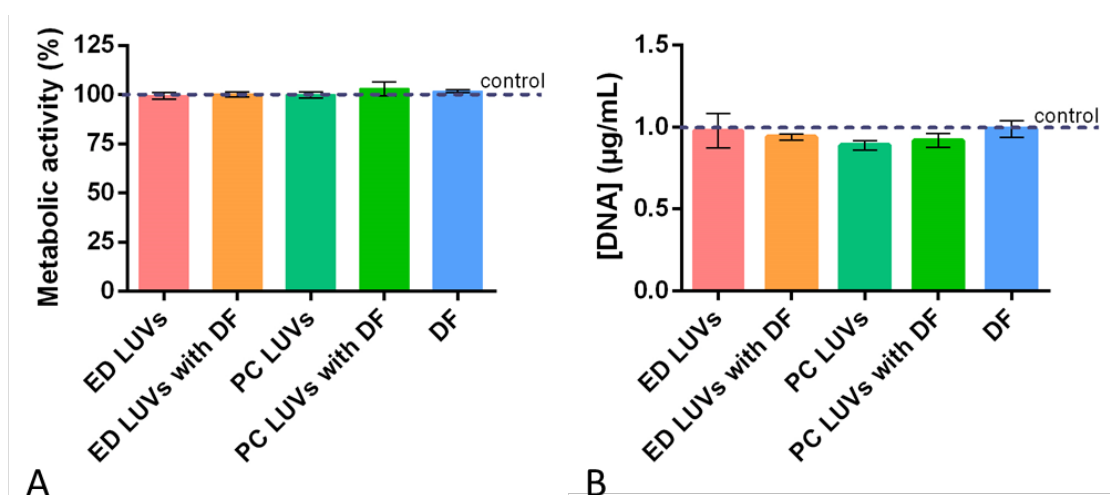


Figure 3.3. Metabolic activity (A) and cell proliferation (B) of non-stimulated macrophages in the presence of either LUVs prepared with erythrocytes membranes lipids or PC (phospholipid concentration of $\sim 124 \mu\text{M}$) incorporating or not diclofenac (DF)) and of the free drug ($55 \mu\text{M}$, concentration similar to the one incorporated in the PC and erythrocyte-derived (ED) LUVs).

In the assays performed with LPS-stimulated THP-1 cells, there were also no significant differences in the metabolic activity of the macrophages between all the tested conditions, namely erythrocyte-based liposomes with and without diclofenac, liposomes made with PC and free NSAID, and the control (without addition of liposomes formulations or free drug, Figure 3.4.).

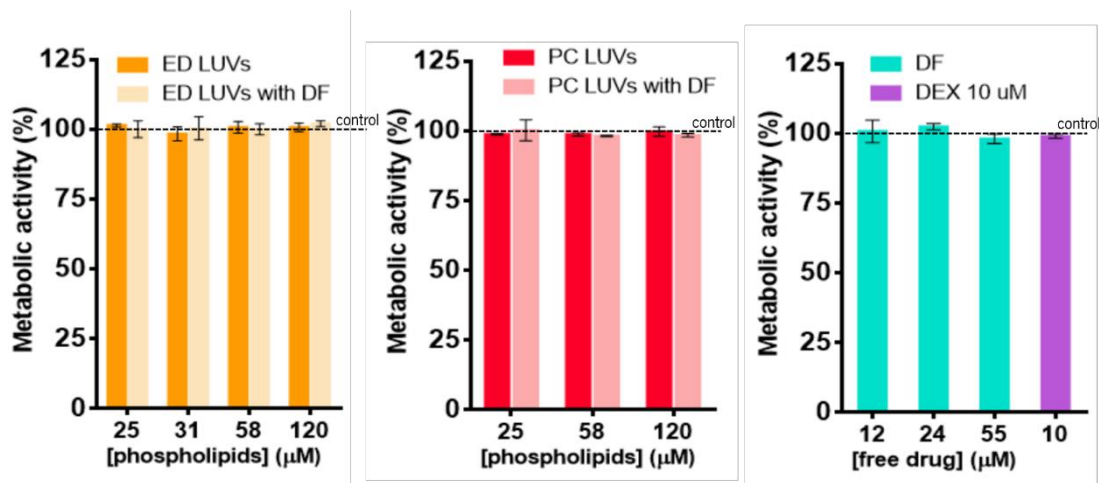


Figure 3.4. Metabolic activity of LPS-stimulated macrophages. Cells were incubated with different phospholipid concentrations of erythrocyte-derived (ED) LUVs (25, 31, 58, 120 μM), PC LUVs (25, 58 and 120 μM) and free diclofenac (DF; 12, 24 and 55 μM). LPS-stimulated macrophages exposed to culture medium were used as control (100%). The ED LUVs with a phospholipid concentration of 31 μM are also functionalized with FA. The concentrations of diclofenac used correspond to the amount incorporated in the DF-loaded erythrocyte-derived and PC LUVs. No significant differences were noted.

The proliferation of the cells after exposure to the different liposomes compositions and free drugs was also assayed. Again, there were no significant differences in the DNA quantification of the cells exposed to the liposomes formulations and free drugs when compared to the control (Figure 3.5.).

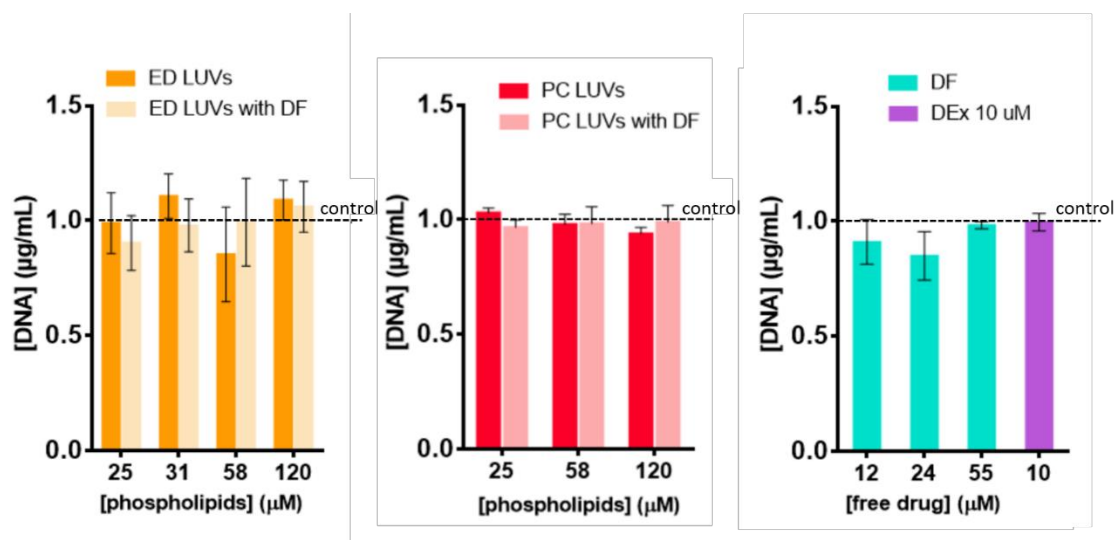


Figure 3.5. Cell proliferation of LPS-stimulated macrophages. Cells were incubated with different phospholipid concentrations of erythrocyte-derived (ED) LUVs (25, 31, 58, 120 μM), PC LUVs (25, 58 and 120 μM) and free diclofenac (DF; 12, 24 and 55 μM). LPS-stimulated macrophages with just culture medium were used as control (100%). The ED LUVs with a phospholipid concentration of 31 μM are also functionalized with FA. The concentrations of diclofenac used correspond to the amount incorporated in the DF-loaded erythrocyte-derived and PCLUVs. No significant differences were noted.

SEM micrographs of the cells exposed to the erythrocyte-based liposomes with and without diclofenac are present in Figure 3.6. There were no noticeable morphological differences when compared to the control (Figure 3.6.), which is in agreement with the results obtained in previous assays.

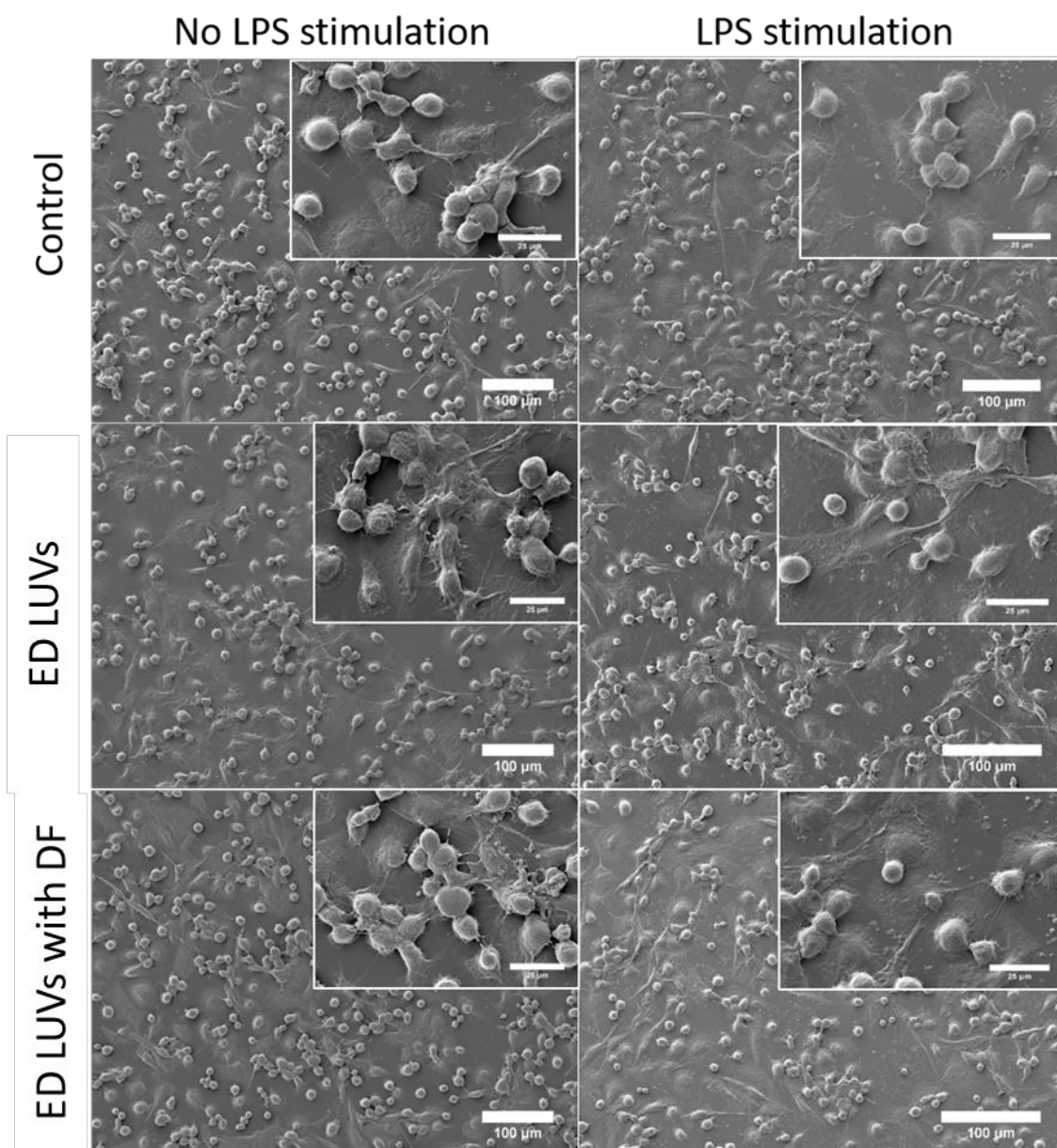


Figure 3.6. SEM micrographs of non-stimulated macrophages and LPS stimulated macrophages in the presence of cell medium (control), empty erythrocyte-derived liposomes (ED LUVs) or incorporating diclofenac (ED LUVs with DF).

3.4.6. Anti-inflammatory activity of the LUVs

The anti-inflammatory activity of the developed liposomes was assessed by quantifying the amount in the media of the pro-inflammatory cytokines IL-6 and TNF- α produced by LPS-stimulated macrophages. Macrophages cultured with LPS-free medium or LPS medium with dexamethasone were used as a negative control and LPS-stimulated macrophages with just RPMI medium (control) were used as a positive control of the pro-inflammatory cytokines production.

The concentration of IL-6 in the medium of cells exposed to erythrocyte-based liposomes was significantly lower than of the controls, PC liposomes and free diclofenac (Figure 3.7.). Moreover,

cytocompatible concentrations of erythrocyte-derived LUVs, with or without diclofenac, (phospholipid concentration of 120 μM), presented similar effects to dexamethasone in reducing IL-6. However, there were no significant differences between the reduction of the IL-6 amount for empty erythrocyte-based liposomes and containing diclofenac for all tested concentrations.

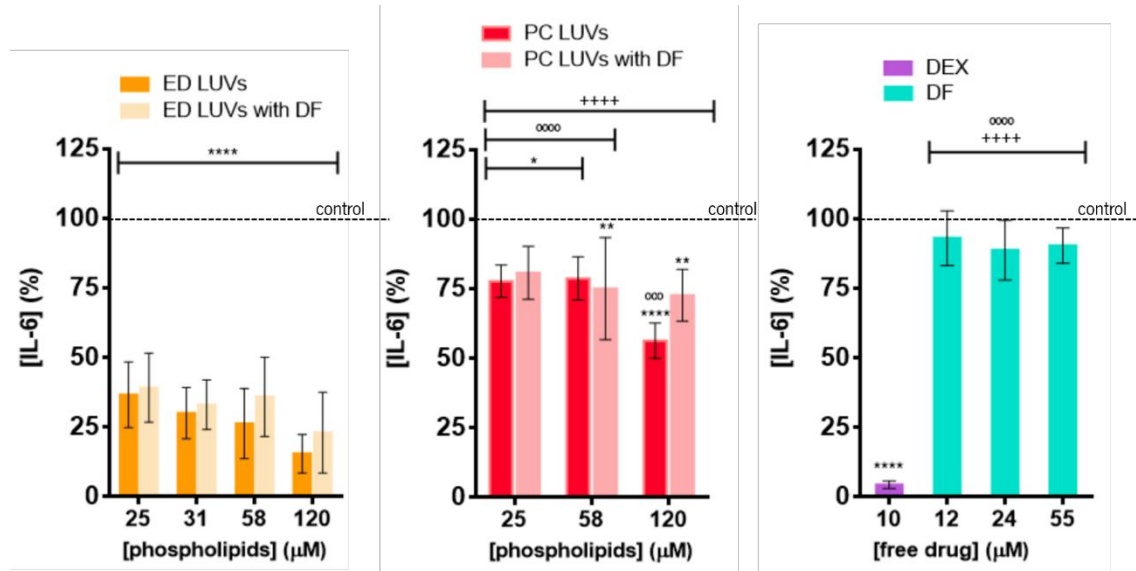


Figure 3.7. Concentration of IL-6 produced by LPS-stimulated macrophages Cells were incubated with different phospholipid concentrations of erythrocyte-derived (ED) LUVs (25, 31, 58, 120 μM), PC LUVs (25, 58 and 120 μM) and free diclofenac (DF; 12, 24 and 55 μM). LPS-stimulated macrophages with just culture medium were used as control (100%). The ED LUVs with a phospholipid concentration of 31 μM are also functionalized with FA. The concentrations of diclofenac used correspond to the amount incorporated in the DF-loaded erythrocyte-derived and PC LUVs. The symbols denote significant differences versus the control (*), versus the ED LUVs (+) and versus the ED LUVs with DF (°). * $p < 0.0361$, ** $p < 0.0044$, **** $p < 0.0001$, + $p < 0.0460$, ++ $p < 0.0017$, +++ $p < 0.0001$, °° $p < 0.0012$, °°° $p < 0.0007$, °°°° $p < 0.0001$.

The concentration of TNF- α in the medium of cells exposed to erythrocyte-based liposomes was also significantly lower than the controls, PC liposomes and free diclofenac (Figure 3.8.). When compared to dexamethasone, the erythrocyte-derived LUVs were similar in reducing TNF- α and the erythrocyte-based liposomes incorporating diclofenac were superior in reducing TNF- α .

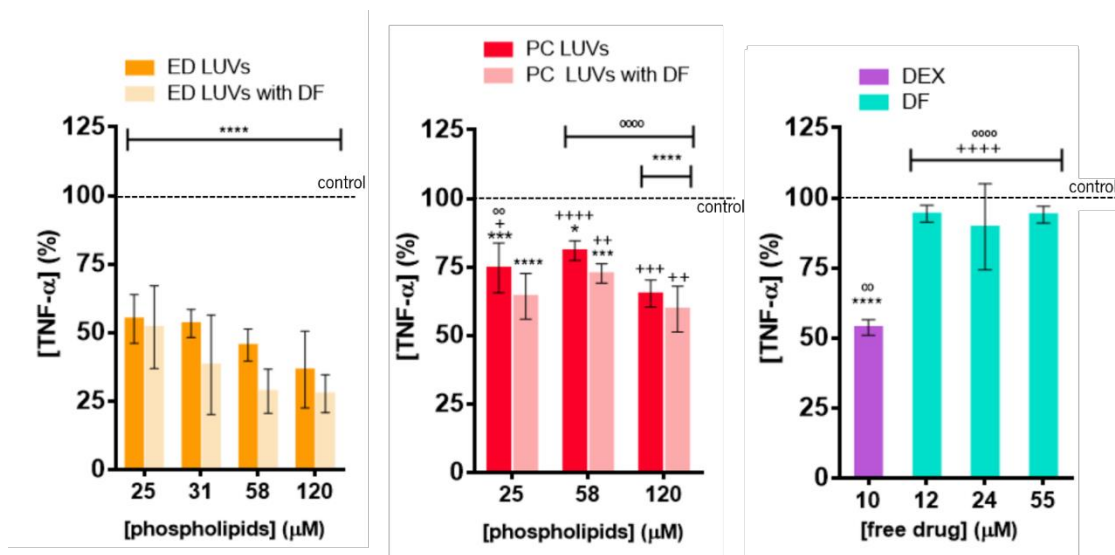


Figure 3.8. Concentration of TNF- α produced by LPS-stimulated macrophages. Cells were incubated or not (control; 100%; stimulation with LPS) with different concentrations (25, 31, 58 and 120 μ M) of erythrocyte-derived (ED) LUVs, (25, 58, 120 μ M) of PC LUVs, (12, 24 and 55 μ M) free diclofenac and (10 μ M) dexamethasone. The ED LUVs with a phospholipid concentration of 31 μ M were functionalized with FA. The concentrations of diclofenac used correspond to the amount incorporated in the DF loaded erythrocyte-derived LUVs. The symbols denote significant differences versus the control (*), versus the ED LUVs (+) and versus the ED LUVs with DF ($^{\circ}$). * p < 0.0183, ** p < 0.0010, **** p < 0.0001, + p < 0.0233, ++ p < 0.0060, +++ p < 0.0006, ++++ p < 0.0001, $^{\circ\circ}$ p < 0.0073 and $^{\circ\circ\circ}$ p < 0.0001.

3.5. Discussion

The main aim of the present work was to extract lipids from erythrocytes membranes to prepare liposomes with intrinsic anti-inflammatory therapeutic properties. The erythrocyte-derived liposomes were characterized, and their drug entrapment ability and anti-inflammatory activity were evaluated to assess their potential to be used as bioactive drug-delivery systems for the treatment of inflammatory diseases. Indeed, liposomes are composed by a phospholipid bilayer, resembling the structure of cell membranes, and are widely used as carriers for drug delivery [39].

As any animal cell membrane, erythrocyte membranes are formed by a bilayer of phospholipids with intercalated cholesterol, proteins and carbohydrates [29–30]. Specifically, their membranes are rich in essential fatty acids and cholesterol (cholesterol/phospholipid ratio of 0.9) [40–41]. Accordingly, the lipidic extracts obtained from the erythrocyte membranes, contained essential fatty acids, namely omega-3 fatty acids EPA and DHA, which are also present after LUVs preparation (Table 3.1.). As phospholipids are constituted by one phosphorus group, it is possible to determine their concentration in a liposome sample by determining the concentration of this mineral, using, e.g., the Bartlett method. Thus, the concentration of phospholipids, in the erythrocyte-derived liposomes was determined, as well as the concentration of cholesterol. Indeed,

the concentration of cholesterol determined in the erythrocyte-derived liposomes resulted in a cholesterol ($764.0 \pm 109.6 \mu\text{M}$) and phospholipid ($866.7 \pm 485.3 \mu\text{M}$) high ratio, which is in accordance with the reported values for the erythrocyte membranes (~ 0.9 , Table 3.4.) [42]. These results suggest that the extraction performed allowed to successfully obtain the phospholipids and cholesterol from the erythrocyte's membranes.

To demonstrate the ability of the developed erythrocyte-derived liposomes as drug delivery devices, diclofenac was used as a model drug. Diclofenac is a widely prescribed NSAID for the treatment of inflammatory diseases, such as osteoarthritis and rheumatoid arthritis [43–45]. The concentration of this drug entrapped into liposomes ($192.7 \pm 30.8 \mu\text{M}$) is superior to its reported therapeutic concentrations, after topical and oral administration, in the synovial fluid (0.006 ± 0.002 and $0.053 \pm 0.038 \mu\text{M}$, respectively) and in plasma (0.015 ± 0.006 and $0.021 \pm 0.014 \mu\text{M}$, respectively) [46]. Consequently, the concentration of this NSAID entrapped into LUVs can reduce the inflammatory response.

The produced erythrocyte-derived LUVs incorporating or not diclofenac presented a heterogeneous size, a significant negative zeta potential and a spherical shape (Table 3.3. and Figure 3.1.). Indeed, the size of the liposomes allows their classification as LUVs [47–48]. Moreover, it is reported in drug delivery applications using lipid-based carriers that a PDI of 0.3 is acceptable and indicates a homogenous population of phospholipid vesicles [49]. As both formulations had PDI values slightly higher than 0.3, they can be considered as having a low level of heterogeneity. The encapsulation of diclofenac led to an increase of LUVs size, however this was not statistically significant (Table 3.3. and Figure 3.1.). On both formulations, the zeta potential was significantly negative. This can be due to the presence of negatively charged phospholipids, which is a main phospholipid of erythrocyte membranes [50]. Furthermore, a decrease in the zeta potential for more negative values was obtained for the liposomes incorporating diclofenac, comparing with the empty ones. Diclofenac has a negative charge in solution and can partition into the lipid bilayer, affecting the net charge of the liposomes and leading to a more negative surface charge [16]. Moreover, the value of zeta potential can be used to predict particles aggregation, with a high module of zeta potential being associated with less possibility of aggregation and, therefore, more stable vesicles suspensions [51]. Both zeta potentials determined for erythrocyte-derived liposomes formulations have a high modulus, suggesting a favourable non-aggregating behaviour.

Another important characteristic of liposomes is their thermal stability. The phase-transition temperature is specific for each phospholipid and depends on its acyl chains lengths, degree of

unsaturation and geometry and location of the double bounds along the chains [52]. Consequently, mixtures of phospholipids can exhibit a complex thermal behaviour [53]. In the present work, two endothermic peaks and one exothermic peak were identified for the empty erythrocyte-derived liposomes and four endothermic peaks and one exothermic peak for the liposomes incorporating diclofenac (Figures 3.2 and 3.3.). Therefore, this thermal behaviour, with a broad peak and high transition temperature, can be attributed to the presence of multiple phospholipids as well as cholesterol. The role of cholesterol in the model lipid bilayers, namely with dipalmitoylphosphatidylcholine liposomes, has been studied, and the results revealed the broadening of the main lipid phase transition peak, which is in accordance with the results here obtained [52]. The onset temperatures of the first endothermic peak for the empty liposomes and incorporating diclofenac (17.5 °C and 23.8 °C, respectively) suggest that at 37 °C the lipids already started to transition from gel to fluid, though the transition is not complete [52]. The fact that the liposomes are not completely fluid is an advantage for clinical application, as it reduces the risk of the drug leaking before reaching the desired target site.

Although the target of the erythrocyte-derived liposomes is the activated macrophages, their effect in the metabolic activity and proliferation of non-stimulated macrophages were also evaluated. The addition of the erythrocyte-derived LUVs did not affect the metabolic activity (Figures 3.4 and 3.5.) nor the proliferation (Figures 3.4 and 3.6.) of both non-stimulated and LPS-stimulated macrophages. This result indicates that the macrophages maintain their biological activity in the presence of the LUVs, which supports the potential of erythrocyte-derived liposomes as drug carriers.

The SEM micrographs (Figure 3.7.) of the monocyte-differentiated macrophages (PMA-stimulated THP-1) after addition of erythrocyte-derived liposomes with and without diclofenac, showed their adherence to wells surface and the presence of membrane ruffling and pseudopodia. These features are in accordance with the reported morphology of healthy macrophages, indicating that the exposure to liposomes did not affect the macrophages morphology [54]. The expected morphology was also verified with the LPS-stimulated macrophages after contact with the erythrocyte-derived liposomes with and without diclofenac (Figure 3.7).

In an inflammatory scenario, activated (M1) macrophages release several pro-inflammatory mediators, including IL-6 and TNF- α , which have key roles in the chronic inflammatory response. Thus, the anti-inflammatory activity of the erythrocyte-derived LUVs was evaluated by their ability to decrease the concentration of these pro-inflammatory cytokines. LUVs activity was very different

in some conditions (corroborated by high SD, Figure 3.7), which can be dependent of the donor's erythrocytes lipid content, varying according to their diet (e.g. rich or not in fish). However, all erythrocyte-derived LUVs were able to significantly decrease the concentration of both cytokines, particularly of IL-6 (Figures 3.8. and 3.9). The erythrocyte-derived LUVs functionalized with folic acid (phospholipid concentration of 31 μM) had a similar behaviour to non-functionalized liposomes. This was expected since in this study the liposomes are readily available for interaction with the desired cells. Moreover, the anti-inflammatory performance of the erythrocyte-derived LUVs was significantly superior to the PC LUVs for both cytokines (Figures 3.8 and 3.9). PC LUVs were used for comparison, as these widely used drug carriers are associated to anti-inflammatory effects [55–56]. The superior anti-inflammatory activity observed for the erythrocyte-derived LUVs can be due to the presence of a high amount of omega-3 fatty acids EPA and DHA. These essential fatty acids, integral components of the erythrocyte membranes, have strong anti-inflammatory properties [57–59]. Indeed, the PC source usually used didn't have significant concentrations of EPA and DHA in its composition [60].

The erythrocyte-derived liposomes incorporating diclofenac had overall better performance than the PC LUVs incorporating diclofenac. Moreover, the anti-inflammatory performance of the erythrocyte-derived LUVs containing or not diclofenac was superior to the free drug in similar concentrations. There were also no significant differences in the reduction of IL-6 and TNF- α by empty and diclofenac-loaded erythrocyte-based LUVs. This can be explained by the mechanism of action of diclofenac, involving mainly the inhibition of COX-2 and not directly IL-6 and TNF- α production. Moreover, cytocompatible concentrations of erythrocyte-derived LUVs (phospholipid concentration of 120 μM) presented similar effects to dexamethasone, a potent anti-inflammatory drug, in reducing IL-6 and TNF- α amounts [47]. Indeed, comparing with dexamethasone, the erythrocyte-derived liposomes incorporating diclofenac had a similar effect in the reduction of IL-6, but induced a superior decrease of TNF- α amount. This reinforces the anti-inflammatory action of the prepared erythrocyte-derived LUVs, since dexamethasone was used as a positive control in the reduction of pro-inflammatory cytokines and is widely used in the treatment of anti-inflammatory diseases [61–62].

Consequently, this suggests that the liposomes by themselves can reduce the production of cytokines and, thus, inflammation, fostering their capability as drug carriers that can act synergistically with the incorporated drug in the treatment of inflammatory conditions.

3.6. Conclusions

Erythrocytes were advantageously used in the present work as a source of lipids to produce liposomes.

The developed erythrocyte-derived LUVs were successfully characterized and present the ability to encapsulate clinically relevant amounts of diclofenac at cytocompatible concentrations. Moreover, due to the presence of omega 3 EPA and DHA fatty acids, the erythrocyte-derived LUVs functionalized with folic acid, to specifically target activated macrophages, were able to drastically reduce the concentration of relevant pro-inflammatory cytokines, namely IL-6 and TNF- α .

Strikingly, the anti-inflammatory performance of the prepared erythrocyte-derived LUVs is superior to established and commonly used PC liposomes, as well as to free diclofenac. Moreover, cytocompatible concentrations of erythrocyte-derived LUVs formulations presented similar or higher effects than dexamethasone, a potent anti-inflammatory drug, in reducing IL-6 and TNF- α . This behaviour highlights the anti-inflammatory properties of the erythrocyte-derived LUVs that can act synergistically with the entrapped anti-inflammatory drugs.

Overall, the developed erythrocyte-derived liposomes show a great potential to be used as drug-delivery systems for the treatment of anti-inflammatory diseases.

3.7. References

- [1] R. H. Straub and C. Schradin, "Chronic inflammatory systemic diseases – an evolutionary trade-off between acutely beneficial but chronically harmful programs," *Evol. Med. Public Heal.*, vol. 2016 (1), pp. 37–51, 2016.
- [2] World Health Organization, *Noncommunicable Diseases Country Profiles 2018*. 2018.
- [3] O. Soehnlein, S. Steffens, A. Hidalgo, and C. Weber, "Neutrophils as protagonists and targets in chronic inflammation," *Nat. Rev. Immunol.*, vol. 17, no. 4, pp. 248–261, 2017.
- [4] R. Medzhitov, "Inflammation 2010: New Adventures of an Old Flame," *Cell*, vol. 140, no. 6, pp. 771–776, 2010.
- [5] D. Okin and R. Medzhitov, "Evolution of inflammatory diseases," *Curr. Biol.*, vol. 22, no. 17, pp. R733–R740, 2012.
- [6] J. Vandewalle, A. Luypaert, K. De Bosscher, and C. Libert, "Therapeutic Mechanisms of Glucocorticoids," *Trends Endocrinol. Metab.*, vol. 29, no. 1, pp. 42–54, 2018.
- [7] N. Osafo, C. Agyare, D. D. Obiri, and A. O. Antwi, "Mechanism of Action of Nonsteroidal Anti-Inflammatory Drugs," in *Nonsteroidal Anti-Inflammatory Drugs*, InTech, 2017, p. 13.
- [8] C. Baigent *et al.*, "Vascular and upper gastrointestinal effects of non-steroidal anti-inflammatory drugs: Meta-analyses of individual participant data from randomised trials," *Lancet*, vol. 382, no. 9894, pp. P769-779, 2013.
- [9] P. McGettigan and D. Henry, "Use of Non-Steroidal Anti-Inflammatory Drugs That Elevate Cardiovascular Risk: An Examination of Sales and Essential Medicines Lists in Low-, Middle-, and High-Income Countries," *PLoS Med.*, vol. 10, no. 2, p. e1001388, 2013.
- [10] A. Ogata *et al.*, "Phase III study of the efficacy and safety of subcutaneous versus intravenous tocilizumab monotherapy in patients with rheumatoid arthritis," *Arthritis Care Res.*, vol. 66, no. 3, pp. 344–354, 2014.
- [11] T. Takeuchi, J. S. Smolen, E. H. Choy, D. Aletaha, I. McInnes, and S. A. Jones, "Considering new lessons about the use of IL-6 inhibitors in arthritis," *Considerations Med.*, vol. 2, no. 1, 2018.
- [12] Y. Yoshida and T. Tanaka, "Interleukin 6 and rheumatoid arthritis," *Biomed Res. Int.*, vol. 2014, p. 698313, 2014.
- [13] A. C. Cannella, "Traditional DMARDs: Methotrexate, Leflunomide, Sulfasalazine, Hydroxychloroquine, and Combination Therapies," in *Kelley and Firestein's Textbook of Rheumatology*, 10th ed., Philadelphia: Elsevier, 2017, pp. 958-982.e7.

- [14] I. Padjen, "Drugs Used in Rheumatic Disease," in *Handbook of Systemic Autoimmune Diseases*, vol. 15, Elsevier, 2018, pp. 39–76.
- [15] H. Ferreira, M. Lúcio, J. L. F. C. Lima, C. Matos, and S. Reis, "Interaction of clonixin with EPC liposomes used as membrane models," *J. Pharm. Sci.*, vol. 94, no. 6, pp. 1277–1287, 2005.
- [16] H. Ferreira, M. Lúcio, J. L. F. C. Lima, C. Matos, and S. Reis, "Effects of diclofenac on EPC liposome membrane properties," *Anal. Bioanal. Chem.*, vol. 382, no. 5, pp. 1256–1264, 2005.
- [17] G. Bozzuto and A. Molinari, "Liposomes as nanomedical devices," *Int. J. Nanomedicine*, vol. 10, pp. 975–999, 2015.
- [18] B. S. Pattni, V. V. Chupin, and V. P. Torchilin, "New Developments in Liposomal Drug Delivery," *Chem. Rev.*, vol. 115, no. 19, pp. 10938–10966, 2015.
- [19] H. Bardania, S. Tarvirdipour, and F. Dorkoosh, "Liposome-targeted delivery for highly potent drugs," *Artif. Cells, Nanomedicine Biotechnol.*, vol. 45, no. 8, pp. 1478–1489, 2017.
- [20] K. Gardikis, C. Tsimplouli, K. Dimas, M. Micha-Screttas, and C. Demetzos, "New chimeric advanced Drug Delivery nano Systems (chi-aDDnSs) as doxorubicin carriers," *Int. J. Pharm.*, vol. 402, no. 1–2, pp. 231–237, 2010.
- [21] J. A. Silverman and S. R. Deitcher, "Marqibo® (vincristine sulfate liposome injection) improves the pharmacokinetics and pharmacodynamics of vincristine," *Cancer Chemother. Pharmacol.*, vol. 71, no. 3, pp. 555–564, 2013.
- [22] V. Usonis and V. Bakasénas, "Antibody titres after primary and booster vaccination of infants and young children with a virosomal hepatitis A vaccine (Epaxal®)," *Vaccine*, vol. 21, no. 31, pp. 4588–4592, 2003.
- [23] D. Dehaini *et al.*, "Erythrocyte-Platelet Hybrid Membrane Coating for Enhanced Nanoparticle Functionalization," *Adv. Mater.*, vol. 29, no. 16, p. 1606209, 2017.
- [24] Q. Jiang *et al.*, "Erythrocyte-cancer hybrid membrane-camouflaged melanin nanoparticles for enhancing photothermal therapy efficacy in tumors," *Biomaterials*, vol. 192, no. 2019, pp. 292–308, 2019.
- [25] A. H. Bryk and J. R. Wiśniewski, "Quantitative Analysis of Human Red Blood Cell Proteome," *J. Proteome Res.*, vol. 16, no. 8, pp. 2752–2761, 2017.
- [26] L. A. L. Fliervoet and E. Mastrobattista, "Drug delivery with living cells," *Adv. Drug Deliv. Rev.*, vol. 106, pp. 63–72, 2016.

- [27] M. Magnani and L. Rossi, "Approaches to erythrocyte-mediated drug delivery," *Expert Opin. Drug Deliv.*, vol. 11, no. 5, pp. 677–687, 2014.
- [28] P. C. Calder, "n-3 Polyunsaturated fatty acids, inflammation, and inflammatory diseases," *Am. J. Clin. Nutr.*, vol. 83, no. 6 Suppl, pp. 1505S-1519S, 2006.
- [29] P. C. Calder, "n-3 fatty acids, inflammation, and immunity - Relevance to postsurgical and critically ill patients," *Lipids*, vol. 39, no. 12, pp. 1147–1161, 2004.
- [30] D. S. Siscovick, "Dietary intake and cell membrane levels of long-chain n-3 polyunsaturated fatty acids and the risk of primary cardiac arrest," *JAMA J. Am. Med. Assoc.*, vol. 274, no. 17, pp. 1363–1367, 2003.
- [31] C. M. Albert *et al.*, "Blood Levels of Long-Chain n-3 Fatty Acids and the Risk of Sudden Death," *N. Engl. J. Med.*, vol. 346, no. 15, pp. 1113–1118, 2002.
- [32] R. N. Lemaitre, I. B. King, D. Mozaffarian, L. H. Kuller, R. P. Tracy, and D. S. Siscovick, "n-3 polyunsaturated fatty acids, fatal ischemic heart disease, and nonfatal myocardial infarction in older adults: The Cardiovascular Health Study," *Am. J. Clin. Nutr.*, vol. 77, no. 2, pp. 319–25, 2003.
- [33] P. S. Low, W. A. Henne, and D. D. Doorneweerd, "Discovery and development of folic-acid-based receptor targeting for imaging and therapy of cancer and inflammatory diseases," *Acc. Chem. Res.*, vol. 41, no. 1, pp. 120–9, 2008.
- [34] A. C. Lima, H. Ferreira, R. L. Reis, and N. M. Neves, "Biodegradable polymers: an update on drug delivery in bone and cartilage diseases," *Expert Opin. Drug Deliv.*, vol. 16, no. 8, pp. 795–813, 2019.
- [35] H. G. Rose and M. Oklander, "Improved Procedure for the Extraction of Lipids From Human Erythrocytes," *J. Lipid Res.*, vol. 6, pp. 428–431, 1965.
- [36] G. R. Bartlett, "Phosphorus assay in column chromatography," *J. Biol. Chem.*, vol. 234, no. 3, pp. 466–8, Mar. 1959.
- [37] D. R. P. Loureiro *et al.*, "Yicathins B and C and Analogues: Total Synthesis, Lipophilicity and Biological Activities," *ChemMedChem*, vol. 15, no. 9, pp. 749–755, 2020.
- [38] A. C. Lima, C. Cunha, A. Carvalho, H. Ferreira, and N. M. Neves, "Interleukin-6 Neutralization by Antibodies Immobilized at the Surface of Polymeric Nanoparticles as a Therapeutic Strategy for Arthritic Diseases," *ACS Appl. Mater. Interfaces*, vol. 10, no. 16, pp. 13839–13850, 2018.
- [39] U. Bulbake, S. Doppalapudi, N. Kommineni, and W. Khan, "Liposomal formulations in

- clinical use: An updated review," *Pharmaceutics*, vol. 9, no. 2, p. 12, 2017.
- [40] S. J. Singer and G. L. Nicolson, "The fluid mosaic model of the structure of cell membranes," *Science (80-.)*, vol. 175, no. 4023, pp. 720–731, 1972.
- [41] Y. Yawata, "Composition of Normal Red Cell Membranes," in *Cell Membrane*, 2004, pp. 27–46.
- [42] Y. Yawata, "Composition of Normal Red Cell Membranes," in *Cell Membrane: The Red Blood Cell as a Model*, Wiley-VCH, 2003, pp. 27–46.
- [43] T. J. Gan, "Diclofenac: An update on its mechanism of action and safety profile," *Curr. Med. Res. Opin.*, vol. 26, no. 7, pp. 1715–31, 2010.
- [44] K. Pavelka, "A comparison of the therapeutic efficacy of diclofenac in osteoarthritis: a systematic review of randomised controlled trials," *Curr. Med. Res. Opin.*, vol. 28, no. 1, pp. 163–178, 2012.
- [45] L. J. Crofford, "Use of NSAIDs in treating patients with arthritis," *Arthritis Res. Ther.*, vol. 15, no. S3, p. S2, 2013.
- [46] S. Miyatake, H. Ichiyama, E. Kondo, and K. Yasuda, "Randomized clinical comparisons of diclofenac concentration in the soft tissues and blood plasma between topical and oral applications," *Br. J. Clin. Pharmacol.*, vol. 67, no. 1, pp. 125–129, 2009.
- [47] S. Emami, S. Azadmard-Damirchi, S. H. Peighambaroust, H. Valizadeh, and J. Hesari, "Liposomes as carrier vehicles for functional compounds in food sector," *J. Exp. Nanosci.*, vol. 11, no. 9, pp. 737–759, 2016.
- [48] R. Nisini, N. Poerio, S. Mariotti, F. De Santis, and M. Fraziano, "The Multirole of Liposomes in Therapy and Prevention of Infectious Diseases," *Front. Immunol.*, vol. 9, p. 155, 2018.
- [49] M. Danaei *et al.*, "Impact of Particle Size and Polydispersity Index on the Clinical Applications of Lipidic Nanocarrier Systems," *Pharmaceutics*, vol. 10, no. 2, p. 57, 2018.
- [50] J. A. Virtanen, K. H. Cheng, and P. Somerharju, "Phospholipid composition of the mammalian red cell membrane can be rationalized by a superlattice model," *Proc. Natl. Acad. Sci.*, vol. 95, no. 9, pp. 4964–4969, 1998.
- [51] M. C. Smith, R. M. Crist, J. D. Clogston, and S. E. McNeil, "Zeta potential: a case study of cationic, anionic, and neutral liposomes," *Anal. Bioanal. Chem.*, vol. 409, no. 24, pp. 5779–5787, 2017.
- [52] C. Demetzos, "Differential Scanning Calorimetry (DSC): A Tool to Study the Thermal Behavior of Lipid Bilayers and Liposomal Stability," *J. Liposome Res.*, vol. 18, no. 3, pp.

159–173, 2008.

- [53] J. Li *et al.*, “A review on phospholipids and their main applications in drug delivery systems,” *Asian J. Pharm. Sci.*, vol. 10, no. 2, pp. 81–98, 2015.
- [54] S. Douglas and A. Douglas, “Part VIII,” in *Williams Hematology*, 2016, pp. 1045–1073.
- [55] I. Treede *et al.*, “Anti-inflammatory Effects of Phosphatidylcholine,” *J. Biol. Chem.*, vol. 282, no. 37, pp. 27155–27164, 2007.
- [56] J. M. Metselaar and G. Storm, “Liposomes in the treatment of inflammatory disorders,” *Expert Opin. Drug Deliv.*, vol. 2, no. 3, pp. 465–476, May 2005.
- [57] M. E. Schober *et al.*, “Docosahexaenoic acid decreased neuroinflammation in rat pups after controlled cortical impact,” *Exp. Neurol.*, vol. 320, p. 112971, 2019.
- [58] J. Cao, K. A. Schwichtenberg, N. Q. Hanson, and M. Y. Tsai, “Incorporation and clearance of omega-3 fatty acids in erythrocyte membranes and plasma phospholipids,” *Clin. Chem.*, vol. 52, no. 12, pp. 2265–2272, 2006.
- [59] R. Wall, R. P. Ross, G. F. Fitzgerald, and C. Stanton, “Fatty acids from fish: the anti-inflammatory potential of long-chain omega-3 fatty acids,” *Nutr. Rev.*, vol. 68, no. 5, pp. 280–289, 2010.
- [60] Sigma, “L- α -Phosphatidylcholine.”
<https://www.sigmaaldrich.com/catalog/product/sigma/p3556?lang=pt®ion=PT>
(accessed Feb. 19, 2019).
- [61] K. D. Huebner, N. G. Shrive, and C. B. Frank, “Dexamethasone inhibits inflammation and cartilage damage in a new model of post-traumatic osteoarthritis,” *J. Orthop. Res.*, vol. 32, no. 4, pp. 566–572, 2014.
- [62] M. Jia *et al.*, “A novel dexamethasone-loaded liposome alleviates rheumatoid arthritis in rats,” *Int. J. Pharm.*, vol. 540, no. 1–2, pp. 57–64, 2018.

CHAPTER IV

General Conclusions and Future Work

CHAPTER IV. General Conclusions and Future Work

4.1. General Conclusions

In this work, erythrocytes were used as a source of lipids, including phospholipids, which were used to produce liposomes. The lipidic extracts from the erythrocyte's membrane were rich in essential fatty acids, such as EPA and DHA in a concentration of 1.5 ± 0.6 and 0.6 ± 0.27 g/L, respectively. Consequently, the developed LUVs also presented in their composition these important fatty acids (EPA: 99.5 ± 38.1 g/L and DHA 41.3 ± 17.1 g/L). To demonstrate the value of the novel liposomes as carriers, diclofenac was used. The size of the LUVs incorporating or not diclofenac was of 296.5 ± 58.1 nm and 221.8 ± 55.2 nm, respectively. The prepared liposomes, with a phospholipid concentration of 650.0 ± 438.7 μ M were able to encapsulate a concentration of diclofenac (192.7 ± 30.8 μ M) superior to the therapeutic concentration of this drug both in the synovial fluid (0.006 ± 0.002 and 0.053 ± 0.038 μ M) and in plasma (0.015 ± 0.006 and 0.021 ± 0.014 μ M), for topical and oral administration, respectively. The LUVs are a stable heterogeneous suspension, as their zeta potential is highly negative. Furthermore, the liposomes at the biological temperature are not fully liquid, reducing the risk of the formulation leaking during administration.

The erythrocyte-derived liposomes are cytocompatible in the presence of LPS-stimulated and non-stimulated macrophages, since the cell's metabolic activity, proliferation and morphology was maintained. Additionally, due to their composition rich in omega 3 EPA and DHA fatty acids, the erythrocyte-derived LUVs reduced strongly the concentration of relevant pro-inflammatory cytokines IL-6 and TNF- α . Strikingly, the anti-inflammatory performance of the prepared erythrocyte-derived LUVs is superior to established and commonly used phosphatidylcholine liposomes, as well as to free diclofenac. Moreover, cytocompatible concentrations of erythrocyte-derived LUVs (phospholipid concentration of 120 μ M) presented similar effects to dexamethasone, a potent anti-inflammatory drug, in reducing IL-6 and TNF- α and the LUVs incorporating diclofenac presented a better performance than dexamethasone in reducing TNF- α . In addition to this, the functionalization of the liposomes with folic acid will allow the specific targeting of activated macrophages.

Empty erythrocyte-derived LUVs have promising anti-inflammatory activity, highlighting their potential to improve the treatment of chronic inflammatory diseases.

Gathering all the results, it is possible to conclude that the developed erythrocyte-derived liposomes present a great potential to be used as drug-delivery systems for the treatment of anti-inflammatory diseases.

4.2. Future Work

The work developed in this Master thesis resulted in liposome formulations with strong anti-inflammatory properties, presenting, consequently, a great therapeutic potential.

The erythrocyte membranes are excellent sources of phospholipids rich in omega-3 fatty acids. Nevertheless, in this study the blood samples used were kindly donated by random donors, whose dietary intake of omega-3 was unknown. In the future, selected samples of donors with high dietary consumption of omega 3 could be used to evaluate if a higher amount of omega-3 EPA and DHA in the lipidic extracts will result in improved anti-inflammatory activity.

Regarding the lipid extraction, this could be improved by using a different method, such as methyl-tert-butyl ether method, which uses an organic solvent more environmentally friendly than chloroform. At the beginning of this work, the method used was the most established and had the advantage of causing iron precipitation, excluding it from the lipidic extract. Nevertheless, novel studies were performed comparing the extractions methods and reported that methyl-tert-butyl ether method can be equally effective in lipid extraction.

The drug encapsulated, diclofenac, produced favorable results, but other drugs, for example that target the IL-6 or TNF- α , could be studied to verify the full power of the combined anti-inflammatory activity of the liposomes and the drugs. Moreover, it would be relevant to study the effect of the liposomes in the concentration of different pro-inflammatory mediators, such as PGE₂, to further understand the potentialities of these liposomes.

Finally, it would be important to test the liposomes *in vivo* in models of osteoarthritis or rheumatoid arthritis, to see the translation of the *in vitro* results.